TECHNICKÁ UNIVERZITA V LIBERCI
Fakulta textilní

Struktura a geometrie jednoduchých a dvouvrstvých (spojkových) tkanin

Disertační práce

Studijní program: P3106 – Textile Engineering
Studijní obor: 3106V015 – Textile Technics and Materials Engineering

Autor práce: **Zuhaib Ahmad, M.Sc.**
Vedoucí práce: Ing. Brigita Kolčavová Sirková, Ph.D.

Liberec 2018

TECHNICAL UNIVERSITY OF LIBEREC
Faculty of Textile Engineering

Structure and geometry of single and two layer stitched woven fabrics

Dissertation

Study programme: P3106 – Textile Engineering
Study branch: 3106V015 – Textile Technics and Materials Engineering

Author: **Zuhaib Ahmad, M.Sc.**
Supervisor: Ing. Brigita Kolčavová Sirková, Ph.D.

Liberec 2018

Prohlášení

Byl jsem seznámen s tím, že na mou disertační práci se plně vztahuje zákon č. 121/2000 Sb., o právu autorském, zejména § 60 – školní dílo.

Beru na vědomí, že Technická univerzita v Liberci (TUL) nezasahuje do mých autorských práv užitím mé disertační práce pro vnitřní potřebu TUL.

Užiji-li disertační práci nebo poskytnu-li licenci k jejímu využití, jsem si vědom povinnosti informovat o této skutečnosti TUL; v tomto případě má TUL právo ode mne požadovat úhradu nákladů, které vynaložila na vytvoření díla, až do jejich skutečné výše.

Disertační práci jsem vypracoval samostatně s použitím uvedené literatury a na základě konzultací s vedoucím mé disertační práce a konzultantem.

Současně čestně prohlašuji, že tištěná verze práce se shoduje s elektronickou verzí, vloženou do IS STAG.

Datum:

Podpis:

DEDICATION

I would like to dedicate this thesis to my beloved parents for nursing me with affections and love and their dedicated partnership for success in my life.

TABLE OF CONTENTS

ACKNOWLEDGEMENT

Firstly, I am thankful to Almighty ALLAH for giving me strength and ability to complete this research work. I am also thankful to the administration of Faculty of Textile Engineering, Technical University of Liberec, Czech Republic, for giving me this unique opportunity to weave my ideas to reality under the guidance of learned faculty. Upon completing this dissertation, I owe my deepest gratitude to so many people for their immense assistance. I would like to begin by expressing my deepest gratitude to my supervisor, Ing. Brigita Kolčavová Sirková, PhD for her encouragement, mentoring, support, cooperation and focused discussions throughout this work. She also helped me to realize the importance of distilling and presenting the ideas in a coherent and accessible fashion.

I am greatly thankful to Ing. Jana Drašarová, Ph.D. (Dean of Faculty of Textile Engineering) and Ing. Gabriela Krupincová, Ph.D. (Vice Dean for Science and Research) for their valued guidance. I also want to thank from the core of my heart to all laboratory attendants, from the Department of Technologies and Structure and Department of Material Engineering, who were always there for helping and especially to Sarka Reznickova and my special friends Muhammad Salman Naeem and Azeem Munir who remained supportive and helpful throughout my stay in Liberec. I would also like to thank Dr. Muhammad Zubair and Dr. Moaz Eldeeb for their valuable suggestions during my work. I am thankful to the management of National Textile University particularly Prof. Dr. Niaz Ahmad Akhtar (former Rector NTU), Prof. Dr. Tanveer Hussain (Rector NTU) and Dr. Sheraz Ahmad who allowed me to avail the extraordinary opportunity provided by Technical University of Liberec.

Completing PhD thesis is a very long journey full of hardships and many turns. At this moment, I am feeling great pleasure to thank all those people who have helped me during this journey. Lastly, but not the least I can never forget my family who really suffered the effects of isolation during my stay away from home.

I would like to thank Faculty of Textile Engineering, Technical University of Liberec for their financial assistance as well.

ABSTRACT

There are different ways of making fabrics but the most common method of producing woven fabric is by interlaced yarns. The woven fabric geometry and structure have significant effects on their behavior. The woven structures provide a combination of strength with flexibility. At high strains the yarns take the load together giving high strength, whereas at small strains the flexibility is achieved by yarn crimp due to freedom of yarn movement. Woven fabrics are key reinforcements which offer ease of handling, moldability, and improved in plane properties. Most of the composites are made by stacking layers of woven performs over each other which can cause the delamination failure in composite materials. This problem has been tackled by using multilayer woven perform as reinforcement, instead of single layer woven fabrics. In the multilayer woven structures, multiple layers of distinctive woven fabrics are being stitched during the weaving process.

The structure and properties of a woven fabric are dependent upon the constructional parameters such as thread density, yarn fineness, crimp, weave etc. As we know, woven fabrics are not capable of description in mathematical forms based on their geometry because these are not regular structures; but many researchers believe that we can idealize the general characters of the materials into simple geometrical forms and physical parameters to arrive at mathematical deductions. It is always assumed that the variation of the fabric structure is insignificant in the analysis. The models given by these researchers can describe the internal geometry of woven fabric by describing some part of the binding wave. But we need a model that can describe binding wave in whole repeat and the validation is good from left or right side. We need to obtain not only geometry of binding wave but also spectral characterization for analyzing individual components, which can react on deformation of the shape of binding wave.

In this study, an attempt is made to create a theoretical model on the geometry of plain single and two layer woven structures and verify them with experimental results. The first part of the work deals with the model development and the second part reports on model validation. In the first part, the basic description of the geometry of woven fabric has been described. The interlacing of one warp and one weft yarn creates the binding cell of the woven fabric. Many attempts have been made by different researchers to find a suitable model for describing the binding cell. They have worked mathematically to express the shape of the

binding wave in a given thread crossing in a woven fabric in a steady state. The geometric models have been studied to find out their limitations as well. After a comprehensive study, the geometry of binding cell in plain weave for single and two layer stitched woven fabrics have been presented for theoretical evaluation by Fourier series. This study shows some interesting mathematical relationships between constructional parameters of single and two layer stitched woven fabrics, so as to enable the fabric designers and researchers to have a clear understanding of the engineering aspects of single and two layer woven fabrics.

In the second part of the work, the theoretical model for the description of mutual interlacing of threads, in multifilament woven fabric structure using Fourier series, derived from plain woven structure has been validated with experimental results. The internal geometry of the woven fabrics and the deformation of the shape of the binding wave in the single and two layer stitched woven structures has been evaluated by the cross-sectional image analysis method. The approximation using the linear function f(x) in Fourier series along longitudinal and transverse cross-section has been performed for single layer and two layer stitched woven fabrics cross-section, which fits well to the experimental binding wave. The spectral characteristics of binding waves obtained by Fourier series (theoretical) has been compared with the experimental values, which are very close to each other in longitudinal and transverse cross-section. By evaluating the geometrical parameters of yarn in the real cross-section of a woven fabric, it is possible to compare it with the theoretical shape of a binding wave by analyzing its individual coordinates. The approximation of the whole binding repeat by a partial sum of FS with straight lines description of central line of the binding wave has also been performed for different repeat sizes and compared with each other to analyze the difference in spectrum.

Keywords: Weaving, fabric structure, geometry, stitched woven fabrics, Fourier Series, multifilament, reinforcement fabrics.

ABSTRAKT

Existují různé způsoby výroby textilií. Jednou z možností výroby je výroba na základě technologie tkaní. Kde tkanina vzniká vzájemným provázáním osnovních a útkových nití. Geometrie a struktura tkanin má významný vliv na její chování. Tkaná struktura je tvořena vzájemným silovým působením a parametry vstupujících soustav nití. Tkaniny jako jeden ze tří plošných útvarů jsou klíčové výztuhy, které nabízejí snadnou manipulaci, tvárnost a zlepšují rovinné vlastnosti. Většina kompozitů je vyrobena vrstvením z tkaných materiálů, kde může nastat separace jednotlivých kompozitních vrstev výztuže. Tento problém může být řešen pomocí použitím vícevrstvé tkané výztuže spojkové, místo jednoduché tkaniny. Ve struktuře vícevrstvé tkaniny spojkové dochází k propojení jednotlivých vrstev už při samotném procesu tkaní.

Struktura a vlastnosti tkanin jsou závislé na konstrukčních parametrech, jako je jemnost nití, dostava (osnovy a útku), vazba, setkání atd. Jak je známo, tkaniny možné popsat pomocí matematických forem založených na jejich geometrii. Lze idealizovat obecné charakteristiky materiálů do jednoduchých geometrických tvarů a fyzikálních parametrů, k vytvoření matematické formulace. Modely mohou popisovat vnitřní geometrii tkanin popisem některé části vazné vlny. Avšak my potřebujeme model, který dokáže popsat vaznou vlnu jako celek – celou střídu vazby.

V této studii se usiluje o vytvoření teoretického modelu geometrie jednoduché a dvouvrstvé tkané struktury a jejich ověření s experimentálními výsledky. První část práce se zabývá vývojem modelu a druhou částí je zpráva o ověření tohoto modelu. V první části, je líčen základní popis geometrie tkanin. Křížení osnovy a útku vytváří základní vaznou buňku tkaniny pro všechny typy provázání. Řada výzkumníků učinila mnoho pokusů najít vhodný model pro popis vazebné buňky. Byly vytvořené matematické modely pro vyjádření tvaru vazebné vlny v příčném řezu plátnového provázání v ustáleném stavu. Tyto geometrické modely byly také studovány z hlediska nalezení jejich limitních hodnot provázání. Po obsáhlých studiích byla geometrie vazné buňky (pro jednoduché a dvouvrstvé tkaniny spojkové) prezentována jako teoretické hodnocení využívající Fourierových řad. Tato studie ukazuje některé zajímavé matematické vztahy mezi konstrukčními parametry jednoduché a dvouvrstvé tkaniny spojkové.

Ve druhé části této práce, byl ověřen teoretický model pro popis vzájemného provázání nití ve struktuře jednoduchých tkanin s plátnovou vazbou s využitím Fourierových řad. Teoretické modely byly porovnaný s experimentálními hodnotami získanými z reálné vazné vlny pomocí obrazové analýzy. Vnitřní geometrie tkaniny a deformace nití ve struktuře tkaniny s jednou a dvěma vrstvami byly hodnoceny metodou analýzy obrazu. Pro jednoduchou a dvouvrstvou tkaninu spojkovou v podélném a příčném řezu byla provedena analýza využitím Fourierových řad, kde vstupní funkce k vyjádření popisu byla použita lineární funkce $f(x)$. Spektrální charakteristika, včetně popisu střednice vazné vlny získaných pomocí Fourierovy řady (teoretické) byla porovnána s experimentálními hodnotami, které jsou v podélném pohledu a příčném průřezu velmi blízké. Hodnocením geometrických parametrů osnovních a útkových nití v reálném průřezu tkaniny je možné porovnávat s teoretickým tvarem vazné vlny pomocí analýzy jejích jednotlivých souřadnic. V rámci práce bylo provedeno hodnocení a porovnání provázání a struktury tkaniny pro různé opakované velikosti střídy dvouvrstvé spojkové tkaniny. Jak je patrné z výsledného hodnocení, poloha a velikost spojky přímo určuje tvar spektrální charakteristiky vycházející z daného rozvoje Fourierovy řady použitého pro konkrétní popis tvaru vazné vlny spojkové dvouvrstvé tkaniny.

Klíčová slova: Tkaní, struktura tkanin, geometrie, tkaniny, Fourierovy řady, multifilament, výztuže, vazba.

خلاصہ

کپڑا بنانے کے مختلف طریقے ہیں لیکن کپڑا بنانے کا سب سے عام طریقہ بُنے ہوئے دھاگوں کے ملاپ سے ہے۔ بُنے ہوئے کپڑے کی جیومیٹری اور ساخت انکے رویے پر اہم اثرات رکھتے ہیں۔بُنے ہوئے ڈھانچے لچکدار ہونے کے ساتھ ساتھ طاقت کا ایک مجموعہ فراہم کرتے ہیں۔ زیادہ کشیدہ صورتحال میں دھاگے مل کر بوجھ کو برداشت کرنے کے لیے طاقت فراہم کرتے ہیں، جبکہ کم کشیدگی میں لچک دھاگوں کی آزادانہ حرکت اور دھاگے کے کرمپ کی وجہ سے حاصل کی جاتی ہے۔ بُنے ہوئے کپڑے وہ اہم ساختیں ہیں جو استعمال میں آسانی، ڈھلائی میں آسانی اور ایک ہی ساخت کی بہتر خصوصیات مہیا کرتی ہیں ۔ زیادہ تر مرکب کپڑے کی تہوں کو ایک دوسرے کے اوپر لگانے سے بنائے جاتے ہیں جس کی وجہ سے تہیں مرکب مواد میں الگ ہونےسےایک ناکامی کا سبب بنتی ہے۔ یہ مسئلہ ایک پرت سے بُنے ہوئے کپڑے کی بجائے کثیر بُنے ہوئے پرتوں کے ڈھانچے کی وجہ سے حل کیا گیا ہے،کثیر بُنے ہوئے پَرتوں کے ڈھانچے میں ایک سے زیادہ پَرتوں کو بُنائی کے دوران آپس میں سلائی کیا جاتا ہے۔

بُنے ہوئے کپڑے کی ساخت اور خصوصیات تعمیراتی پہلوؤں پر مُنحصر ہوتی ہیں جیسا کہ دھاگے کی کثافت ، دھاگے کی باریکی،کرمپ اور بُنائی وغیرہ۔ جیسا کہ ہم جانتے ہیں، کہ بُنے ہوئے کپڑے ابھی جیومیٹری کی بنا پر ریاضیاتی شکلوں میں وضاحت کے قابل نہیں ہیں کیونکہ یہ کوئی باقائدہ ڈھانچے نہیں ہیں؛لیکن بہت سے محققین کا خیال ہے کہ ہم مواد کی عام خصوصیات کو سادہ جامیاتی شکلوں اور طبیعیاتی پہلوؤ ں میں ریاضیاتی کٹوتیوں تک پہنچنے کے لیے مثالی طور پر عزم کر سکتے ہیں۔ یہ ہمیشہ فرض کیا جاتا ہے کہ کپڑے کی ساخت میں تبدیلی دورانِ تجزیہ نہ ہونے کے برابر ہے۔ ان محققین کی طرف سے پیش کردہ یہ نمونے بُنے ہوئے کپڑے کی اندرونی ساخت کی وضاحت ،بائینڈگ لہر کے کُچھ حصے کو بیان کرتے ہوئے کر سکتے ہیں۔ لیکن ہمیں ایک ایسے نمونے کی ضرورت ہے جو کہ بائینڈنگ لہر کی پوری دُہرائی میں وضاحت کرے اور اسکی پڑتال بائیں اور دائیں جانب سے درست ہو۔ ہمیں بائینڈنگ لہر کی ساخت کے ساتھ ساتھ اسکے انفرادی اجزاء کا تجزیہ کرنے کے لیے سپیکٹرل خصوصیات بھی حاصل کرنی ہیں جو کہ بائینڈنگ لہر کی شکل کے بگاڑ پر ردّ عمل کر سکتی ہیں۔

اس مطالعے میں ،ایک اور دو پَرتوں کے بُنے ہوئے کپڑے کے ڈھانچے کی جیو میٹری پر نظریاتی نمونہ تخلیق کرنے کی کوشش کی گئی ہے اور تجرباتی نتائج سے انکی توثیق کی گئی ہے۔ اس کام کے پہلے حصے میں نمونےکو بنانا اور دوسرے حصے میں اس نمونے کی پڑتال کرنا شامل ہے۔ اس کام کا پہلا حصہ بُنے ہوئے کپڑے کی جیومیٹری کی بنیادی ساخت کی وضاحت کرتا ہے۔ بُنے ہوئے کپڑے میں تانہ اور بانہ کا ایک ایک دھاگہ مل کر ایک سیل تخلیق دیتا ہے۔ بائینڈنگ سیل کی وضاحت ایک خاص نمونے سے کرنے کے لیے مختلف محققین کی طرف سے بہت سی کوششیں کی گئی ہیں۔ انہوں نے مستحکم حالت میں بُنے ہوئے کپڑوں میں دھاگوں کے ملاپ کی جگہ پر بائینڈنگ لہر کی شکل کی وضاحت کے لیے ریاضیاتی طور پر کام کیا ہے۔ اسی طرح جیومیٹری کے نمونوں کی حدود کو تلاش کرنے کے لیے بھی ان کا مطالعہ کیا گیا ہے۔ ایک جامعہ مطالعہ کے بعد، ایک اور دو پَرتوں کے سلائی کئے گئے بُنے ہوئے کپڑوں کے بائینڈنگ سیل کی جیومیٹری کو نظریاتی تشخیص بزریعہ فورئیر سیریز کے پیش کیا گیا ہے۔ اس مطالعہ سے ایک

اور دو پَرتوں کے سلائی کئے گئے بُنے ہوئے کپڑوں کے تعمیراتی پہلوؤ ں کے درمیان کچھ دلچسپ ریاضیاتی تعلقات ظاہر ہوتے ہیں ،لہذا اس کی مددسے کپڑے کے نقشہ نگاروں اور محققین کو ایک اور دو پَرتوں کے بُنے ہوئے کپڑوں کے انجینئرنگ کے پہلوؤ ں کو سمجھنے میں واضع مدد ملے گی۔

اس کام کے دو سرے حصے ہیں اُس نظریاتی نمونےکی، جو کہ دھاگوں کے باہمی ملاپ کی وضاحت کے لیے فورئیر سیریز کو کثیر ریشوں سے بُنے ہوئے کپڑے کے ڈھانچے اورسادہ بُنے ہوئےکپڑے کی ساخت سے حاصل کردہ ہے، تجربہ کار نتائج کے ساتھ توثیق کی گئی ہے۔ بُنے ہوئے کپڑوں کی اندرونی ساخت اور ایک اور دو پَرتوں والے سلائی کئے گئے بُنے ہوئے کپڑوں کے بگاڑ کے عمودی تراش کا جائزہ تصویری تجزیہ کے طریقے سے کیا گیا ہے۔ لکیری اصول کو فورئیر سیریز میں استعمال کرتے ہوئے ایک اور دو پَرتوں کے سلائی کے ذریعے بُنے ہوئے کپڑوں میں لمبائی اور چوڑائی کے عمودی تراش کی قُربت حاصل کی گئی ہے،جو کہ تجربہ کے ذریعے حاصل کردہ بائینڈنگ پر درست بیٹھتی ہے۔ فورئیر سیریز (نظریاتی) کی وجہ سے بائینڈنگ لہر کی حاصل کردہ سپیکٹرل خصوصیات کا تجرباتی شماریات کیساتھ موازنہ کیا گیا ہے ،جو کہ لمبائی اور چوڑائی کے عموی تراش میں ایک دوسرے کے بہت قریب ہیں۔ ایک بُنے ہوئے کپڑے کے حقیقی عمودی تراش میں دھاگے کی جیومیٹری کے پہلوؤ ں کا اندازہ لگاتے ہوئے ،اس کابائینڈگ لہر کے انفرادی مُحدّد اور نظریاتی شکل کیساتھ موازنہ کرنا ممکن ہے۔ ایک مکمل بائینڈنگ دُہرائی، جسکی بائینڈگ لہرکی درمیانی لکیر کو سیدھی لکیر کے ذریعے واضع کیا گیا ہے، کی قُربت فورئیر سیریز کے جُزوی مجموعہ سے کی گئی ہے اور یہ کام مختلف دُہرائی کی پیمائیشوں اور ایک دوسرے کیساتھ اِنکے سپیکٹرم کاموازنہ کرنے کے لیے بھی انجام دیا گیا ہے۔

مطلوبہ الفاظ: بُنائی، کپڑے کی ساخت، جیومیٹری، بُنے ہوئے سلائی کردہ کپڑے،فورئیر سیریز،کثیرالمقدار ریشے،تقویت یافتہ کپڑے۔

LIST OF FIGURES

LIST OF TABLES

LIST OF SYMBOLS

Symbol	Description
B1-7	Basalt woven fabric samples
d	Diameter of thread [μm]
p	Thread spacing [μm]
h	Maximum displacement of thread axis (crimp height) [μm]
θ	Angle of thread axis to the plane of cloth [^{o}]
l	Length of thread axis between planes through axes of consecutive cross-threads
c	Crimp of thread
T_1	Yarn count of warp [tex]
T_2	Yarn count of weft [tex]
A	Distance between two warp yarns [μm]
B	Distance between two weft yarns [μm]
D_1	Setting of warp threads [1/cm]
D_2	Setting of weft threads [1/cm]
ρ_1	Fiber density of warp yarn [kg.m^{-3}]
ρ_1	Fiber density of weft yarn [kg.m^{-3}]
μ_1	Packing density of warp yarn []
μ_2	Packing density of weft yarn []
d_1	Diameter of warp yarn [μm]
d_2	Diameter of weft yarn [μm]
d_s	Mean diameter [μm]

$d_{eff.}$	Effective diameter [µm]
g	Constant of deformation
h_1	Height of warp crimp wave [µm]
h_2	Height of weft crimp wave [µm]
e_1	Waviness of warp yarn [-]
e_2	Waviness of weft yarn [-]
n_1	Number of ends in weave repeat
n_2	Number of picks in weave repeat
pp_1	Number of crossing parts in weave repeat in warp
pp_2	Number of crossing parts in weave repeat in weft
fl_1	Length of float part of warp threads
fl_2	Length of float part of weft threads
FS	Fourier Series
k	Slope of linear function in single layer plain woven fabric
k_1 and k_2	Slope of linear functions in two layer stitched woven fabrics in stitching and non-stitching section
Δy	Change in y direction
Δx	Change in x direction
h_{f^1} and h_{f^2}	The height of first warp and weft binding waves in two layer woven fabrics
h_{s^1} and h_{s^2}	The height of second warp and weft binding waves in two layer woven fabric
e_{f^1} and e_{f^2}	Relative waviness of first warp and weft yarn in two layer woven fabrics
e_{s^1} and e_{s^2}	Relative waviness of second warp and weft yarn in two layer woven fabrics
f (x)	Analytic function

a_o	Coefficient of Fourier Series [µm]
a_n	Coefficient of Fourier Series [µm]
b_n	Coefficient of Fourier Series [µm]
T	Specific interval for one repeat [µm]
n	Harmonic component (1, 2, 3, …)
α	Number of terms (1, 2, 3, …)
m	Number of Intervals (0, T)
j	even numbers (2,4,6, . . .)
l	odd numbers (3,5,7, . . .)
A_n	Amplitude of component [µm]
ϕ_n	Phase shift of component [^{o}]

1. INTRODUCTION

In recent years, the woven fabrics have gained much attention because they have superior properties over conventional materials used in engineering structures. The woven fabric geometry and structure have significant effects on their behavior. For example, for the multilayer structures, a good reinforcement material should be chosen as a good reinforcement material ensures better properties of a final product. Whereas, to access the better properties of reinforcement material, it is very important to understand the internal geometry of the woven fabric [1]–[3].

As we know, woven fabrics are not capable of description in mathematical forms based on their geometry because these are not regular structures; but many researchers believe that we can idealize the general characters of the materials into simple geometrical forms and physical parameters to arrive at mathematical deductions. Researchers have put forward many different forms of fabric geometry to represent the configuration of threads in woven fabrics. To understand the internal geometry of woven fabric, which refers to the spatial orientation of yarns in the structure of a fabric, many studies have been performed in the past [4], [5]. Pierce's, Kemp's, Olofsson's and Hearl's model are known as the most used and best known models [6]–[15]. Moreover, there are some investigations in which these mentioned models has been compared and evaluated [16], [17]. The principles on which all these models are based remain unaltered. It is always assumed in these models that the geometric shape is constant for each model of the unit cell or it can be said the variation of the fabric structure was considered insignificant in the analysis.

In another study Jaume et al. applied Fourier transform on woven fabric structures by image analysis, it is a non-destructive and non-contact testing technique to obtain the fabric structure or the pattern of weaving textile structures [18]. Similarly, Bohumila Koskova and Stanislav Vopicka worked on the determination of yarn waviness for eight-layer carbon composites by the application of discrete Fourier transform (DFT) [19]. Whereas it has been described by Brigita Sirkova that by using the sum of Fourier series, the spectral characteristic of the approximated course can be obtained. The spectral characteristic consists of amplitude and phase characteristics of individual wavelengths [20].

It is very complex to build up a direct mathematical relationship to predict the structural properties of the woven fabric. Moreover, it is not possible to rely only on theoretical models,

however it can be combined with empirical findings as well. In this regard, it is necessary to find out the best possible approach, which may use a special method of analyzing the cross-section of woven structures to evaluate the fabric geometry in a better way and to correlate it with predicted theoretical findings. Kawabata et al. developed a 3D sawtooth geometry, which allows the implementation of biaxial response in a mechanistic way. The warp and weft axes are assumed to be straight lines for simplifications. The current work focuses on a macroscopic length scale geometrical model for woven fabrics using the mesoscopic sawtooth geometry developed by Kawabata et al. [21].

The main aim of this work is creation of model as well as the development of a methodology to analyze the shape of the binding wave in the whole weave repeat and yarn deformation in plain woven fabrics and analysis of mutual interlacing of threads in multifilament single layer and two layer stitched woven fabric structure using Fourier series as it has not been possible by the other described models.

2. RESEARCH OBJECTIVES

The purpose of the work is the description and expression of geometry of woven fabric structure - two layer stitched woven fabrics with plain weave in the cross-section. Evaluation and analyzation of cross-sectional image of single layer and two layer stitched woven fabric structures with plain weave, which can be used as reinforcement fabrics. The main aim is the creation of model as well as the development of methodology to analyze the shape of binding wave as well as yarn deformation in single layer and two layer stitched woven fabrics with plain weave and to validate it with theoretical models. The work has been divided into the following parts.

a) Analysis of the fiber and yarn

Understanding the behavior of fiber and yarn by analyzing its physical properties like fineness, diameter, twist per meter, tenacity and elongation etc.

b) Construction of woven structures

The objective is to prepare the single and two layer stitched woven structures with different material, weft settings and stitching (connection) points on a sample weaving loom.

c) Creation of theoretical model (idea)

The basic geometric models will be studied, and their limitations will be analyzed. An improved theoretical model for the description of geometry of cross-section of woven multifilament fabric structure – single and two layer stitched woven fabrics with plain weave will be presented.

d) Evaluation of the internal geometry of the woven fabrics

The objective is the evaluation of the internal geometry of the woven fabrics and analysis of deformation in the single and two layer stitched woven structures by the cross-sectional image analysis method.

e) Fourier analyses

It will be performed by the mathematical modeling of geometry of binding wave in woven fabric structure using Fourier series. Mathematical modelling creates information about shape – geometry of binding wave and characteristic of weave and interlacing - the spectrum for

single layer and two layer stitched woven fabrics with plain weave. The approximation of two layer stitched woven fabrics with different repeat size will be performed and their spectrum will be analyzed as well.

f) Model validation

The experimental values will be validated by the proposed theoretical model which is going to be proposed for the evaluation of single layer and two layer stitched woven structures.

3. LITERATURE REVIEW

Textile structures are recognized for their exclusive combination of light weight and flexibility and their capability to offer a combination of strength and toughness [22]. Because of the growing need to offer specialized products at finest quality and low cost, satisfying at the same time the fast cycles of fashion trends, the automation and integration of processes in the textile industry is increased. Similarly, in the case of technical applications the delivery of products of exact properties and of high quality are required as well. The prediction of the properties and the aesthetic features of the product before the actual fabrication can really benefit the textile research community [23]. The textile materials can be used to produce an extensive range of technical products nowadays, such as reinforcements in composites for aerospace or marine applications or textiles for medical applications. Therefore the prediction of the mechanical properties of end-product is of major importance [24]–[26].

The textile structures are flexible, inhomogeneous, anisotropic, porous materials with distinct viscoelastic properties. These unique characteristics makes the textile structures to behave differently as compared to other engineering materials. Moreover, textiles are characterized by an increased structural complexity that is why their properties mainly depend on a complicated combination of their structural units and their interactions. The weave patterns of woven fabrics as well as the deformation mechanisms of their consistent yarns make the modelling of these structures extremely challenging [27]. An extended literature review for the deformation of woven fabrics by the computational models is presented in this study. On the basis of these models, the problems towards a comprehensive model for textile structures are highlighted as well.

The study of fabric mechanics often leads to the introduction of models with simplifying assumptions. The yarn is considered as the basic structural unit of the fabrics. As yarns are assumed as homogeneous materials, the contact phenomena dominate the deformation procedure of the fabrics. The stability of the textile structures is supported by the friction effects. Whereas the stress and strain distribution in fabric subjected to deformation is also affected by the contact phenomena. The study of fabrics mechanics requires special attention due to the large deflection effects and the nonlinearity of the textile structures deformation phenomena [24].

3.1 Structure of woven fabric

The textile fabrics are made of interlaced yarns which consist of the basic element of every textile product called as the fibers. While the fabrics are classified according to their manufacture process as knitted, woven and non-woven. Whereas, woven fabrics are made of two set of yarns which are warp and weft yarns. These yarns are interlaced perpendicular to each other [28]–[30]. The method of mutual interlacing of these two sets of threads in woven fabric gives the weave. The correct choice of weave in woven fabric is important not only for the construction of the fabric, but it adds additional necessary mechanical and end-use properties (strength, elongation, permeability, roughness, feel, flexibility, etc.) [31]–[33].

Weave in woven fabric are usually illustrates by patterns, which show the fabric design and way of interlacing. Patterns are usually drawn on squared paper on which each vertical space represents a warp thread and each horizontal space represents a weft thread. Each square therefore indicates an intersection of warp and weft thread. To show the warp overlap, a square is filled in or shaded. The blank square indicates that the weft thread is placed over the warp i.e. weft overlap [34]–[36].

The three basic weave designs are plain, twill and satin as shown in Figure 1. These basic weaves are characterized by small repeat size, ease of formation, and recognition [28] [37]. The simplest interlacing pattern for warp and weft threads is over one and under one. The weave design resulting from this interlacement pattern is termed as plain or 1 / 1 weave. The 1 / 1 interlacement of yarns develops more crimp and fabric produced has a tighter structure. The plain weave is produced using only two heald frames. The variations of plain weave include warp rib, weft rib and matt or basket weave. Whereas the twill weave is characterized by diagonal ribs (line) across the fabric. It is produced in a stepwise progression of the warp yarn interlacing pattern. The interlacement pattern of each warp starts on the next filling yarn progressively. The two sub categories based on the orientation of twill line are Z and S-twill or right-hand and left-hand twill, respectively. Some of the variations of twill weave include pointed, skip, and herringbone twill [38]. While the satin /sateen weave is characterized by longer floats of one yarn over several others. The satin weave is warp faced while sateen is a weft faced weave. A move number is used to determine the layout in a weave repeat of satin, and number of interlacements is kept to a minimum. The fabrics produced in satin/sateen weave are more lustrous as compared to corresponding weaves [29].

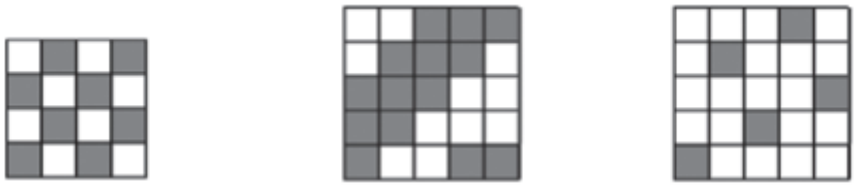

Figure 1. Weave diagram for basic weaves [29]

Warp yarns run lengthwise through the fabric or along the weaving machine direction while weft (filling) yarns run widthwise through the fabric [39]. The pattern of interlacing, weave diagram and cross-sectional view for plain weave has been shown in Figure 2.

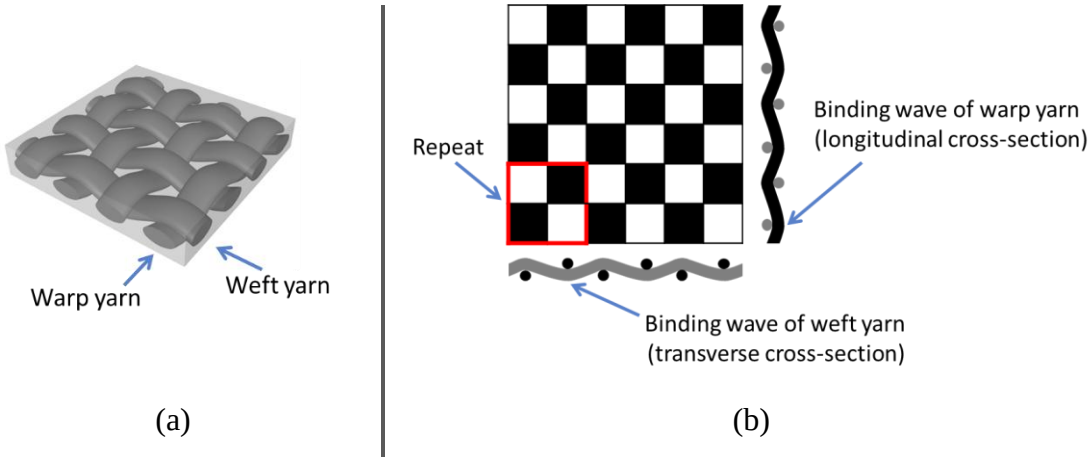

Figure 2. Plain woven fabric (a) Interlacing of warp and weft yarn (b) Weave diagram and cross-sectional view

In addition to these basic designs, there are complex structures produced by the combination of these basic weaves, for example, multilayer fabrics, pile weave structures, and jacquard designs. These structures are widely used for a number of applications. Woven fabrics are key reinforcements which offer ease of handling, moldability, and improved in plane properties. Most of the composites are made by stacking layers of woven performs over each other which can cause the delamination failure in composite materials. This problem has been tackled by using multilayer woven perform as reinforcement instead of multiple layer stacking of single layer woven fabrics. In the multilayer woven structures, multiple layers of distinctive woven fabrics are being stitched during the weaving process [40]–[42].

The structure of multilayer fabrics is based on the stitching pattern of the individual layers. It is either layer to layer or through the thickness [34]. Two-dimensional (2D) weaving may be utilized to produce both conventional sheet like two-dimensional fabrics and some three-dimensional (3D) fabrics. 2D weaving is characterized by the interlacing of two orthogonal sets of yarns and by mono-directional shedding. Khokar defines the 2D weaving process as "the action of interlacing either a single or a multiple-layer warp with a set of weft". The process by which the 2D weaving process is used for producing both 2D fabrics and 3D fabrics can be observed in Figure 3 [43], [44].

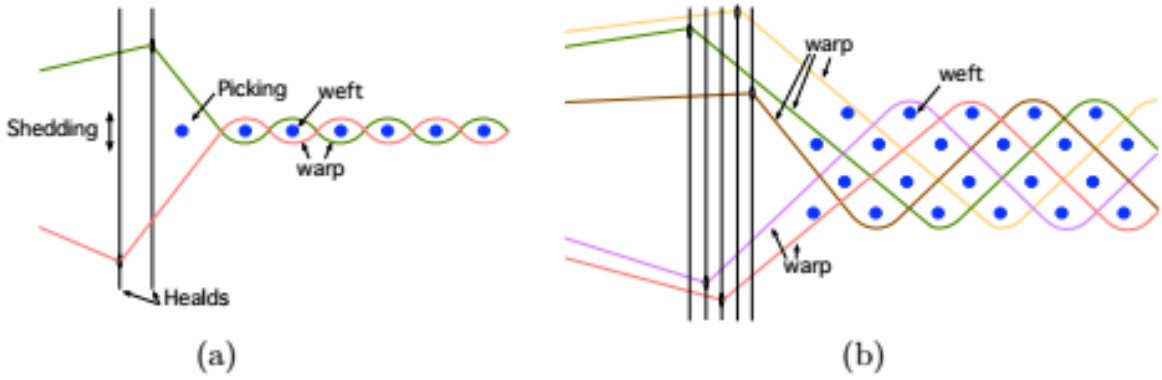

Figure 3. Illustration of the 2D-weaving principle for a) 2D-fabrics and b) 3D-fabrics [44]

3D woven fabrics are produced principally by the multiple warp weaving method which has been used for the manufacturing of double and triple cloths for bags, webbings and carpets. By using the weaving method, various fiber architectures can be produced including solid orthogonal panels, variable thickness solid panels, and core structures simulating a box beam or a truss-like structure [22] [45], [46].

Woven fabrics in the form of crimp (binding) waves are considered as a repeating network of identical unit cells and assumed to have constant yarn cross-section in their structure. Mathematical relationships could be obtained by linking this kind of geometry with physical parameters. The yarn configuration (deformation) in the fabric is mainly determined by the form of crimp waves (binding wave) and the cross-sectional shape of yarns in each position [24] [47], [48]. As we know that the geometry of the fabrics has considerable effects on their behavior. Therefore, studies of fabric geometry have played an important role in the following areas:

- Prediction of the fabric dimensional properties and maximum set of a fabric.

- Prediction of mechanical properties by combining fabric geometry with yarn properties such as bending rigidity, Young's modulus, and torsional rigidity.
- Derivation of the relationship between geometrical parameters, such as crimp and weave angle.
- To understand the fabric performance in terms of fabric handle and surface effects [24].

By considering a geometrical model of the woven fabric, the interrelation between fabric parameters can be obtained. The model is not just an exercise in mathematics and not only useful in determining the entire structure of a fabric from a few values, which are given in technological terms. Whereas the model establishes a base for calculating various changes in woven fabric geometry when it is subjected to known extensions or compressions in a given direction or a complete swelling in aqueous medium. It has been found useful for weaving of structures with maximum sett and also in the analysis and interpretation of structure property relationship of woven fabrics [40].

3.2 Classification of modelling approaches

Several methods were adopted for the modelling and analysis of the textile structures during the last decades, According to the different modelling method used, a basic classification divides them into the analytical and numerical or computational approaches. Another essential classification of the modelling of the textile structures is made according to the scale of the model which is micromechanical, mesomechanical and the macromechanical modelling [49]–[56]. Although the mentioned modelling stages were developed as distinct analysis approaches but their integration in a compound modelling approach was directly raised. Thus the textile society implemented a modelling hierarchy [14], [57], [58] based on three modelling scales: the micromechanical modelling of yarns, the mesomechanical modelling of the fabric unit cell and the micromechanical modelling of the fabric sheet.

3.3 Modelling of woven fabric structures

In 1937, Peirce [6] proposed a "flexible thread" model in which a two-dimensional unit cell (repeat) of fabric was built up by superimposing linear and circular yarn segments to produce the desired shape as shown in Figure 4. His model of plain weave fabrics could be valid if the yarns have a circular cross-section and highly incompressible, but at the same time, perfectly flexible so that each set of yarns had a uniform curvature imposed upon it by the circular

cross-sectional shape of the interlacing yarns. The main advantages in considering this simple geometry are as follows.

- It helps to establish the relationships between various geometrical parameters.
- It is possible to calculate the resistance of the cloth to mechanical deformation such as initial extension, bending and shear in terms of the resistance to deformation of individual fibers.
- Information is obtained on the relative resistance of the cloth to the passage of air, water or light.
- It provides a guide to the maximum density of yarn packing possible in the cloth [40].

The derivation of the relationships between the geometrical parameters and parameters such as thread-spacing, weave angle, weave crimp, and fabric thickness forms the basis of the analysis. This model is convenient for their calculations and is especially valid for open structures. But the assumptions of circular cross-section, uniform structure along the longitudinal direction, perfect flexibility, and incompressibility are all unrealistic, which leads to the limitations of the application of this model.

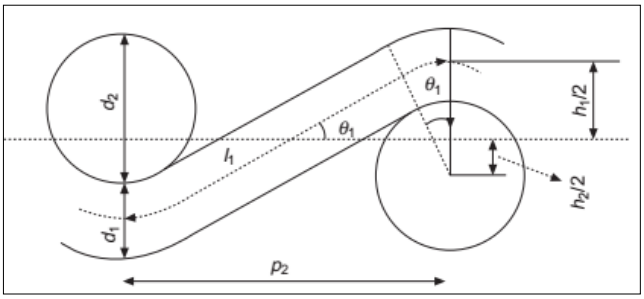

Figure 4. Peirce's circular cross-section geometry of plain-weave fabrics [6]

However, in high density woven structures, the inter-thread pressures built during weaving cause considerable thread flattening, normal to the plane of the cloth. Peirce recognized this and proposed an elliptic cross-section-based theory as shown in Figure 5. But it is also not valid as increased flattening also means increased error in fundamental geometrical relationships which has been derived by Pierce.

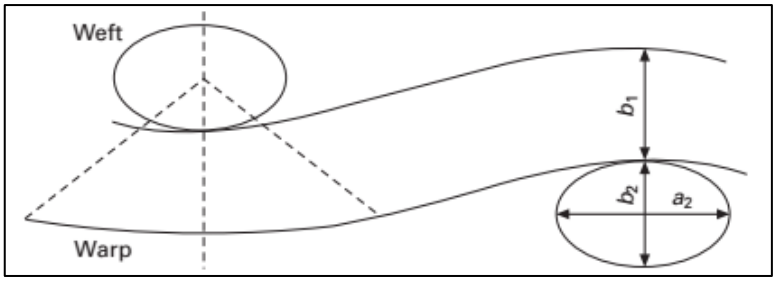

Figure 5. Peirce's elliptic cross-section geometry of plain-weave fabrics [11]

Peirce did not extend his treatment of non-circular threads for jammed structures, where the formal relations for elliptic sections would be required. In this note, Kemp [7] suggested a racetrack section in 1958 as shown in Figure 6 to modify the cross-sectional shape proposed by Pierce. It consisted of a rectangle enclosed by two semicircular ends and had the considerable advantage that it allowed the use of relatively simple relations of circular thread geometry, already utilized and tabulated by Peirce, to be applied to a comprehensive treatment of flattened threads. It was much more suitable for the jammed structures.

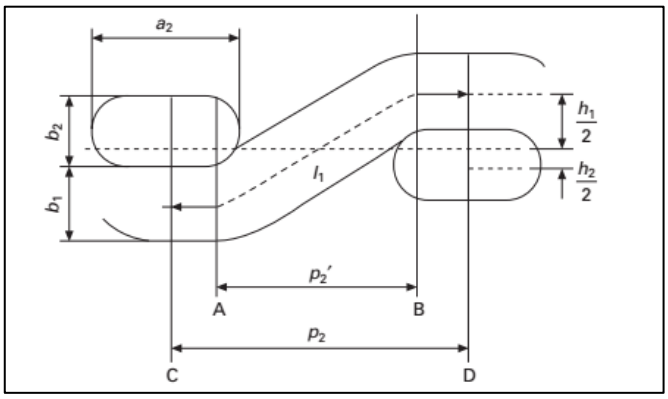

Figure 6. Kemp's racetrack section geometry of plain-weave fabrics [7]

A lenticular geometry as shown in Figure 7, was proposed by Hearle Shanahan in 1978, which was the most general model mathematically. This geometry is an attempt to avoid the difficulties encountered with racetrack geometry. The geometry is a modification of the Peirce geometry. The curvature of the crossing yarn will clearly be reduced as the yarn cross-section becomes flatter, so that more sensible behavior should be obtained when the interaction between yarn-bending and yarn-flattening is considered [59][9].

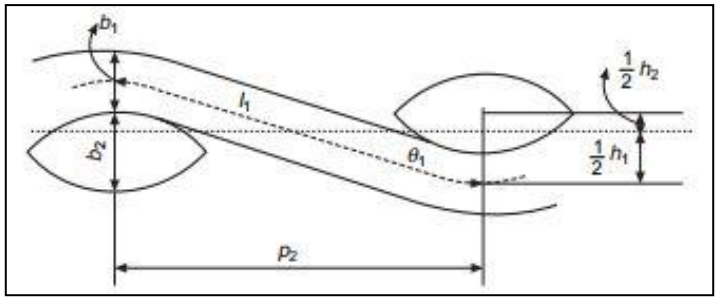

Figure 7. Hearle's lenticular section geometry of plain-weave fabrics [9]

Table 1 lists the basic descriptions of these models and their differences [44]. The principles on which all these models are based remain unaltered. It is always assumed that the geometric shape is constant for each model of the unit cell or it can be said that the variation of the fabric structure was considered insignificant in the analysis. Therefore, the direct application of these models is limited.

Table 1: The comparison of three geometrical models

Model type	**Cross-section shape**	**Yarn tracing or crimp style**	**Features**
Peirce's model	Circular or elliptic	Incompressible, flexible and uniform curvature, including linear and circular or elliptic yarn segments	Valid for open fabrics
Kemp's model	Racetrack	Incompressible, flexible and uniform curvature, including linear and racetrack sections	Valid for jammed fabrics
Hearle's model	Lenticular	Incompressible, flexible and uniform curvature, including linear and lenticular sections	Compressive treatment of flatted threads

An elastic model deducted from the assumption of the normal shape of yarn cross-section was introduced by Olofsson [8]. Yarn cross-sectional shape was considered as a function of the external forces acting on them and reaction forces in the fabric. Important fabric parameters are calculated, and different force combinations considered. A mathematical

analysis is given of equilibrium conditions, of stress-strain relationships in extension and compression, and of energy in bending. He has also criticized the previous models as follows:

- The effective diameter which may be very different from the diameters found experimentally and are primarily unknown.
- The cross-section of the thread is assumed to be circular and corrections for flattening can be introduced, but increased flattening also means increased error in the fundamental geometrical relationships (this objection is not valid for the racetrack section introduced by Kemp [7]).
- Bending stiffness (and torsional stiffness) of the yarn are neglected.
- The model does not consider the setting of the yarn crimp in the fabric, i.e., the residual crimp of the yarn after it has been released from the fabric.
- If the plain weave, considered especially by Peirce, is replaced by a more complicated design, the corresponding modification to the model is often inadequate [8].

Similarly, in a recent study, Ozgen and Gong [60] aimed to achieve a more realistic representation of the yarns in fabric, suggested an ellipse model with a variable yarn cross-sectional shape in different regions as shown in Figure 8. The model is based on the various variables including fiber type, yarn count, yarn twist factor, and cover factor. The fabric samples were scanned using the synchrotron facility and three-dimensional images of fabric samples were achieved [61]. The ImageJ software [62] was used for volume visualization (slice by slice) and for the measurements to locate the data points which describe the yarn path. The Matlab script was written to generate best fit ellipse models from a yarn cross-section image. The response surface methodology (RSM) is used to analyze the data which uses statistical models to find the best approximation. However, this approach did not provide statistically satisfying models that describe the data.

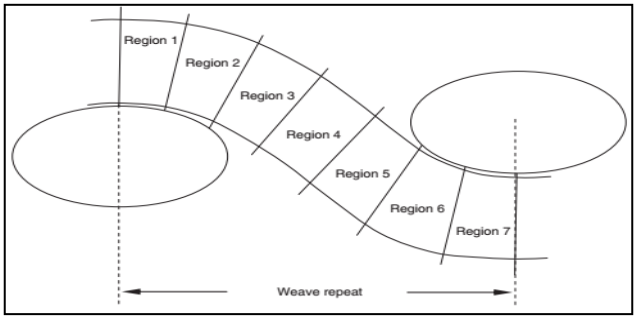

Figure 8. Schematic representations of binding wave regions [60]

It is a characteristic of a woven fabric that its pattern of binding is periodic across the whole width of fabric [24]. The periodically repeated pattern of binding waves can be mathematically modeled by a sinusoidal function when the deformations and irregularities are not high. In another case, when deformations are higher, the Fourier series fits the shape of the binding wave as it takes part of this sine and cosine functions to create better information about deformation. A mathematical model using Fourier series was used by Birgita in which she analyzed the experimental binding wave by Fourier series as shown in Figure 9. It responds well to the deviations in the real interlacing [63]. Predicted warp and weft crimp was calculated from experimental yarn parameters in cross-section (real value of warp and weft diameter, waviness, real value of heights of binding wave, etc.). All necessary information about the fabric can be deduced from the description of mutual relations of the binding cell. By using the sum of Fourier series, the spectral characteristic of the approximated course can be obtained. The spectral characteristic consists of amplitude and phase characteristics of individual wavelengths [20].

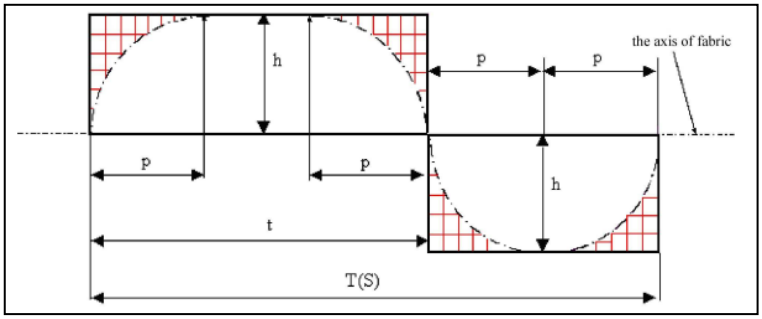

Figure 9. Description of binding wave in fabric for Fourier mathematical model [63]

As we know the analysis of woven structures in most laboratories is still visually and manually made by cutting a sample and unravelling thread crossing. Jaume et al. [18] applied a non-destructive and non-contact testing technique to obtain the woven fabric structure or the pattern of weaving textile structures as shown in Figure 10. The techniques can be grouped in two basic classes: Some of them are based on Fourier analysis of the fabric image and the others are based on image analysis in the spatial domain. Based on the convolution theorem, the definition of a woven structure in terms of an elementary unit with a minimum number of thread crossings and a basis of two non-perpendicular vectors is equivalent to that of the conventional weaving diagram. But it is also more compact because it drastically reduces the amount of redundant information. The new expression is therefore advantageous for storing information about weaving patterns in looms and simulators. In a real fabric

structure, the data for this new expression can easily be extracted from the peak distribution of the magnitude of the Fourier transform for the most common structures (plain, twill, satin).

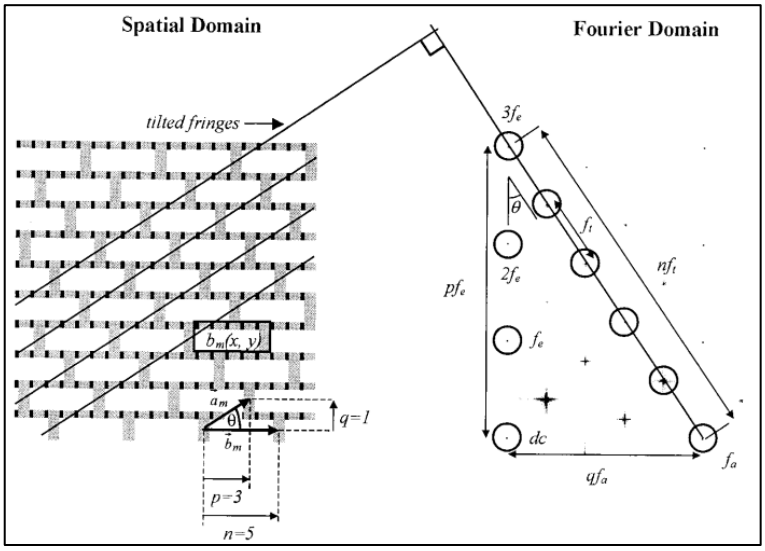

Figure 10. Schematic of correspondence between the spatial and the frequency domains for a fabric structure [18]

The woven composite reinforcements are created by different yarn interlacing, which produces yarn undulation (waviness). Yarn waviness strongly influences the elastic properties of woven composites. Therefore, the prediction of properties is based upon detailed geometric description of the reinforcement. Bohumila and Stanislav worked on the determination of yarn waviness for eight-layer carbon composites by the application of discrete Fourier transform (DFT) [19]. Yarn waviness is usually quantified by means of inclination angle distribution. Inclination angles can be derived from mathematical description of actual yarn shape. The actual quasi-periodic yarn shape *y(x)* can be considered as a superposition of a definite number of harmonic courses with amplitudes A_1, phase angles ϕ_i and wavelength L.

$$y(x) = A_o + A_1 sin\left(\frac{2\pi x}{L} + \phi_1\right) + \ldots + A_n sin\left(\frac{2\pi x}{L} + \phi_n\right) \quad (1)$$

The compression level of carbon composites has been changed as well and Discrete Fourier transform was applied to yarn centreline coordinates as shown in Figure 11. The program allows to select the dominant harmonics, or selects the given number of the highest harmonics automatically, calculates the approximate yarn axis using equation (1) and

compares it with an experimental shape. The values of inclination angle rise with increasing compression level namely in plain weave composites.

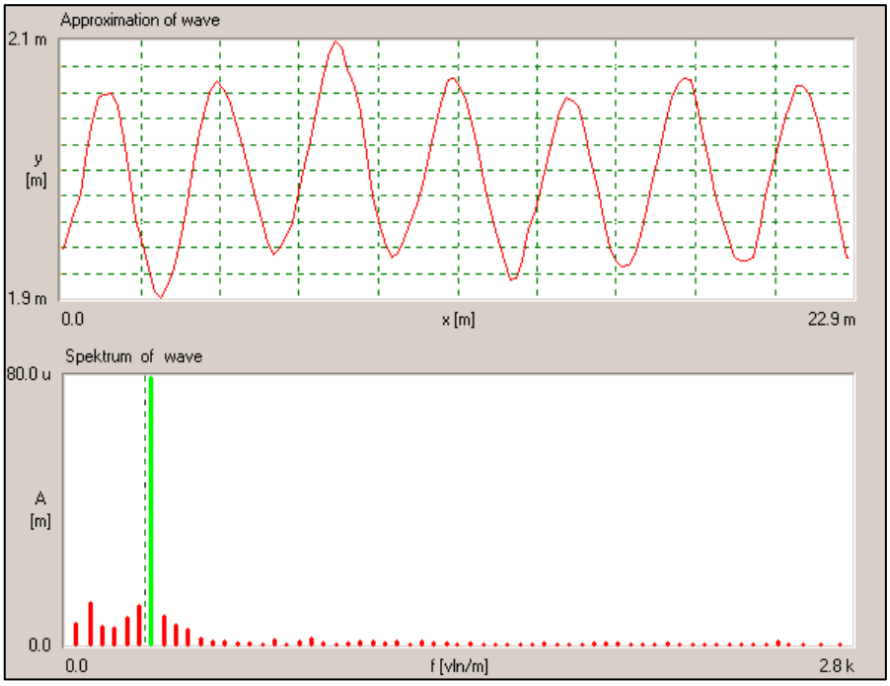

Figure 11. Yarn centerline approximation and DFT spectrum [19]

Many researchers measured the warp and weft densities according to the brightness and interstices among the yarns. In the transmitted or reflective fabric image, the grey projection was used to locate the yarns or interstices by finding the peaks in the projection curve. They have used the method of Fourier transform, image reconstruction and threshold processing [64]–[69]. Some researchers have also analysed the weave pattern of woven fabrics while others performed the defect detection of fabric using the Fourier image analysis technique [70]–[74].

Kawabata et al. [21] presented a biaxial tensile-deformation theory with the aid of the model, and the forces required to stretch the fabric along the warp and weft directions at the same time are theoretically calculated from the properties of yarns and from the structure of the fabrics. He developed a 3D sawtooth geometry, which allows the implementation of biaxial response in a mechanistic way. The warp and weft axes are assumed to be straight lines for simplifications as shown in the unit structure in Figure 12.

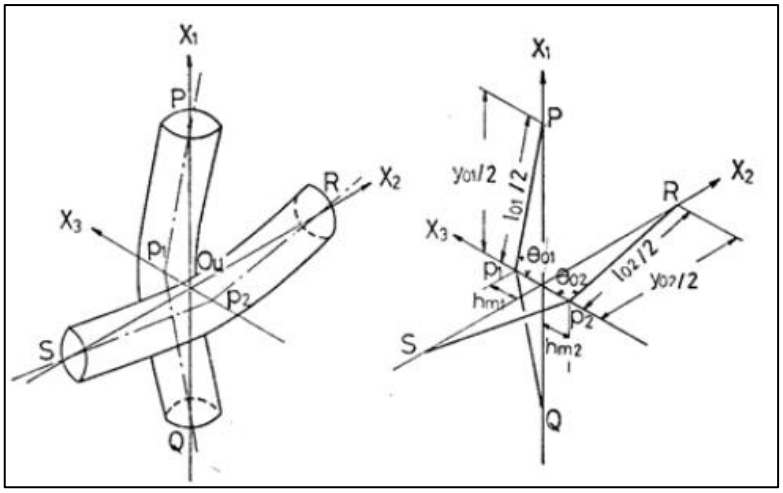

Figure 12. The unit structure of a plain woven fabric or "Saw-tooth" model of plain woven fabric [21]

These models can describe the internal geometry of woven fabric by describing some part of the binding wave, but we need a model that can describe binding wave in whole repeat and the validation is good from left or right side. We need to obtain not only geometry of binding wave but also spectral characterization for analyzing individual components, which can react on deformation of the shape of binding wave. So, it can be used as possible substitution of classic models because the description of the shapes of binding wave is continuous and smooth functions as in the real binding wave. Fourier approximation method can be used to analyze the yarn deformation in single layer and two layer stitched woven structures and it is possible to analyze the structures woven by multifilament yarns to evaluate the properties of individual and two layer fabrics. This could give a better description of the binding wave in woven structures and it is important to apply this model for comparison of deformation of binding wave in experimental data as well.

4. THEORETICAL MODELLING OF TWO LAYERS STITCHED WOVEN FABRIC GEOMETRY STRUCTURE

Many attempts have been done in the past to find a suitable model describing the binding cell, i.e. to express mathematically the shape of the binding wave in each thread crossing in woven fabric in the steady state. Pierce model, Ollofsson model, hyperbolic model, parabolic shapes are registered as the most used and best-known models [75]. These models are related to the plain weave. Other than plain kinds of interlacing could theoretically arise from the models created before. But additional mathematical formulations, which are used for expressing the irregularity of interlacing in bindings, describe the real binding conditions in a more complex way, which is not a satisfying manner.

A mathematical model that permits the characterization of fabric structure and surface profile is to be developed. For simplification, here we investigate only a model for woven fabrics with basic weave patterns. One factor that is common to all weave designs is that of the repeating pattern or the unit cell. The unit cell represents the smallest repeat unit of the weave architecture and describes the whole reinforcing fabric, so it is necessary to understand it [76]. This model is based on the following assumptions:

1. The yarn is monofilament, without twist and having smooth surface.
2. The crimp of the yarn is an ideal cosine or sine function.
3. The yarn is circular in cross-section; no thickness variance exists along the yarn length.
4. The yarn can be bent into any crimp shape without changing its cross-sectional shape.
5. Both warp and weft are perpendicular to each other and evenly distributed, without any distortion and having same diameters [44].

The most detailed geometric analysis would consider the path of each single fibre in the unit cell. The greatest practical problem, however, is caused by the fact that the complete set of input data necessary for such a detailed geometric description is very large and difficult to quantify. Therefore, the geometric analysis is carried out on the yarn level. We assume that all individual fibres in the yarn run in the same direction as the yarn [22].

The geometric characteristics of a weave can be subdivided in three groups (Table 2). The first group, the know group, contains those parameters that are supplied by the weaving company. All the parameters that one has to measure on a real woven fabric are put together in the second group, the measure group. This fabric information can be obtained by

microscopic observation of warp and weft sections of the fabric longitudinal and transverse cross-sections. Finally, the third group, the calculate group, contains all values that are calculated from the previous parameters, using formulas based on simple geometric considerations [22].

Table 2. Classification of geometric parameters

1. Known parameters	Number of fibres in the yarn, diameter of the fibre, yarn spacing, yarn count, stitch distance.
2. Measure parameters	The diameter of yarns, yarn tenacity, their deformation, yarn spacing, height of binding wave, the angle of the yarn axis (interlacing angle), the length of the yarn axis in the cross-section of the fabric, the crimp of yarns in the fabric, the real shape of the binding wave through the wave coordinates, and the fabric thickness.
3. Calculated parameters	The approximated binding wave and spectrum analysis for single layer and two layer stitched woven fabrics

4.1 Geometry of binding cell in plain weave for single and two layer woven fabric and parameters description of woven fabrics

The woven fabric is treated as an assembly of unit cells and the unit cell is the smallest repeating pattern in the structure. The plain fabric is created by the mutual interlacing of two set of threads. The manner of the mutual interlacing of threads defines the final structure of the fabric. The shape of the binding (crimp) wave and basic geometry of the binding cell changes according to the dimension and number of threads in the weave repeat [77]. The geometry of the binding cell is characterized by the following parameters and dimensions:

T_1 and T_2 = the yarn count for warp and weft yarn

D_1 and D_2 = setting of warp and weft threads

d_1, d_2 and d_s = yarn diameters for warp and weft and their mean diameter

A and B = the distances of warp and weft threads

e_1 and e_2 = relative waviness of warp and weft yarn in single layer woven fabrics

h_1 and h_2 = the heights of warp and weft binding waves in single layer woven fabrics

n_1 and n_2 = number of ends and picks in weave repeat

pp_1 and pp_2 = number of crossing parts in weave repeat in warp and weft direction

fl_1 and fl_2 = length of float part of warp and weft threads

The geometry of the binding point in the plain weaves, for the mathematical model used later, is based on the Brierley theory of the tight weave (Figure 13) [78]. A woven fabric in which warp and weft yarns do not have mobility within the structure as they are in intimate contact with each other are called jammed structures. In such structures the warp and weft yarns will have minimum thread spacing and their geometry is called limit geometry. These are closely woven fabrics and find applications in wind-proof, water-proof and bullet-proof requirements [47]. Whereas the structures other than limit are called looser structures, in which warp and weft yarn have some thread spacing and mobility within the structures. As we know that the simple woven fabric is produced by the interlacement of two set of threads (warp and weft), similarly when the conventional 2D weaving process is designed to interlace two orthogonal sets of yarns (warp and weft) with an additional set of yarns functioning as binder yarn or interlaced yarns in through the thickness or Z direction. Then it is referred to as multilayer weaving [79]–[84]. The two layer stitched woven fabric is composed of two layers of simple woven fabric and these layers are joined together by the interlaced or binder yarn. The limit, semi-loose and looser geometry of two layer stitched woven fabrics with plain weave have been derived from simple plain weave in single layer woven fabrics and it can be observed in Figure 14, Figure 15 and Figure 16 respectively.

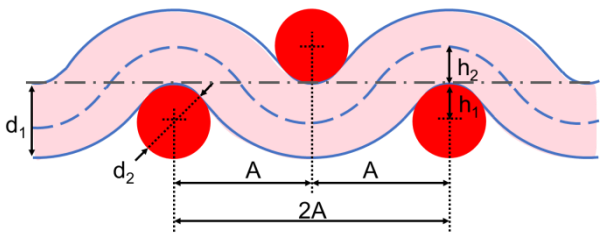

Figure 13. Limit geometry of single layer woven fabrics with plain weave

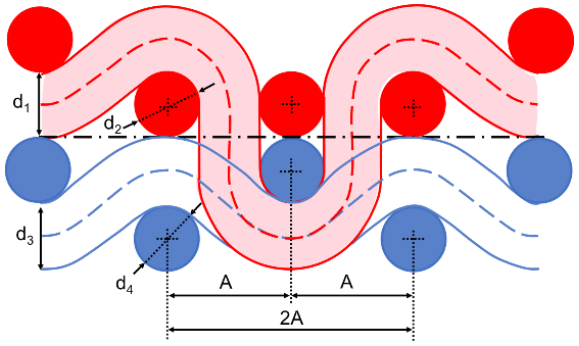

Figure 14. Limit geometry of two layer stitched woven fabrics with plain weave

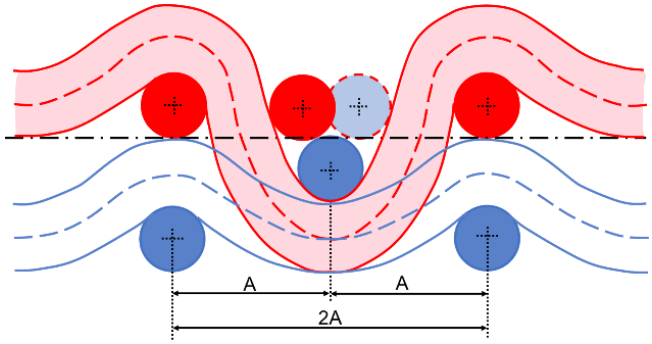

Figure 15. Semi-loose geometry of two layer stitched woven fabrics with plain weave (geometry between limit and loose)

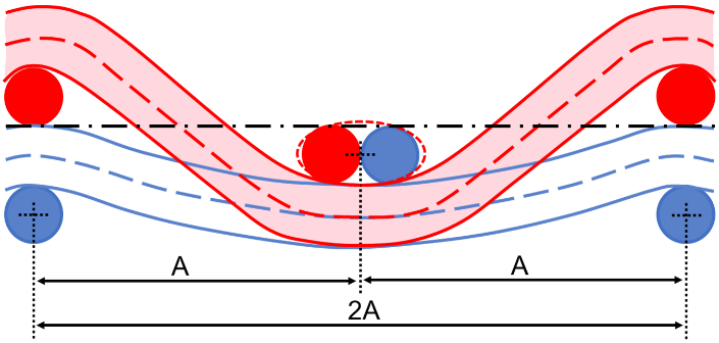

Figure 16. Looser geometry of two layer stitched woven fabrics with plain weave

The geometry of two layer stitched woven fabrics with plain weave can be divided into stitching and non-stitching section as shown in Figure 17. While the geometry of the binding cell for other than plain weaves can be derived from the plain weave as well. The looser interlacing of the fabric depends on the type of material being used and on the type of machine.

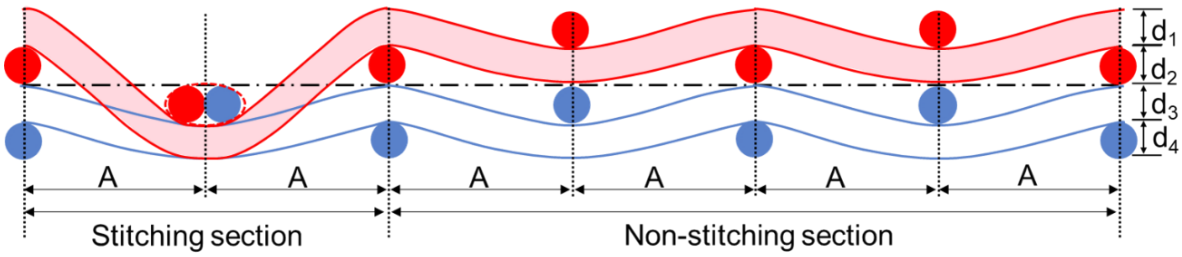

Figure 17. Geometry of two layer stitched woven fabrics with plain weave (stitched and non-stitched section)

The parameters which are necessary for the calculation of the binding waves are given below.

$$A = \frac{1}{D_1} \quad , \quad B = \frac{1}{D_2} \tag{2}$$

$$d_{1,2} = \sqrt{\frac{4.T_{1,2}}{\pi.\rho_{1,2}.\mu_{1,2}}} \tag{3}$$

$$d_s = \frac{d_1 + d_2}{2} \tag{4}$$

$$d_{effective} = d_s * g \tag{5}$$

Where 'g' is the constant of deformation obtained from experimental values of yarn cross-sectional diameter. The difference between the theoretical yarn diameter and the experimental diameter in the woven fabric has been obtained which gives us the value of constant 'g'. It can be used to obtain the effective diameter and as output for modelling of this type of structure and material.

The parameter (h_1 and h_2) height of binding waves can be determined on the basis of:

a. Experimental methods - from transverse and longitudinal cross-section of woven fabric by using image analyse, the real heights of the warp and weft crimp waves from fabric centre line can be obtained.
b. Theoretical methods – it is necessary to know effective diameter of threads and rate of warp and weft waviness e_1 and e_2, which can be used in equation (4) and equation (5) for determination of heights. The rate of thread waviness e_1 and e_2, can be estimated on the basis of individual phases of interlacing from Novikov work [85].

$$h_1 = e_1 \,.\, d_{effective}\,, \qquad h_2 = e_2 \,.\, d_{effective} \tag{6}$$

$$e_1 + e_2 = 1 \tag{7}$$

The distance between warp and weft yarn axis and $e_1 = e_2 = 0.5$ is given by equation (8). This equivalency is valid every time, independently to a theoretical model used.

$$h_1 + h_2 = (d_1 + d_2)/2 \tag{8}$$

4.2 Mathematical model for the description of binding wave by using Fourier series (FS)

The description of the shape of binding waves can be provided in the fabric, in the longitudinal cross-section (the shape of the binding wave of the warp thread) and in the transverse cross-section (the shape of the binding wave of the weft thread), to define the mutual position of the warp threads towards weft threads.

Due to spatial threads distribution in the cross-section of a cloth, the shape of the binding waves obtains the form which is near to the harmonic sinus course. That leads to the idea to approximate the binding wave by a sum of Fourier series (FS). For the weave of the fabric, as it is characteristic that the pattern of binding is repeated regularly (periodically) across the whole fabric width, and that it is continuous. The Fourier approximation respects this periodicity and shape of the binding wave, in the contrary to the above-mentioned models of single threads crossing. In our case of the periodically repeated pattern of thread waves, it means to substitute the binding wave by a system of sine curves with increasing frequencies (decreasing wavelengths), with different amplitudes and phase shifts. Apart from the approximated course, we also obtain the spectral characteristic of the course, by approximations using the sum of Fourier series. Spectral characteristic consists of amplitude and phase characteristics of individual wavelengths. The wavelengths are the whole fractions of the basic wavelengths of the pattern on the interval of the binding repeat (0, binding repeat).

For the creation of spectral characteristics of the repeat of binding in the longitudinal and transverse cross-sections, it is necessary first to describe the spectral characteristics of individual binding waves in the binding repeat in both the longitudinal as well as transverse cross-section. It has been said, that in the basic weaves, the interlacing of threads is identical in the longitudinal as well as in the transverse cross-section (using identical parameters of threads). This is not true for derived higher weaves or special weaves. The shapes of the

binding waves in the derived weaves are different in the longitudinal and transverse section. Resulting from individual sections, spectral characteristics of the repeat of the binding in the derived weaves will be different for the longitudinal and for the transverse cross-sections. The difference of individual spectral characteristics depends on the number of threads (binding waves) in the binding repeat and on their mutual interlacing.

The shape of the binding wave or its course can be possibly obtained by two methods:

4.2.1 FS approximation of binding wave (theoretical general description of model)

There is a tendency to avoid labored and tardy procedure of the creation of the cross-sections experimentally. The values of the course of one binding wave will be obtained by substitution of the wave shape by a well-known analytic function $f(x)$ (linear, circular, parabolic, hyperbolic, etc.), or created by a sum of functions defined on the specified interval 'T'. The interval is given by the width of the repeat of binding.

For a function $f(x)$, periodic on an interval $[0, T]$, the Fourier series of a function $f(x)$, is given by.

$$f(x) = \frac{a_0}{2} + \sum_{n=1}^{\infty} a_n \cos\left(\frac{n.2.\pi.x}{T}\right) + \sum_{n=1}^{\infty} b_n \sin\left(\frac{n.2.\pi.x}{T}\right) \tag{9}$$

Where the coefficients are,

$$a_0 = \frac{2}{T}\int_0^T f(x)\,dx \tag{10}$$

$$a_n = \frac{2}{T}\int_0^T f(x).\cos\left(\frac{n.2.\pi.x}{T}\right)dx \qquad (n = 0,1,2,\dots) \tag{11}$$

$$b_n = \frac{2}{T}\int_0^T f(x).\sin\left(\frac{n.2.\pi.x}{T}\right)dx \qquad (n = 1,2,3,\dots) \tag{12}$$

During the modelling and searching for certain dependencies, it is necessary to consider the equilibrium between the efficiency of the used model and its accuracy to the expressed parameter. This model has been extended for single layer and two layer stitched woven fabrics and explained further.

A) Modelling of binding wave of single layer plain woven fabric cross-section

Mathematical expression of geometry of binding wave using Fourier series - construction of structure of woven fabric of single layer of plain woven fabric geometry

Modelling of central line of threads in cross-section in woven fabric is based on Fourier series. For mathematical definition of binding wave, in this case as an input function f(x) in Fourier series, it is possible to use different mathematical shapes like linear, circular arc, parabolic, hyperbolic, sine or rectangular description [20]. Based on literary research [63] [86], [87] for mathematical modelling of binding wave using the Fourier series, it is sufficient that the simplest description of the central line of the binding wave is given by the linear description by means of two straight lines as shown in Figure 18 for single layer woven fabric. This description is applicable in every interlacing of basic weaves as well as of higher derived weaves. It allows the evaluation of the warp and weft threads in the interlacing. In the case of single layer plain weave, it represents the weaving with the simplest interlacing, therefore, only two different interlacing threads appear in the binding repeat along the longitudinal and transverse cross-sections.

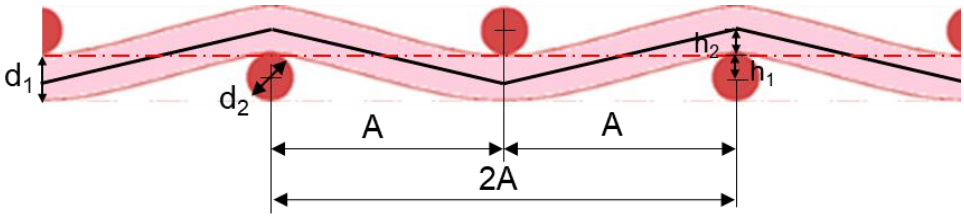

Figure 18. Geometry and graphical illustration of linear description of central line of thread in cross-section of single layer woven fabrics with plain weave

For the approximation of a single layer woven fabric by a partial sum of FS with straight lines description of central line of the binding wave, the period of the periodic function has been taken as $P = T = 2A$ in single layer woven fabrics and parameters mentioned below have been taken.

$$h_2 = 59\ \mu m, \qquad A = 1220 \mu m, \qquad d_s = 280\ \mu m, \qquad g = 0.6$$

The equations of the linear functions were used in the Fourier equations to find the coefficients a_0, a_n and b_n. The final equations are;

$$a_0 = \frac{2}{T}\left[\int_0^A (k.x + h_2)\,dx + \int_A^{2A} (-k.(x-A) - h_2)\,dx\right] \quad (13)$$

$$a_n = \frac{2}{T}\left[\int_0^A (k.x + h_2)\,cos\left(\frac{n.2.\pi}{T}x\right)dx + \int_A^{2A} (-k.(x-A) - h_2)\,cos\left(\frac{n.2.\pi}{T}x\right)dx\right] \quad (14)$$

$$b_n = \frac{2}{T}\left[\int_0^A (k.x + h_2)\,sin\left(\frac{n.2.\pi}{T}x\right)dx + \int_A^{2A} (-k.(x-A) - h_2)\,sin\left(\frac{n.2.\pi}{T}x\right)dx\right] \quad (15)$$

Where k is the slope of the linear function in single layer plain woven fabric. It can be calculated by the general formula to calculate the slope of linear function as described by the Figure 19 and given in equation (16) for first linear function.

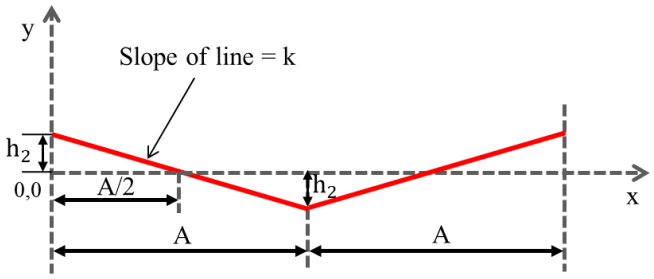

Figure 19. Graphical illustration of linear description of single layer woven fabric

$$k = \frac{change\ in\ y}{change\ in\ x} = \frac{\Delta y}{\Delta x} = -\frac{h_2}{A/2} = -\frac{2.h_2}{A} \quad (16)$$

The final approximation function is,

$$F_\alpha(x) = \frac{a_0}{2} + \sum_{n=1}^{\alpha} a_n\,cos\left(\frac{n.2.\pi}{T}x\right) + \sum_{n=1}^{\alpha} b_n\,sin\left(\frac{n.2.\pi}{T}x\right) \quad (17)$$

$$(where, \alpha = 1,2,3,\dots)$$

By applying Fourier approximations, it changes the shape and gives us the shape which is comparable to the real shape of binding wave. The FS approximation and spectral characteristics of a single layer woven fabric can be observed in Figure 20. First and second binding wave in the binding of the plain weave is identically. The binding wave in a repeat form the spectral characteristic, which evaluates the given course of the binding wave regarding the geometry of binding wave, eventual deformation and random changes of the state of stress of the individual threads. The spectral characteristics (spectral characteristics of the binding waves) of the individual cross-sections and their possible differences between theoretical (idealised) characteristics and real characteristics will supposedly allow to find the

typical signs of the real weaving process (shuttles, shuttleless, multished weaving) and various transition processes connected with starting of the loom, transition to different bindings (borders), change of the tension of the threads in the interlacing etc. In the Figure 20b, the first harmonic component ($A1$) represents the amplitude of the first binding wave, while second harmonic component ($A2$) is the difference between first and second binding wave and as these are identical so the difference between them is zero. In the similar way, the difference between the other binding waves has been calculated which is continuously decreasing.

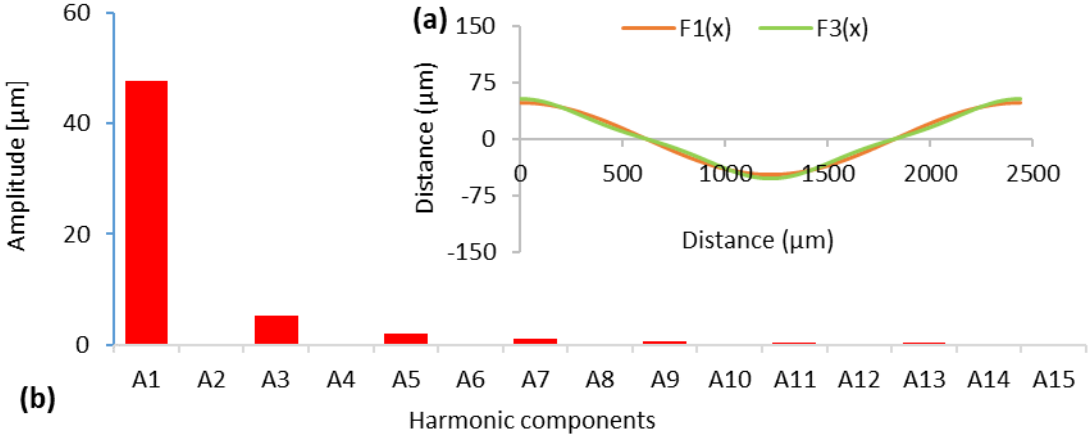

Figure 20. FS (a) approximation and (b) spectral characteristics of binding wave in cross-section of plain woven fabric

B) Modelling of influence of plain weave repeat in non-stitched part of binding wave of two-layer stitched woven cross-section

a. Mathematical expression and description of binding wave in two-layer stitched cross-section of woven fabric - construction of structure of woven fabric with minimum time plain weave repeat in non-stitching section

The geometry of two layer stitched woven fabrics with plain weave can be divided into stitching and non-stitching section as shown by upper binding wave in Figure 21. For regular repeat of the interlacing the minimum number of plain weave repeat in non-stitching section is one-time as given in figure. The linear description of the central line of the binding wave in two layer stitched woven fabric has also been illustrated in Figure 21. For the approximation of a two layer woven fabric by a partial sum of FS with straight lines description of central line of the binding wave, the period of the periodic function has been taken as $P = T = 4A$.

Some additional parameters have been described for the geometry of the binding cell of two layer stitched woven fabric as under.

h_{f^1} and h_{f^2} = the height of first warp and weft binding waves in two layer woven fabrics

h_{s^1} and h_{s^2} = the height of second warp and weft binding waves in two layer woven fabrics

e_{f^1} and e_{f^2} = relative waviness of first warp and weft yarn in two layer woven fabrics

e_{s^1} and e_{s^2} = relative waviness of second warp and weft yarn in two layer woven fabrics

h'_{f^2} = the height of first warp binding waves in two layer woven fabric in non-stitching section ($h_{f^2} \neq h'_{f^2}$)

$$h'_{f^2} = h_{f^2} - (h_1 + h_2) \tag{18}$$

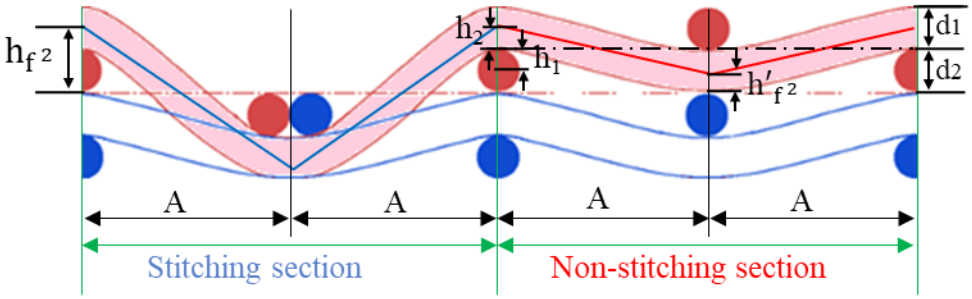

Figure 21. Geometry and graphical illustration of linear description of central line of thread in cross-section of two layer stitched woven fabrics with plain weave

The equations of the linear functions were used in the Fourier equations to find the coefficients a_0, a_n and b_n. There are four linear equations in these coefficients, the first two are for stitching section and the last two are for non-stitching section. The final equations are given by:

$$a_0 = \frac{2}{T}\left[\left(\int_0^A (k_1.x + h_{f^2})\,dx + \int_A^{2A} (-k_1.(x-A) - h_{f^2})\,dx\right) + \left(\int_{2A}^{3A} (k_2.(x-2A) + h_{f^2})\,dx + \int_{3A}^{4A} (-k_2.(x-3A) + h'_{f^2})\,dx\right)\right] \tag{19}$$

$$a_n = \frac{2}{T}\left[\left(\int_0^A (k_1.x + h_{f^2}) \cos\left(\frac{n.2.\pi}{T}x\right) dx + \int_A^{2A} (-k_1.(x-A) - h_{f^2}) \cos\left(\frac{n.2.\pi}{T}x\right) dx\right) + \left(\int_{2A}^{3A} (k_2.(x-2A) + h_{f^2}) \cos\left(\frac{n.2.\pi}{T}x\right) dx + \int_{3A}^{4A} (-k_2.(x-3A) + h'_{f^2}) \cos\left(\frac{n.2.\pi}{T}x\right) dx\right)\right] \quad (20)$$

$$b_n = \frac{2}{T}\left[\left(\int_0^A (k_1.x + h_{f^2}) \sin\left(\frac{n.2.\pi}{T}x\right) dx + \int_A^{2A} (-k_1.(x-A) - h_{f^2}) \sin\left(\frac{n.2.\pi}{T}x\right) dx\right) + \left(\int_{2A}^{3A} (k_2.(x-2A) + h_{f^2}) \sin\left(\frac{n.2.\pi}{T}x\right) dx + \int_{3A}^{4A} (-k_2.(x-3A) + h'_{f^2}) \sin\left(\frac{n.2.\pi}{T}x\right) dx\right)\right] \quad (21)$$

Where k_1 and k_2 are the slopes of the linear functions in two layer stitched woven fabrics in stitching and non-stitching sections respectively. The graphical illustration of linear description of two layer stitched woven fabric has been shown in Figure 22 to understand the calculation of slopes.

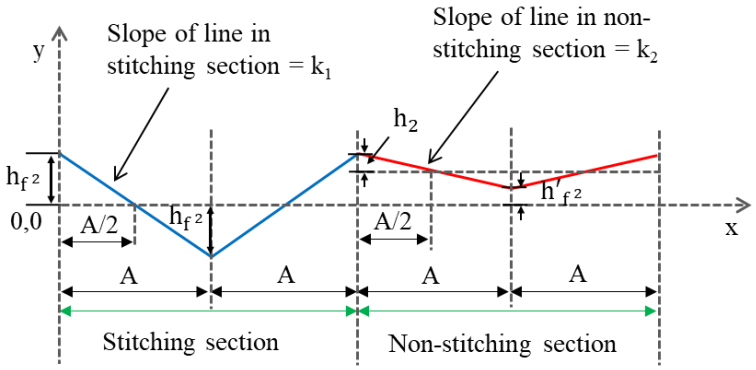

Figure 22. Graphical illustration of linear description of two layer stitched fabric

$$k_1 = -\frac{h_{f^2}}{A/2} = -\frac{2.h_{f^2}}{A} \quad (22)$$

$$k_2 = -\frac{h_2}{A/2} = -\frac{2.h_2}{A} \quad (23)$$

The final approximation function is,

$$F_\alpha(x) = \frac{a_0}{2} + \sum_{n=1}^{\alpha} a_n \cos\left(\frac{n.2.\pi}{T}x\right) + \sum_{n=1}^{\alpha} b_n \sin\left(\frac{n.2.\pi}{T}x\right) \quad (24)$$

$$(where, \alpha = 1,2,3,\dots)$$

The FS approximation and spectral characteristics of two layer stitched woven fabric can be observed in Figure 23. This approximation is for both sections of two layer woven fabric and it can be observed in spectral characteristics that after certain number of intervals ($A3$) we get a better approximation for two layer stitched woven fabric.

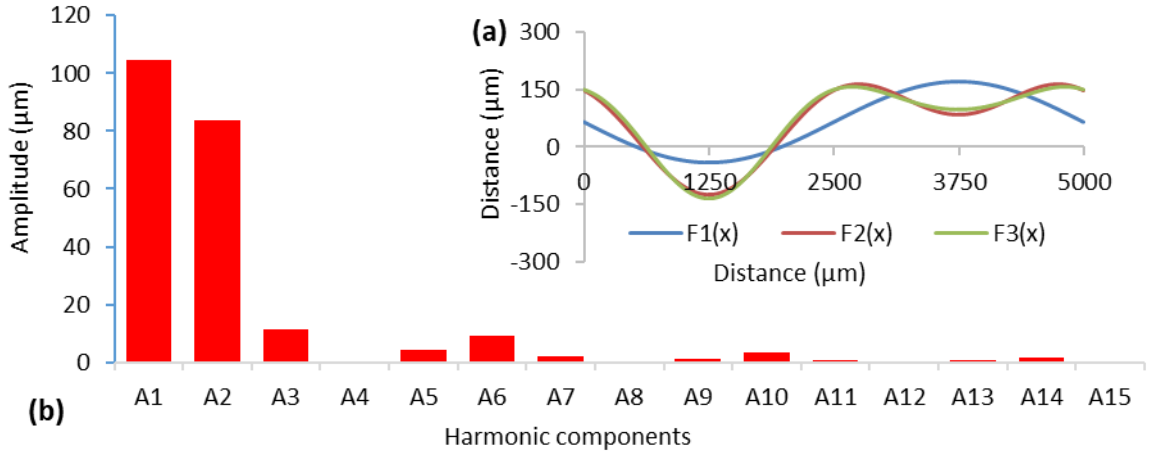

Figure 23. FS (a) approximation and (b) spectral characteristics of stitched binding wave in cross-section of two layer plain woven fabric with minimum time plain repeat

b. Mathematical expression and description of binding wave in two-layer stitched cross-section of woven fabric - Construction of structure of woven fabric with maximum (j) time plain weave in non-stitching section

If we have more number of plain weave repeats in non-stitching section, then we can illustrate the geometric description accordingly and the equation for FS will be different. Suppose we have 'N' number of times of plain weave in non-stitching section (Figure 24). In this case the equation for non-stitching section will be the sum of 'N' number of times of plain repeat.

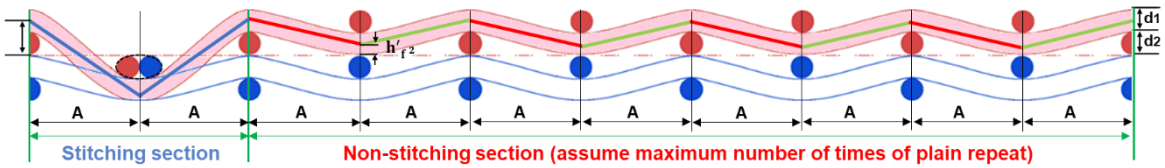

Figure 24. Graphical illustration of linear description of central line of thread in cross-section of two layer stitched woven fabrics with plain weave (assuming it maximum time)

The equations of the linear functions will be used in the Fourier equations to find the coefficients a_0, a_n and b_n. It is explained in the final equations given below:

$$a_0 = \frac{2}{T}\left[\left(\int_0^{A}\left(k_1.x + h_{f^2}\right)dx + \int_A^{2A}\left(-k_1.(x-A) - h_{f^2}\right)dx\right) + \left\{\left(\int_{(j)A}^{(j+1)A}\left(k_2.(x-j.A) + h_{f^2}\right)dx\right) + \int_{(l)A}^{(l+1)A}\left(-k_2.(x-l.A) + h'_{f^2}\right)dx\right\}\right] \tag{25}$$

Where, $j = 2,4,6,\ldots, number\ of\ repeats\ (only\ even\ numbers)$

and $l = 3,5,7,\ldots, number\ of\ repeats\ (only\ odd\ numbers)$

$$a_n = \frac{2}{T}\left[\left(\int_0^{A}\left(k_1.x + h_{f^2}\right)cos\left(\frac{n.2.\pi}{T}x\right)dx + \int_A^{2A}\left(-k_1.(x-A) - h_{f^1}\right)cos\left(\frac{n.2.\pi}{T}x\right)dx\right) + \left\{\left(\int_{(j)A}^{(j+1)A}\left(k_2.(x-j.A) + h_{f^2}\right)cos\left(\frac{n.2.\pi}{T}x\right)dx\right) + \int_{(l)A}^{(l+1)A}\left(-k_2.(x-l.A) + h'_{f^2}\right)cos\left(\frac{n.2.\pi}{T}x\right)dx\right\}\right] \tag{26}$$

$$b_n = \frac{2}{T}\left[\left(\int_0^A (k_1.x + h_{f^2}) \sin\left(\frac{n.2.\pi}{T}x\right) dx + \int_A^{2A} (-k_1.(x-A) - h_{f^2}) \sin\left(\frac{n.2.\pi}{T}x\right) dx\right) + \left\{\left(\int_{(j)A}^{(j+1)A} (k_2.(x-j.A) + h_{f^2}) \sin\left(\frac{n.2.\pi}{T}x\right) dx\right) + \int_{(l)A}^{(l+1)A} (-k_2.(x-l.A) + h'_{f^2}) \sin\left(\frac{n.2.\pi}{T}x\right) dx\right\}\right] \quad (27)$$

Where k_1 and k_2 are the slopes of the linear functions as calculated in equation (22) and (23). The final approximation function is,

$$F_\alpha(x) = \frac{a_0}{2} + \sum_{n=1}^{\alpha} a_n \cos\left(\frac{n.2.\pi}{T}x\right) + \sum_{n=1}^{\alpha} b_n \sin\left(\frac{n.2.\pi}{T}x\right) \quad (28)$$

$$(where, \alpha = 1,2,3,\dots)$$

The FS approximation and spectral characteristics of two layer stitched woven fabric can be observed in Figure 25. It has been divided in two sections, the first section I the approximation of the stitching portion of a woven fabric while the second section is the approximation of non-stitching portion of two layer stitched woven fabric. It can be observed that approximation of non-stitching section can be continuous up to next stitching point.

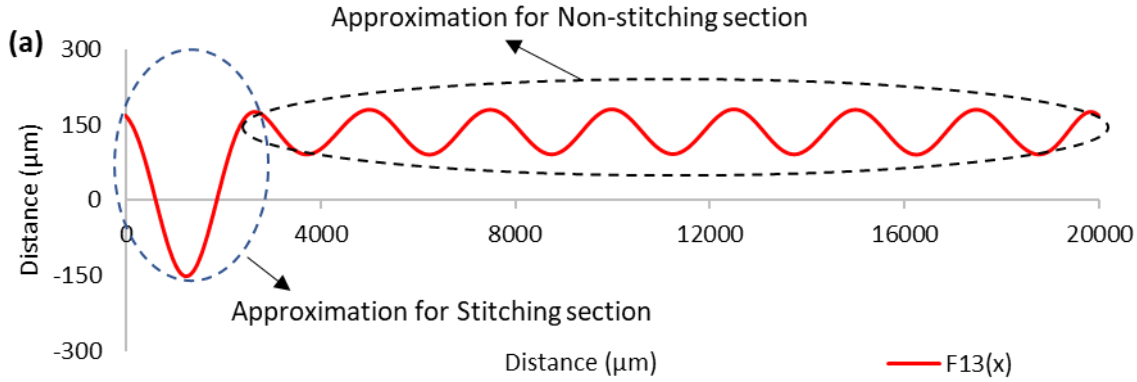

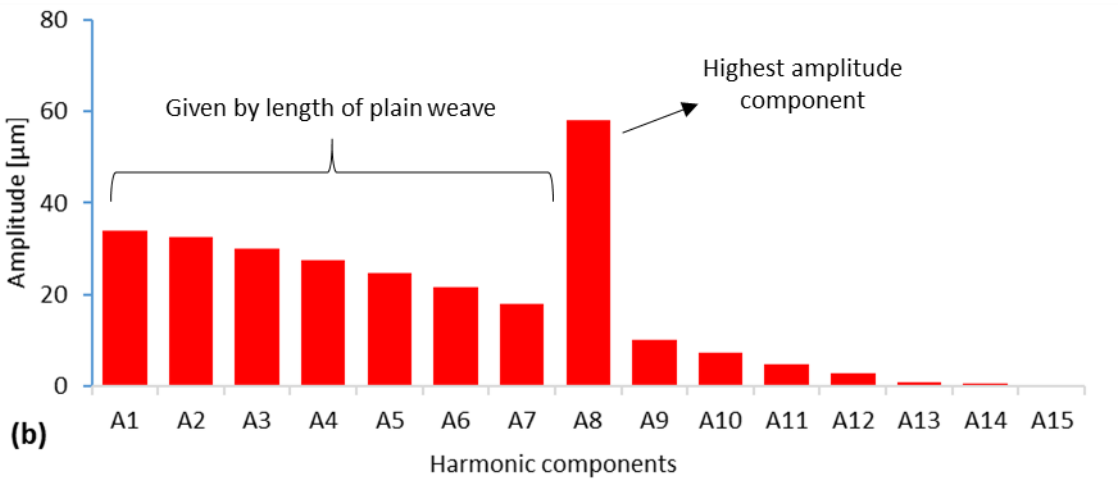

Figure 25. FS (a) approximation and (b) spectral characteristics of stitched binding wave in cross-section of two layer plain woven fabric with maximum time plain repeat

Whereas in spectral analysis we can observe two parts, the first part is before higher amplitude component and second is after it. The first part is given by the length of the plain weave and it depends on number of plain weave in non-stitching section. In the second part we can observe the maximum amplitude at (A8), because in this case we have seven repeats of plain weave (n=7) in non-stitching section. After this highest amplitude the approximated crimp wave holds good with the sample crimp wave. So, it can be concluded that when the repeat size is increasing, the number of binding waves required to get a better approximation as per woven structure are also increasing, hence the repeat size is directly proportional to the number of harmonic components.

4.2.2 Mathematical expression and description of real binding wave using Fourier series (experimental analyses of binding wave in cross-section of woven fabric)

It is the approximation of the whole binding wave course obtained experimentally by a partial sum of Fourier series (harmonic synthesis). The series is given by the table of equidistant co-ordinates which will be obtained from the real fabric (real longitudinal and transverse cross-sections) by the visual analysis.

The basic parameters of binding wave in real conditions are detected based on image analysis (using the software NIS elements as shown in Figure 26), which are needed to obtain the coefficient of Fourier series, i.e. a_0, a_n and b_n.

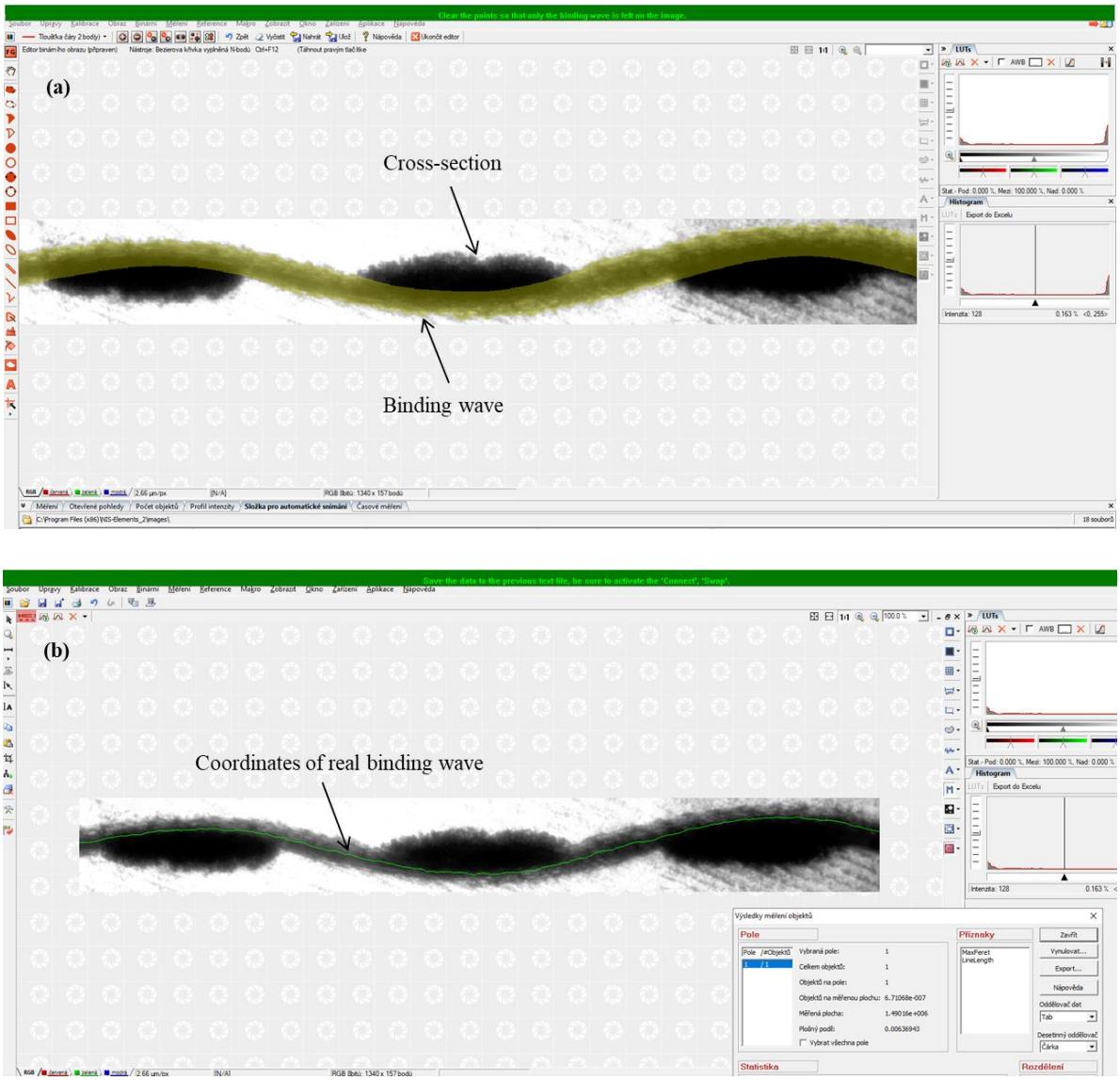

Figure 26. Single layer plain woven fabric with its (a) real cross-section, binding wave and (b) individual coordinates of binding wave (image analysis software NIS element)

The period of the periodic function can be taken as $P = T$, which is the total length of the periodic wave. The coefficients of FS are;

$$a_0 = \frac{2}{m}\,(y_i) \tag{29}$$

$$a_n = \frac{2}{m}\sum_{i=1}^{m}\left[y_i.cos\left(\frac{n.2.\pi.i}{m}\right)\right] \tag{30}$$

$$b_n = \frac{2}{m}\sum_{i=1}^{m}\left[y_i.sin\left(\frac{n.2.\pi.i}{m}\right)\right] \tag{31}$$

Where

m = number of Intervals $(0, T)$

y_i = function value of course at a given point x_i $\quad (x_i = x + ih; \quad h = \frac{T}{m}; \quad i = 0, \ldots, m)$,

n = harmonic component.

The application of Fourier transformation enables to find the wavelength and phase angle of crimp wave as well. For individual components amplitude and phase shift pays the same relationship as in the case of normal equation and are given by;

$$A_n = \sqrt{(a_n)^2 + (b_n)^2} \tag{32}$$

$$\phi_n = atan(\frac{b_n}{a_n}) \tag{33}$$

The final approximation function is;

$$T_\alpha(x) = \frac{a_0}{2} + \left[\sum_{n=1}^{\alpha} A_n \, sin\left(\frac{n.2.\pi}{T}x + \phi_n\right)\right] \qquad (where, \alpha = 1,2,3,\ldots) \tag{34}$$

The FS approximation and spectral characteristics using above equations of a single layer stitched woven fabric can be observed in Figure 27. It can be observed that approximation performed by FS is in accordance with the experimental binding wave. The spectral characteristics obtained by experimental FS analysis can be compared with the spectral characteristics obtained by theoretical FS analysis.

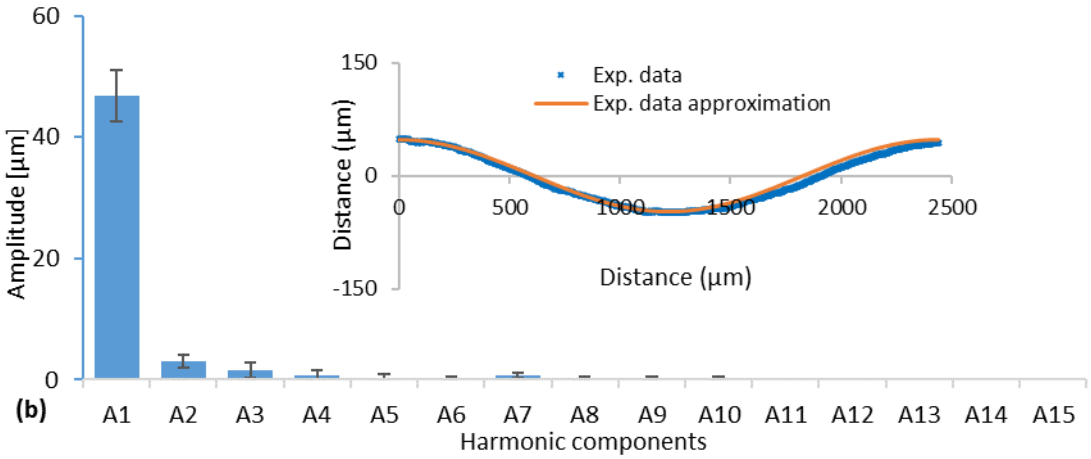

Figure 27. FS (a) approximation and (b) spectral characteristics of binding wave obtained from real fabric (experimental analyses of binding wave of plain woven fabric)

5. MATERIAL AND METHODS

5.1 Materials

Basalt 66x2 Tex continuous multifilament plied twisted yarn was used as a raw material. The plied twisted yarn with small number of twist has been used to avoid fibrillation during weaving of multifilament yarn. Sample weaving loom (CCI SL-7900) was used to make the woven structures, keeping same yarn count in warp and weft. All other parameters like weft insertion speed and warp tension was kept the same for all fabric samples. Woven samples were produced with different pick density, stitch distance, weave and number of layers, according to the experimental plan shown in Table 3 [88]. The sample B1-B3 are single layer woven structures with plain weave and B4-B7 are two layer stitched woven structures. The plain weave was selected to validate the theoretical model described earlier as plain weave is the simplest of all weaves and interlacing pattern is identical in longitudinal and transverse cross-section. The basic fabric structures for single layer and two layer stitched woven fabrics are shown in Figure 28. Yarns were kept in a conditioning room for 24 hours at standard temperature (20±2°C) and relative humidity (65±2%) before yarn testing and fabric production.

Table 3. Construction parameters of woven fabrics

Sample code	Ends/cm	Picks/cm	Design
B1	8.1	6.5	Single layer plain weave
B2	8.1	8.5	Single layer plain weave
B3	8.1	10.8	Single layer plain weave
B4	16.2	18.2	Two layer stitched plain weave (S.D.= 0.5 x 0.5)
B5	16.2	18.2	Two layer stitched plain weave (S.D.= 1x1)
B6	16.2	18.2	Two layer stitched plain weave (S.D.= 1x1.5)
B7	16.2	18	Two layer stitched plain weave (S.D.= 1x2)

*B = Basalt, S.D. = stitch distance (cm)

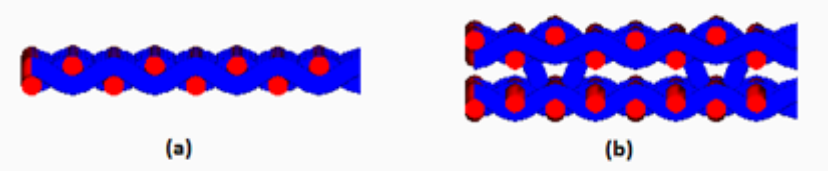

Figure 28. (a) Single layer plain woven fabric, (b) Two layer stitched plain woven fabric

5.2 Methodology

The standard test methods for evaluation of different parameters fiber fineness, fiber force and elongation, yarn fineness, yam force and elongation, yarn diameter, yarn twist, yarn cross-section has been described as under.

5.2.1 Fiber testing

Tensile force, elongation, titre and tenacity of Basalt fibers were measured on Vibroskop-400 by LENZING Instruments Austria according to the standard test method ISO 1973:1995 [89]. A total of fifty measurements were made. The gauge length was 20 mm and force was applied at a rate of 10 mm / min. The stress-strain curves and data for filament fibers was obtained from the equipment software which was used to produce mean curve for both fibers. The test setup for tensile testing of fibers is shown in Figure 29. The stress-strain curves data has been shown in Appendix A, whereas the fibers specifications are shown in Table 4.

Figure 29. Test setup for tensile testing of Basalt and Glass fibers

5.2.2 Yarn testing

The tensile properties of Basalt yarn were tested using TIRA 2300 instrument as shown in Figure 30 in accordance with ASTM D885 [90]. The yarn was tested for the force and elongation at the corresponding speeds 100 mm / min and the gauge length being 250 mm for

both yarns. The individual raw stress-strain curves and breaking force and elongation for some samples of yarns is given in the Appendix A. A total of fifty tests were performed on yarn. The force and elongation were measured directly from the instrument. The individual raw stress-strain data of yarn was used to obtained average stress-strain curve using linear interpolation and Matlab software.

Yarn twist per meter was measured by MesdanLAB twist tester machine according to standard procedure ISO 2061:1995 [91]. Ten samples from specimen were tested and mean value of twist was determined. The twist meter used for measurement of twist is shown in Figure 31.

Figure 30. Test setup for tensile testing of Basalt and Glass yarns

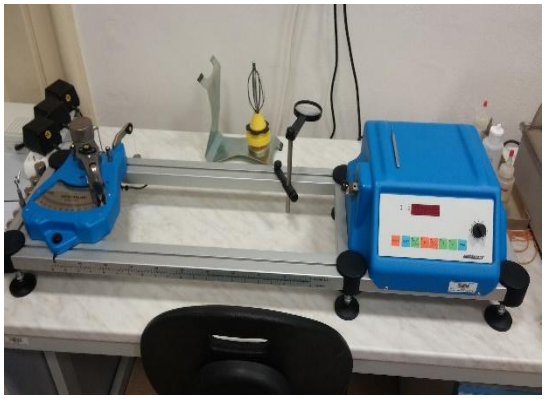

Figure 31. Test setup for yarn twist measurement

The yarn linear density was measured from a lea of one hundred meters according to standard test procedure ISO 1144:2016 [92]. Five samples of yarn were prepared on lea making machine and each sample was weighed in grams on weighing balance and yarn Tex was determined from average of five samples. The physical characteristics of Basalt yarn are presented in the Table 4.

Table 4. Basalt fiber and yarn properties

Parameters	Basalt fiber	Basalt yarn
Fineness (tex)	0.172	132
Diameter (um)	10	440

Tenacity (cN/tex)	96.97	46
Breaking strain (%)	3.66	2.96
Density (g/cm^3)	2.8	
Twist per meter	-	94

Yarn diameter was determined by longitudinal view method with the help of instrument as shown in the Figure 32 and Figure 33 in accordance to IS 22-102-01/01[93]. The longitudinal section is a section parallel to the direction of material output. To scan the yarn in tight state by a microscope, it is necessary to lead the yarn into the brakes of a bridge guide and then images of the yarn longitudinal views are captured using a microscope set on a lower exposure and an appropriate objective magnification. Three hundred observations were taken for determination of the mean diameter of yarn, at the recommended distance for scanning a random selection of yarn sections which is approximately 30cm. The image analysis of the yarn was performed by software LUCIA.

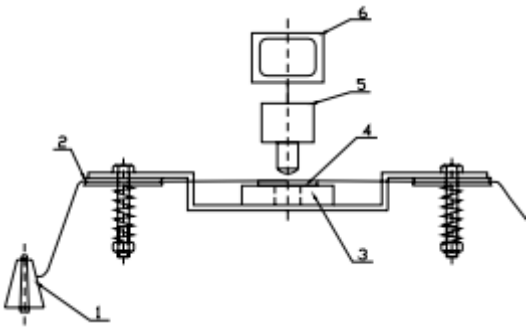

1 – bobbin with the yarn; 2 – disc brake; 3 – bridge gate; 4 – objective of the microscope; 5 – camera; 6 – PC

Figure 32. An order of the yarn image capturing [93]

Figure 33. Test setup for yarn diameter measurement

5.2.3 Cross-sectional image analysis

A) Yarn cross-sectional diameter

Cross-sectional diameter of yarn is usually considered as the diameter of the cylinder, where most of the fibers are concentrated [94]. The cross-section of yarn is a section perpendicular to the direction of the output material. Image analysis method was used to measure the cross-

sectional diameter of yarn. Ten yarn samples were randomly selected from yarn cone with cutting dimension of 15 cm. Afterwards, these were completely impregnated in a mixture of Epoxy and Hardener in 100:23 ratio under a relax condition. Then these samples were kept for first drying (pre-curing) for 24 hours. These fixed samples were put into tinny tubs having notch of 1 mm width and tub edges were sealed with the gluing tape to prevent the leakage of the mixture. After that epoxy resin was poured into these tubs and upon cooling of epoxy in the tubs, the samples were placed in the oven at 80^{o}c for 60 minutes (post curing) [95].

After the resin is fully cured, the hardened blocks were removed from the tub. The samples were polished with sanding papers (P320, P600, P1200, P2000 and P2500) and were cut (sliced) out with a diamond saw. The samples were analyzed by a scanning electron microscope (SEM), an optical microscope from Nikon which was later processed by LUCIA software to calculate the effective diameter of yarn. One section was obtained from each block.

B) Yarn cross-sectional shape in fabric

To measure the geometry of the yarn cross-section in fabric, 10 fabric samples were selected randomly from each fabric sample with cutting dimension of 10x10 cm. After that, the same procedure of impregnation in the epoxy mixture was done and pre-curing and post-curing was performed in the same way as performed for yarns earlier. The prepared hard bodies were then cut into pieces of 3 mm thickness in a manner that the cutter was perpendicular to the fabric surface and one group of either warp or weft ends to cut them vertically. This time samples were fixed into tinny tubs having notch of 4 mm. The epoxy resin was poured into these tubs and upon cooling of epoxy in the tubs, the samples were placed in the oven at 80^{o}c for 60 minutes (post curing). Later, the same procedure of slicing used for yarns was followed, while the real images has been taken using the projection microscope equipped with digital camera [95]. The real image is a term used for the image obtained from real pattern. The test procedure with all the steps involved for cross-sectional image analysis of woven fabric has been shown in Figure 34.

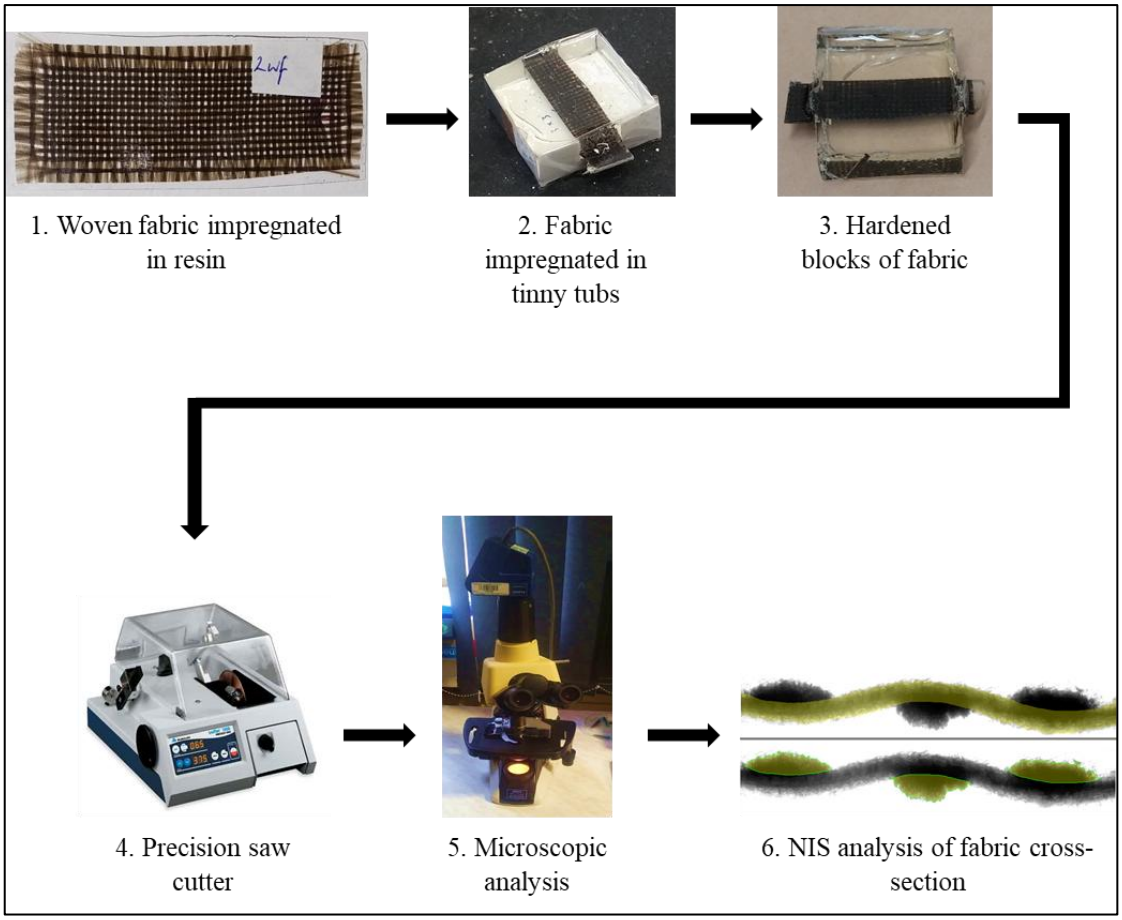

Figure 34. Method for cross-sectional image analysis of woven fabric

C) Image processing technique

The cross-sectional image analysis of the fabrics was performed by NIS Elements software in accordance with IS 46-108-01/01 [95]. The software is semi-objective based and uses specific macro for determination of image properties. The user intervention was adopted, and all necessary measurements were obtained stepwise from the fabric real image.

Before carrying out any test, calibration was done. Usually, micrometric scale is used for calibration of the given objective. The focusing is provided and the scale divisions of the image are attached to the real values. It is essential to apply calibration for the used zoom of the microscope before carrying out any measurements. The input of the macro is colored image of fabric longitudinal and transverse cross-section, this real image has been processed and transformed to binary system (grey structure), in which we are able to analyze easily where are the fibers in the picture. The test procedure has been showed in Figure 35.

The preprocessing and image transformation was performed in a way that a series of operations was carried out on the image in the sense of elimination of noise to make it more readable, and then the required part of the image was selected for further processing (binary image). The binary image is expressed in gray scale as combination of 0 (black color) and 1 (white color). The binary image comprises the main features of the real image i.e., contours from which it is possible to measure the image as a function of area, length, perimeter, center of gravity, etc.

Binary transformation was obtained by image thresholding and interactive tracing of contours or points of the image. The contour of fiber cross-section refers to that line, which creates the outline of the image of the fiber cross-section on the background. Then after that the boundary of the image was selected for the measurement of length and width. Later, the bending wave was overlaid first and then the cross-sections were overlaid and measured. The center and boundary points of the cross-sections were also measured in the next step. The output of the macro is a text file, in which all the readings of stepwise measurement are indicated.

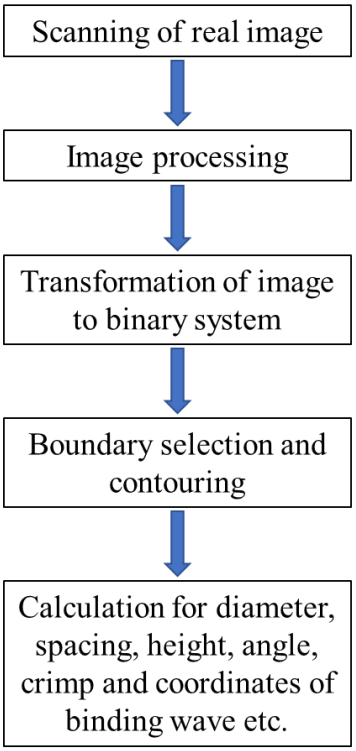

Figure 35. Test procedure for image processing by NIS element software

5.2.4 Shape of yarn in cross-section of woven fabric

Shape (roundness) is a factor which can influence the appearance of the end product of the yarn. Spinning methods have an immediate effect on the shape and density of yarns [96]. It is the ratio of short to long axis of ellipse (circular = 1). Initially the yarn cross-section is assumed to be circular with diameter *'d'* and incompressible, which becomes a flattened shape after being woven into fabric, due to different stresses on it as shown in Figure 36. After deformation it has the shape having the yarn width (major diameter, in a plane parallel to the fabric surface) *'a'* and yarn height (minor diameter, in a plane perpendicular to fabric surface) *'b'*, and usually $a > d$ and $b < d$. It is supposed that the yarn axis is in the middle of *'a'* and *'b'* and may be specified by the equation given below [60].

$$\frac{x^2}{a^2} + \frac{y^2}{b^2} = 1 \tag{35}$$

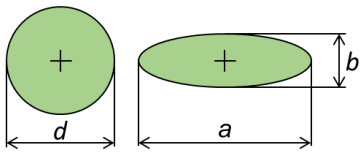

Figure 36. Geometry of yarn cross-section

To calculate the shape factor of the yarn cross-section, the major diameter (*a*) of yarn in the plane approximately parallel to the fabric surface and minor diameter (*b*) of yarn in the plane approximately perpendicular to the fabric surface of the elliptical yarn, were measured in each image as shown in Figure 37 [97].

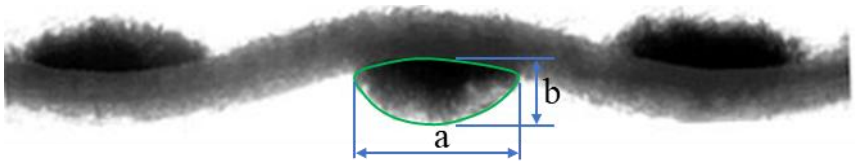

Figure 37. Measuring method of yarn cross-section

6. RESULTS AND DISCUSSIONS

6.1 Cross-sectional image analysis of woven fabrics

In the Figure 38 the basalt woven fabric impregnated in resin can be observed while the segmented cross-sectional image of a woven fabric (B1) can be seen in Figure 39. It is possible to measure the geometry of the individual fabric cross-section; the diameter of yarns, their deformation, yarn spacing, height of binding wave, the angle of the yarn axis (interlacing angle), the length of the yarn axis in the cross-section of the fabric, the crimp of yarns in the fabric, the real shape of the binding wave through the wave coordinates, and the fabric thickness.

Figure 38. Basalt woven fabric impregnated in resin

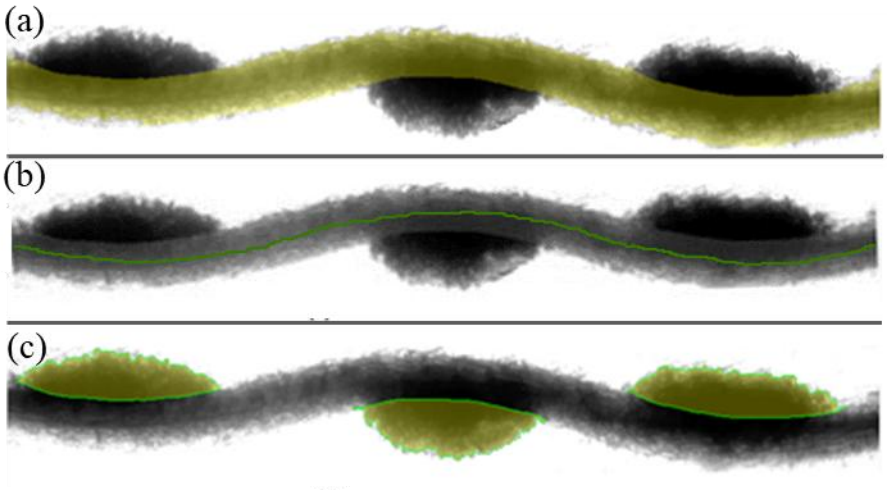

Figure 39. Cross-sectional image of a segmented woven fabric (B1) in NIS software – Overlay image of (a) binding wave, (b) coordinates of center line of binding wave and (c) cross-sections

The binding wave data of ten samples for each fabric type were obtained and the central line of the average binding wave was calculated. The average binding wave can be seen in Figure 40 for fabric sample (B1). Similarly, in Figure 41, the average cross-sections of fabric sample (B1), can be seen along with the individual coordinates of the binding wave, the central line of fabric, the minimum and maximum diameter of elliptical cross-sectional shapes, and the space between them. The outputs of the description of the warp and weft cross-sections are the geometrical parameters of the woven fabric, the binding wave, and the yarn cross-sections.

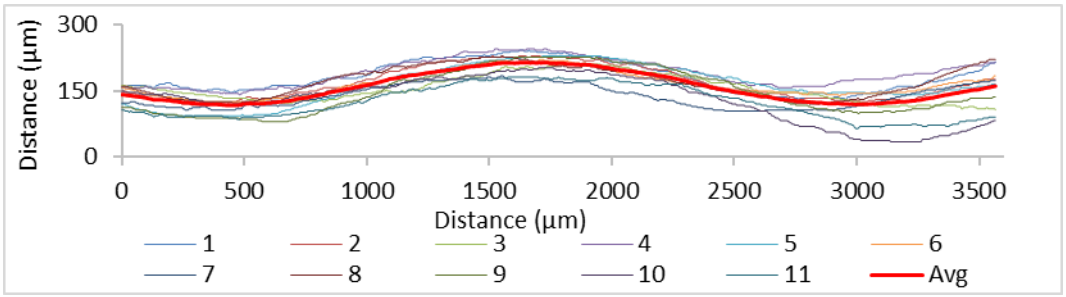

Figure 40. Average binding wave of a single layer fabric (B1) in transverse cross-section

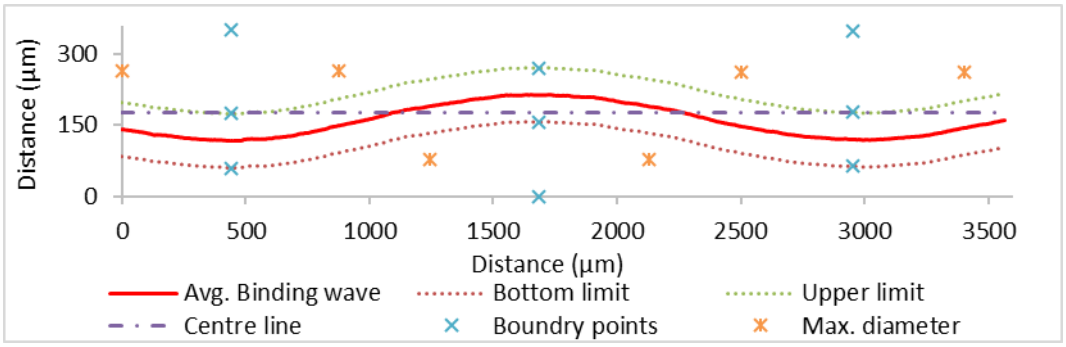

Figure 41. Cross-section of woven fabric (B1) with individual coordinates of binding wave, central line of fabric, and cross-sectional points

6.2 Evaluation of deformation of thread in cross-section of woven fabric

The shape of the binding wave and that of individual yarns in the cross-section of woven fabric can be evaluated from the real woven fabric. The shape of binding wave and yarn deformation changes based on fabric parameters like threads sett, weave and threads tension on the weaving loom, etc. Therefore, we can get bigger or smaller compression in comparison with diameter of free yarn (not woven). It is also possible to substitute the shape of yarn in the cross-section of woven fabric according to the models of yarn deformation which has been described earlier. The elliptical substitution of yarn (based on Pierce elliptical model) in the cross-sectional image of woven fabric can be seen in Figure 42 and it has been used to calculate the effective values of yarn diameter, which should be used later in Fourier analysis. It is not necessary to use Fourier series analysis for yarn cross-sections but for the binding wave in woven fabric. To analyze the yarn cross-section, it is necessary to use some other theories of prediction. The Fourier series is for periodic function which holds good for the binding wave analysis, while the yarn cross-section is the shape which is given by Pierce's, Kemp's, and Hearl's models.

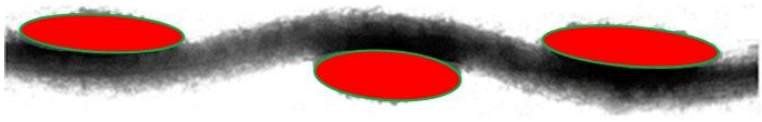

Figure 42. Elliptical substitution of the yarn cross-sectional shape in the cross-section of woven fabric

To study the effect of change in pick density on shape of binding wave and yarn cross-section, the major *(a)* and minor diameter *(b)* of elliptical shape of each woven fabric sample was measured and the results are shown in Figure 43. It can be observed in figure that major diameter *(a)* of weft yarn is greater than that of adjacent warp yarns, which means more flatness in weft yarns. The major diameter *(a)* is decreasing from (B1) to (B3) and minor diameter *(b)* is increasing for warp yarn, while it is opposite in case of weft yarns. As the pick density increases, the yarn height *(b)* for warp yarn increases which can result in higher crimp and waviness for the binding wave of weft yarn [98].

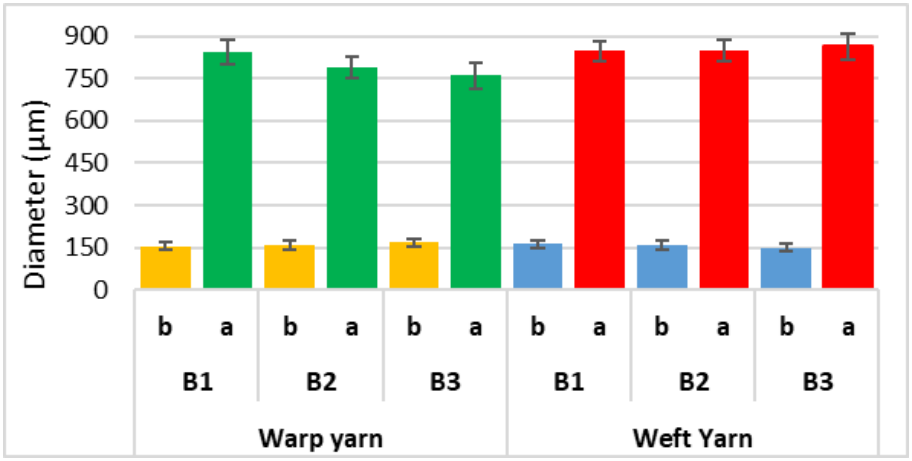

Figure 43. Effect of pick density on major and minor diameter of single layer woven fabrics

6.3 Approximation of binding wave of single layer basalt woven fabrics in cross-section using Fourier series

For the approximation of binding wave in cross-section in single layer of plain woven fabrics by a partial sum of FS with a linear description of the central line of the binding wave, the parameters required are given in Table 5. The linear descriptions of the binding wave in longitudinal and transverse cross-sections for fabric sample (B1) are shown in Figure 44.

Table 5. Input parameters for the mathematical modeling (sample B1)

Yarn count (Tex)	T	132	Height of warp from center (µm)	h_1	109
Warp yarn diameter (µm)	d_1	168	Height of weft from center (µm)	h_2	59
Weft yarn diameter (µm)	d_2	168	Density of warp yarns (1/cm)	D_1	8.15
Mean yarn diameter (µm)	d_s	168	Density of weft yarns (1/cm)	D_2	6.5
Warp yarn spacing (µm)	A	1220	Weft yarn spacing (µm)	B	1539

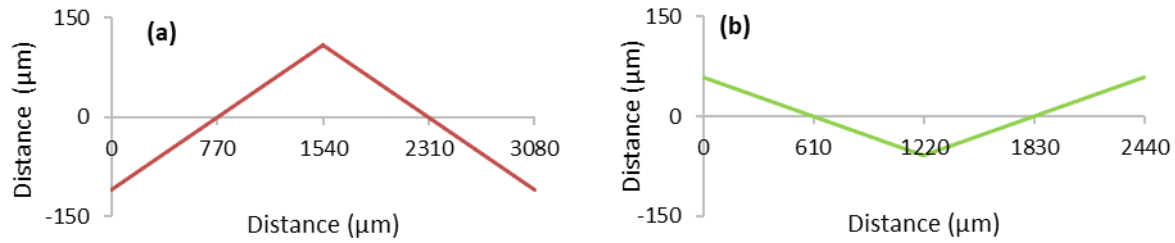

Figure 44. Graphical illustration of linear description of central line of thread in cross-section for sample (B1) in (a) longitudinal, and (b) transverse cross-section of woven fabric

The real cross-section for the sample (B1), its experimental binding waves and FS approximation using equation (34) along longitudinal cross-section can be observed in Figure 45. It can be observed that the approximation done by Fourier series fits well to the experimental binding wave. Each of the binding waves obtained by Fourier series (where $\alpha = 1,2,3,..$) has its spectral characteristic which evaluates the course of the binding wave in terms of geometry, eventual deformation and random changes resulted from the stress of individual threads. The spectral characteristics of the single layer fabric sample (B1) in longitudinal cross-section has been calculated using equation (32) and are also shown in Figure 45. First and second binding waves are identical in the longitudinal and transverse cross-sections. Similarly, the third and fourth binding waves are also identical and so on. The first harmonic component *(A1)* represents the amplitude of the first binding wave, while second harmonic component *(A2)* is the difference between first and second binding wave and as these are identical so the difference between them is zero. In the similar way, the difference between the other binding waves has been calculated which is continuously decreasing. The interlacing in the plain weave is the interlacing with the smallest binding repeat, with only two different interlacing threads in both cross-sections. The height of the first harmonic component *(A1)* also tells us about the deformation of binding wave in comparison with other fabrics. While the third component *(A3)* tells us about the rigidity of woven fabric, when the difference between second and third binding wave is high then this value is more. The higher value of the amplitude of *(A3)* means the fabric *(B1)* is more rigid in longitudinal cross-section. The FS approximation of average binding wave has been performed theoretically using equation (17) and experimentally using equation (34), while their spectral characteristics has been obtained using equation (32) and compared with each other given in Figure 45 as well. It can be observed that our predicted (theoretical) values obtained by Fourier model are close to experimental spectral characteristics values. The

difference is in the even number of harmonic components, which is not equal to zero in experimental values. Moreover, it has been observed that just by adding few number of sines and cosines series we can get a better approximation of binding wave. As the Fourier series is an expansion of a periodic function $F(x)$ in terms of an infinite sum of sines and cosines. In the figures $F_1(x)$ (orange line) is the sum of one term of Fourier series, while in $F_3(x)$ (green line) it is the sum of three terms of Fourier series to get better approximation.

Similarly, in Figure 46 and Figure 47 the real cross-sections, Fourier approximation and spectral characteristics of binding wave in longitudinal cross-section for fabric sample (B2) and (B3) can be observed as well. It can also be observed from the Figure 45 to Figure 47 that with the increase in pick density, the deformation in bending wave of warp yarn in longitudinal cross-section is consecutively increasing from (B1) to (B3), while the height of their crimp wave is continuously decreasing, which can also be observed with amplitude of the first harmonic component *(A1)*. The reason for this is that at high pick setting, the weft yarn gets less space to be flat and warp yarn more space, in fabric plane and hence, the binding wave of warp yarn attains more deformation.

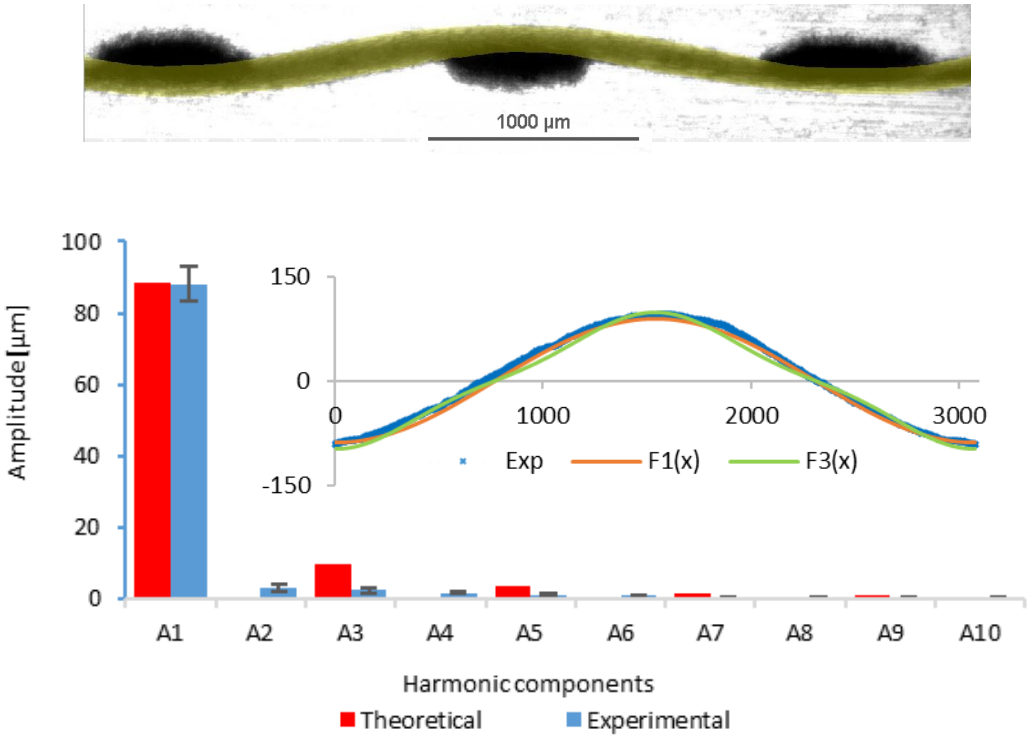

Figure 45. Cross-section of real binding wave of woven fabric, Fourier approximation and spectral characteristics of binding wave in longitudinal cross-section for fabric sample (B1)

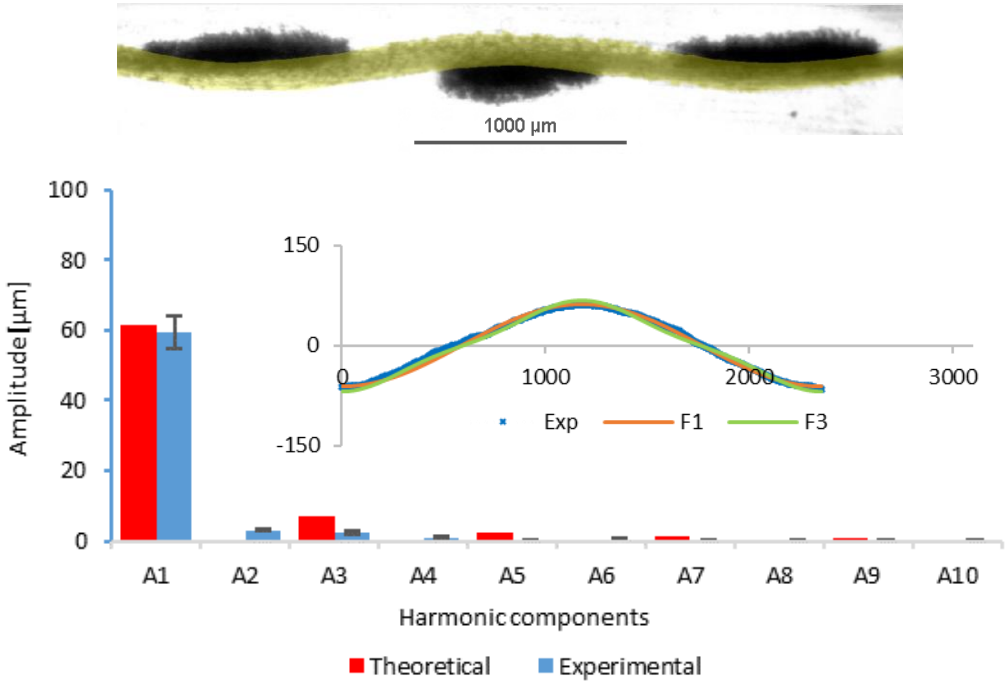

Figure 46. Cross-section of real binding wave of woven fabric, Fourier approximation and spectral characteristics of binding wave in longitudinal cross-section for fabric sample (B2)

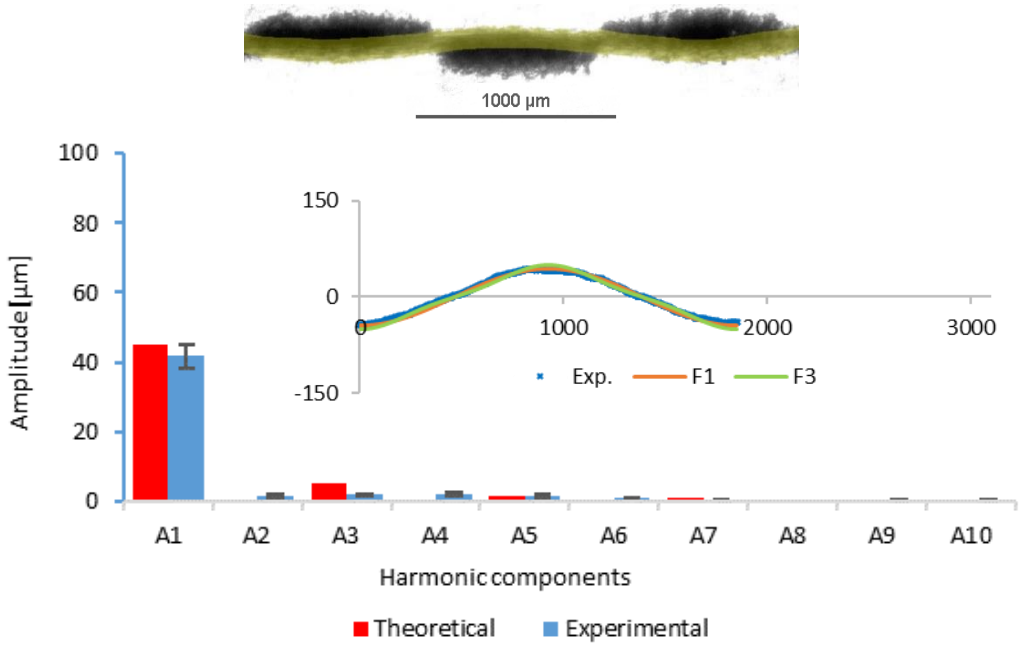

Figure 47. Cross-section of real binding wave of woven fabric, Fourier approximation and spectral characteristics of binding wave in longitudinal cross-section for fabric sample (B3)

The real cross-section for the sample (B1), its experimental binding waves and FS approximation using equation (34) along transverse cross-section can be observed in Figure 48. It can be observed that the approximation done by Fourier series fits well to the experimental binding wave. The difference in amplitude can be analyzed as well, the deformation in transverse cross-section (binding wave of weft) is more as compared to deformation in longitudinal cross-section (binding wave of warp). The spectral characteristics of fabric sample (B1) in transverse cross-section has been calculated using equation (32) and are shown in Figure 48 as well.

Similarly, in Figure 49 and Figure 50 the real cross-sections, Fourier approximation and spectral characteristics of binding wave in transverse cross-section for fabric sample (B2) and (B3) can be observed as well. It can also be observed from the Figure 48 to Figure 50 that with the increase in pick density, the deformation in bending wave of weft yarn in transverse cross-section is consecutively decreasing from (B1) to (B3), while the height of their crimp wave is continuously increasing, which can also be observed with amplitude of the first harmonic component *(A1)*. This is because, at low pick setting, the weft yarn gets more space to be flat in fabric plane and hence, its binding wave attains more deformation.

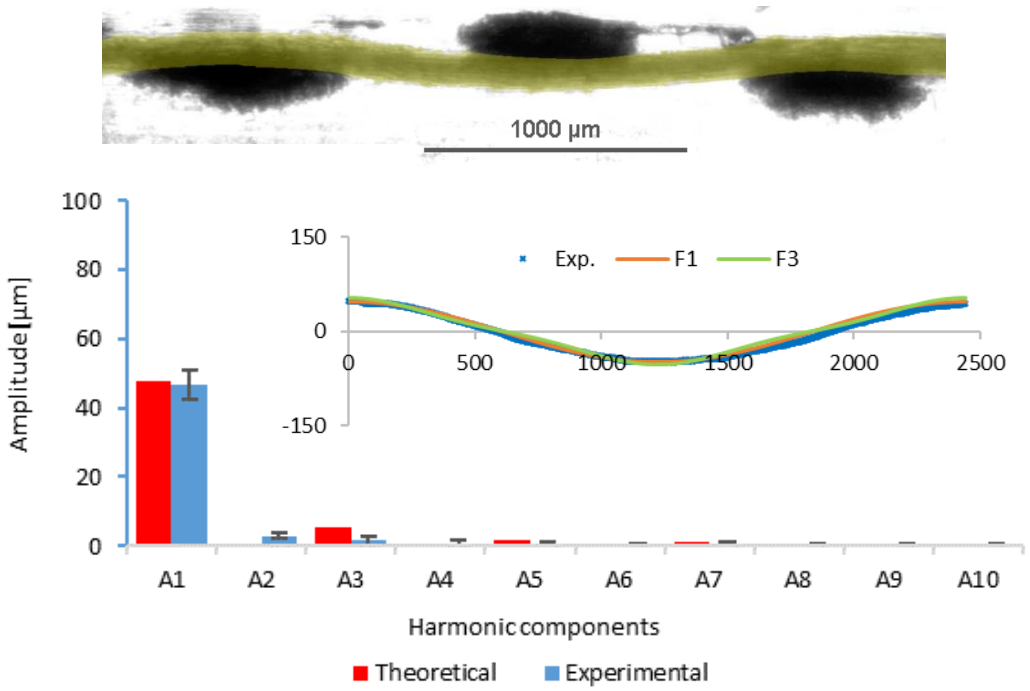

Figure 48. Cross-section of real binding wave of woven fabric, Fourier approximation and spectral characteristics of binding wave in transverse cross-section for fabric sample (B1)

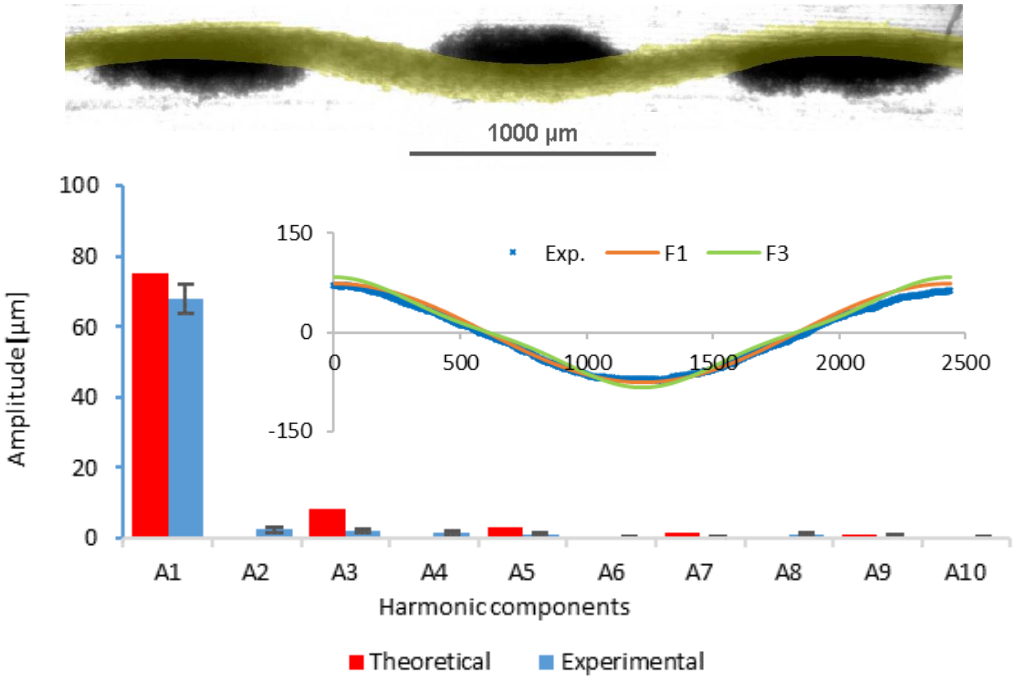

Figure 49. Cross-section of real binding wave of woven fabric, Fourier approximation and spectral characteristics of binding wave in transverse cross-section for fabric sample (B2)

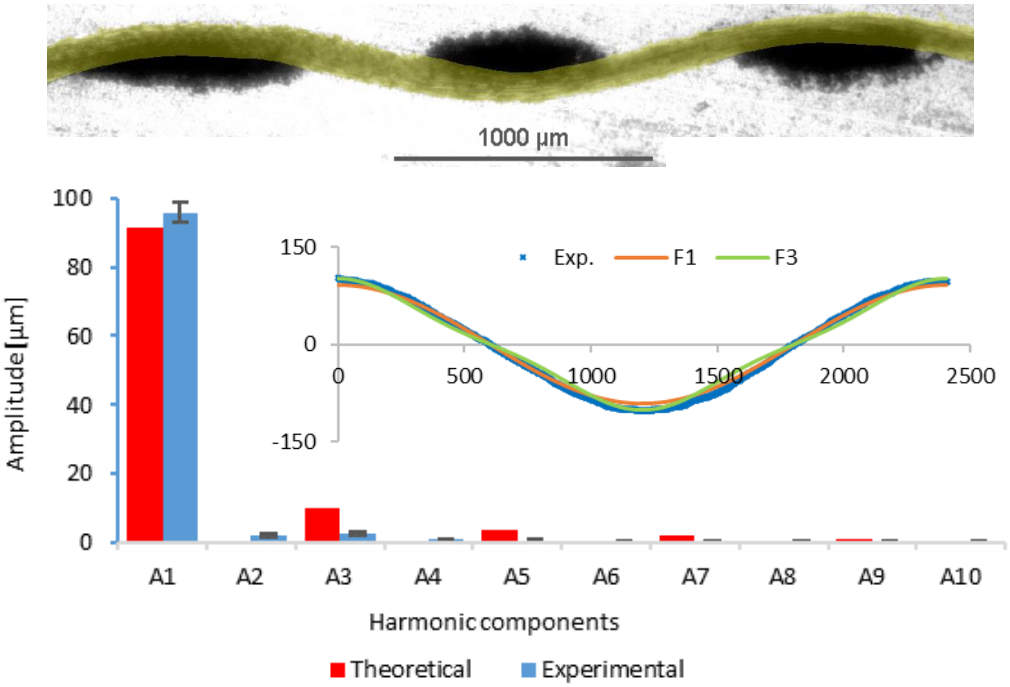

Figure 50. Cross-section of real binding wave of woven fabric, Fourier approximation and spectral characteristics of binding wave in transverse cross-section for fabric sample (B3)

In Figure 51 and Figure 52, the experimental values of binding waves and their spectrum can be observed in longitudinal and transverse cross-section, to analyze their deformation in comparison with each other. It can be analyzed in Figure 51, as the weft density is continuously increasing from (B1) to (B3), it is affecting the width (period) and deformation of the binding wave of warp yarn. It can also be explained by the effect of density in Figure 52 as the interval or density in transverse cross-section is fixed so there is no change in the period of the binding waves of weft yarn, but in the heights (amplitudes). It can be observed, when the density is low (sample B1) the deformation of binding wave of weft yarn is high because of the availability of more yarn spacing, which lets the yarn to deform easily even on small tensions. While at higher densities (sample B3) the spaces between weft yarns are so less that they do not let the weft yarns to get higher deformations. In this case the stresses increase on binding wave of warp yarn and eventually it deforms more. It is the balance of force from the law of action and reaction, the longitudinal and transverse cross-sections complement each other.

The difference in amplitude can be analyzed by the harmonic analyses as well, the deformation in longitudinal cross-section (binding wave of warp) is less for sample (B1) as compared to deformation in transverse cross-section (binding wave of weft). When one yarn

gets more deformation then the other yarn connected to it, deforms less as in case of the binding wave of warp yarn. It is called the balance of crimp between warp and weft [99]. Similarly, it can be observed how the amplitude of first harmonic component is decreasing in longitudinal cross-section from (B1) to (B3), while it is increasing in transverse cross-section of woven fabric.

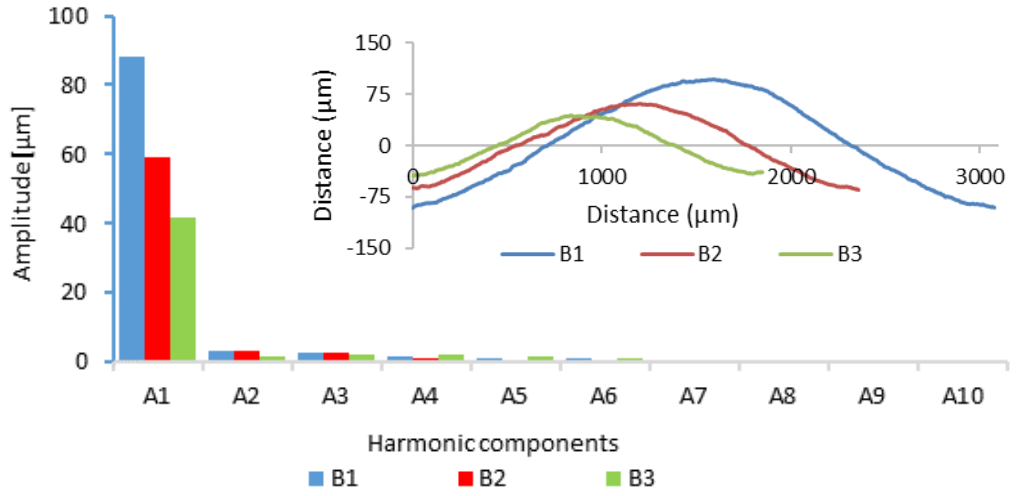

Figure 51. Shape deformation of binding wave in plain woven fabrics (B1-B3) in longitudinal cross-section

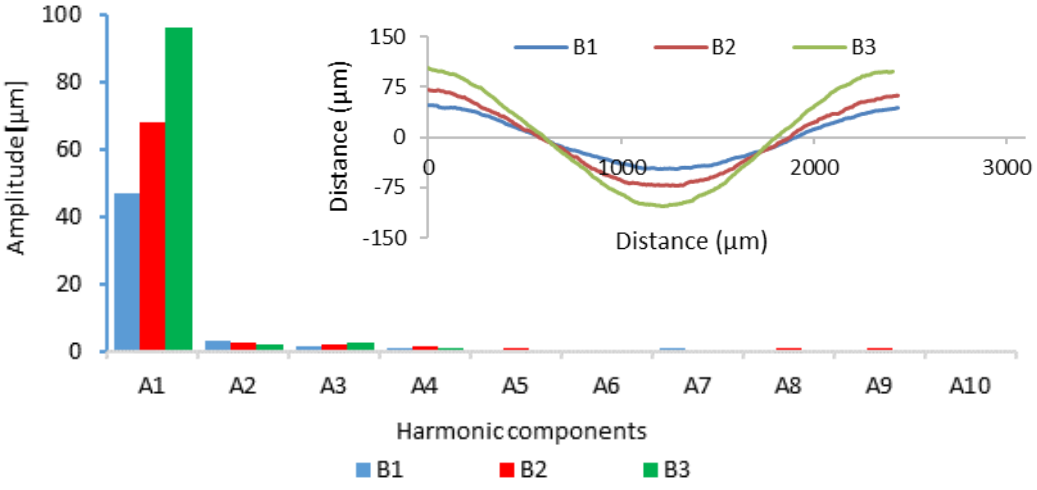

Figure 52. Shape deformation of binding wave in plain woven fabrics (B1-B3) in transverse cross-section

The FS approximation of single layer plain Glass woven fabrics by a partial sum of FS with a linear description of the central line of the binding wave have been performed as well [100].

All the parameters were kept same as of Basalt woven fabric and results are shown in Appendix B. As we have the same Glass and Basalt material and their linear density is also almost same, so we have obtained the similar results of approximation and harmonic analysis. Some small changes in deformation are given by the irregularity and non-uniformity of the structures.

6.4 Approximation of binding wave of two layer stitched basalt woven fabrics in cross-section using Fourier series

The fabric design and their real cross-sectional images of binding wave of two layer woven fabrics (B4-B7) with varying stitching distance are shown in Figure 53. The binding wave in two layer stitched plain woven fabric can be analyzed and approximated in different methods. These methods are described further.

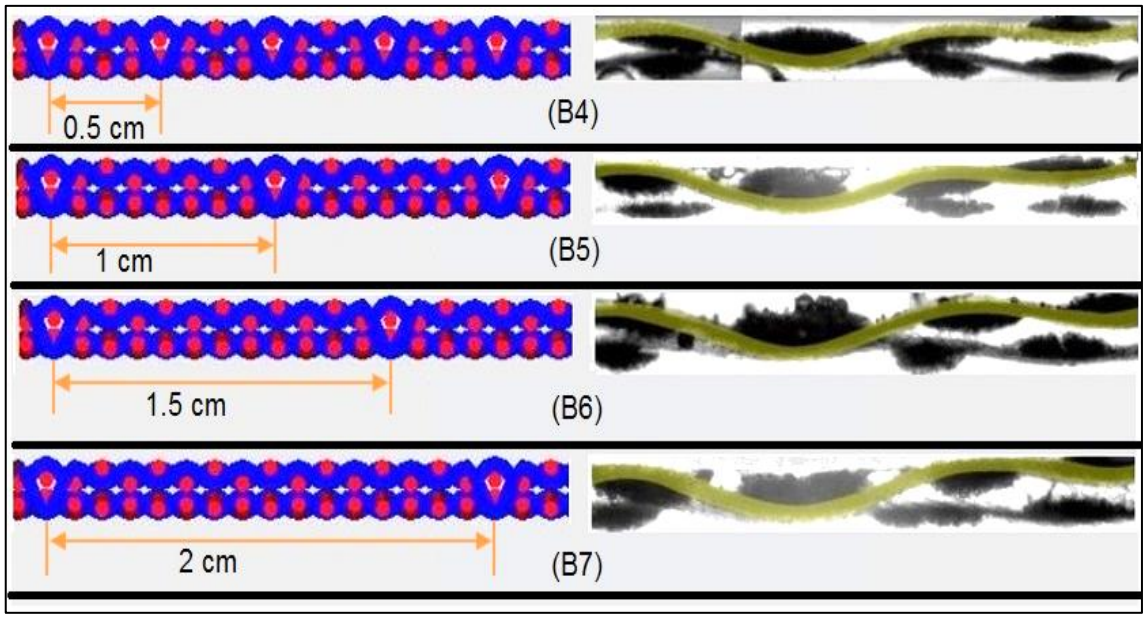

Figure 53. Cross-sectional image of binding wave of two layer woven fabrics (B4-B7) in longitudinal cross-section with varying stitching distance along warp thread (left side: theoretical simulation of cross-section, right side: real cross-section of woven fabric)

6.4.1 FS approximation of stitching section of binding wave of two layer stitched woven fabric in cross-section

The geometry of two layer stitched woven fabrics with plain weave has been divided into stitching and non-stitching section as shown in Figure 54. When the number of stitching

points decreasing from (B4) to (B7), it increases the forces inside the thread during weaving. So, we need to analyze that whether the deformation is different at stitching points or not. The linear description of binding wave in two layer stitched fabric can be observed in Figure 54 as well. This description allows us to evaluate the warp and weft threads in the interlacing at stitching sections.

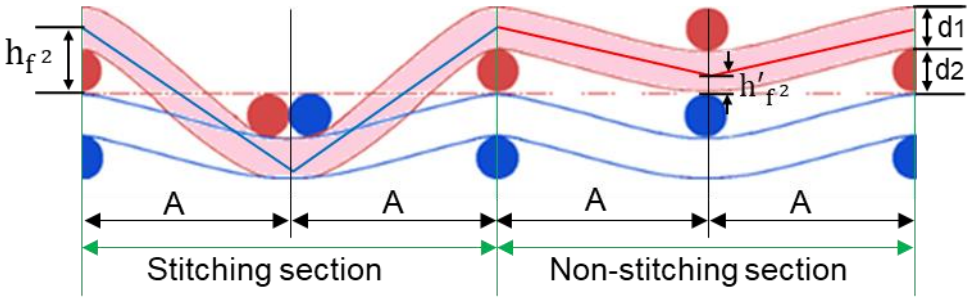

Figure 54. Graphical illustration of linear description of central line of thread in cross-section of two layer stitched woven fabrics with plain weave (stitched and non-stitched section)

The experimental binding wave of samples (B4-B7) and its approximation using equation (17) in longitudinal cross-section can be observed in Figure 55 to Figure 58 for stitching sections. It also contains the spectral characteristics of binding wave. Each of the binding waves obtained by Fourier series (where $\alpha = 1,2,3,..$) has its own spectral characteristic which evaluates the course of the binding wave in terms of geometry, eventual deformation and random changes, resulted from the stress of individual threads. It can be observed in all figures that the approximation done by Fourier series fits well to the experimental binding wave. The deformation is slightly changing in stitching sections of binding wave in two layer woven samples (B4-B7), which can be analyzed accurately by the harmonic analysis. The shape of the binding wave is not similar in all cases. The spectral characteristics obtained by theoretically and experimentally approximated binding wave has been calculated using equation (32) for stitched sections. The first harmonic component *(A1)* represents the amplitude of the first binding wave, second harmonic component *(A2)* is the difference between first and second binding wave and so on. The difference between the binding waves has been rapidly decreasing, which shows that it is not necessary to use higher number of harmonic components to get the better approximation.

The amplitude of the first harmonic component *(A1)* for the first binding wave is increasing in all four cases from (B4) to (B7). All the input parameters are same for these fabric samples

except of the stitch distance, which explains the effect of stitch distance in two layer woven structure is significant on the deformation of the binding wave. As the amplitude of first harmonic component *(A1)* is increasing from (B4) to (B7), it means the deformation is decreasing in stitching section. In other words, it can also be said that the woven fabric sample (B4) possess maximum deformation of binding wave, while woven fabric sample (B7) possess less deformation of binding wave as compared to other fabric samples. This change in amplitude or deformation is due to varying number of stitch points in all woven structures. When there are more number of stitch points and stitch distance is short, then more length of stitching yarn will be required by the same input weaver beam. Therefore, the tension on stitching yarn increases, which result in higher deformation of binding yarn in the stitching area. The second harmonic component *(A2)* gives the information about the rigidity of woven fabric, when the difference between first and second binding wave is higher, then this value is high. The amplitude of harmonic components after *(A1)* is not high which shows good approximation and only few terms will be required for better approximation.

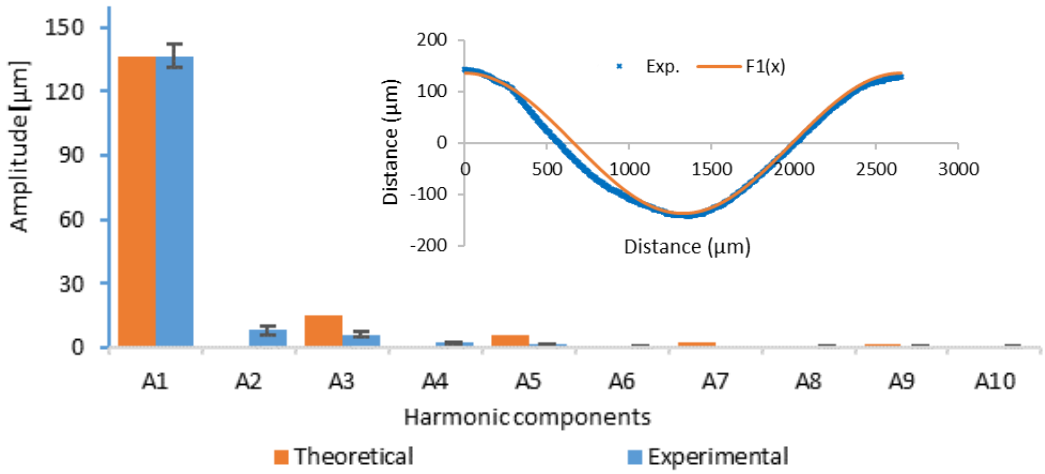

Figure 55. Fourier approximation and spectral characteristics of binding wave in stitched section of binding wave for sample (B4)

It can also be observed in Figure 55 to Figure 58 that our predicted (theoretical) values of harmonic components obtained by Fourier model are in accordance with the experimental spectral characteristics values. First and second binding waves obtained using theoretical model are identical in the longitudinal cross-section. Similarly, the third and fourth binding waves are also identical and so on. As these binding waves are identical, so the difference

between them is zero in spectral characteristics. In the similar way, the difference between the other binding waves has been calculated, which is continuously decreasing.

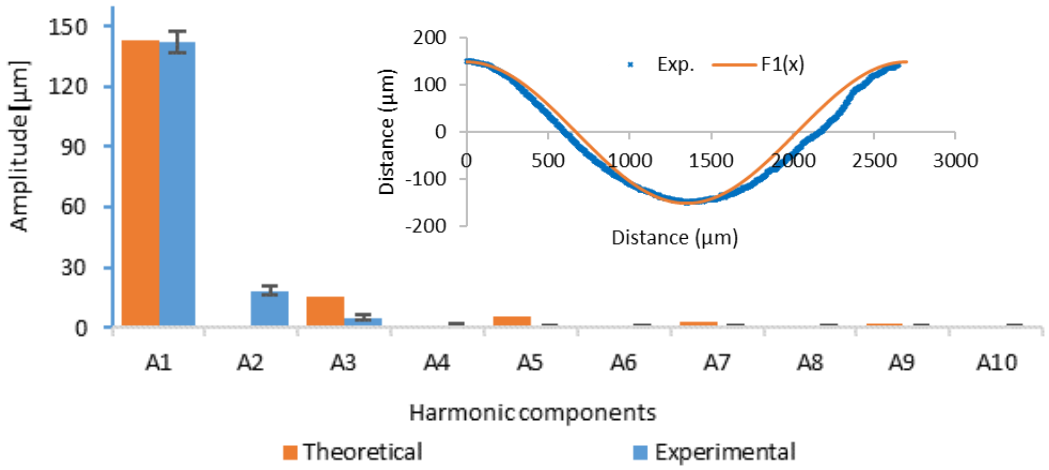

Figure 56. Fourier approximation and spectral characteristics of binding wave in stitched section of binding wave for sample (B5)

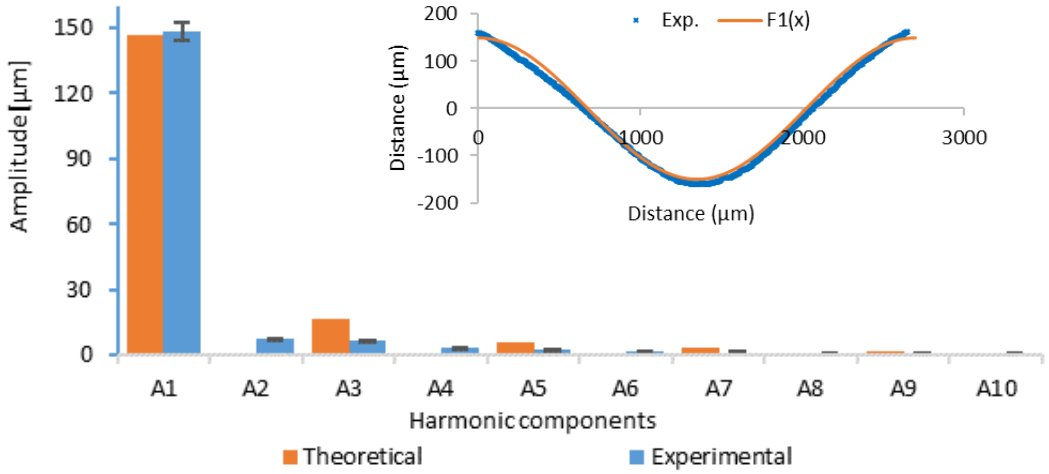

Figure 57. Fourier approximation and spectral characteristics of binding wave in stitched section of binding wave for sample (B6)

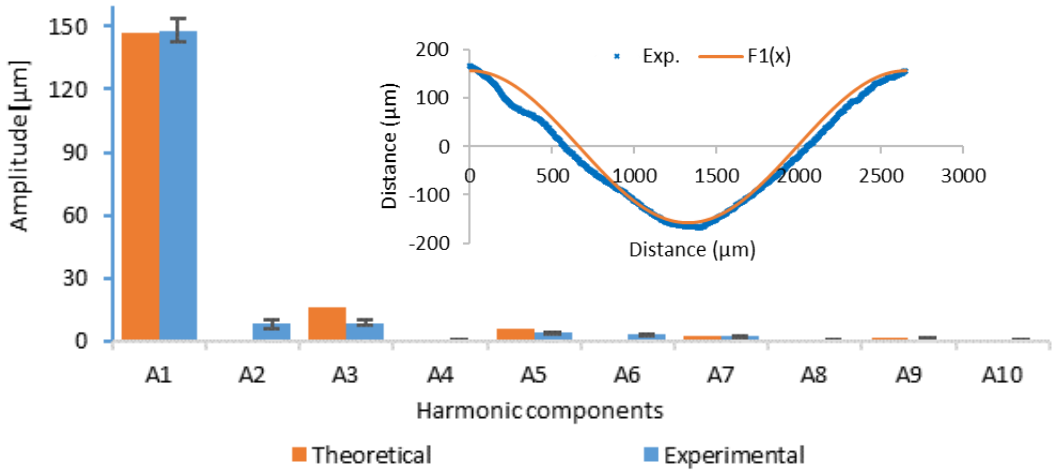

Figure 58. Fourier approximation and spectral characteristics of binding wave in stitched section of binding wave for sample (B7)

In Figure 59, the binding wave for two layer woven fabrics at stitching area obtained by the cross-sectional image analysis of real fabric can be observed. It can be analyzed that there is a slight change in the course of binding wave in all woven fabric samples, which depicts different amplitudes and deformations for different fabric structures at stitching area. This difference has been calculated and explained by the harmonic analysis of experimental binding wave as well and can be observed with a slight increase in amplitude of first harmonic component from (B4) to (B7).

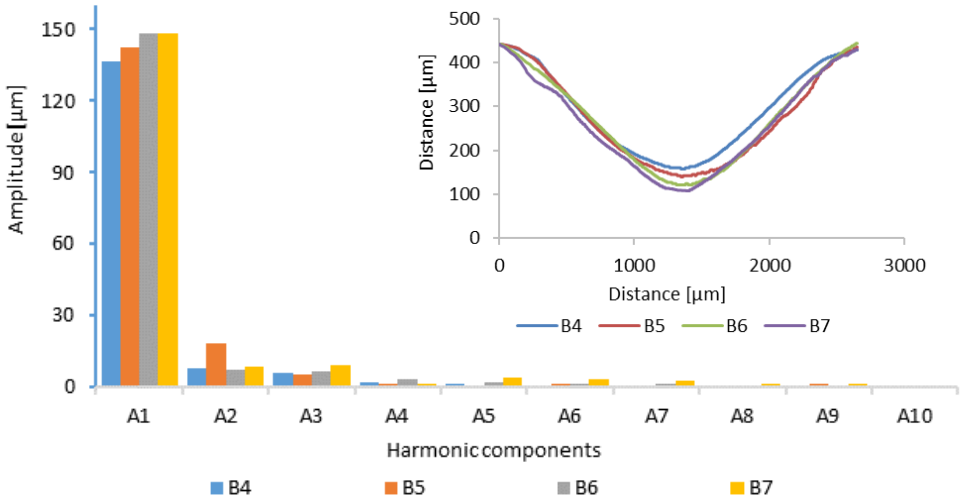

Figure 59. Shape deformation of binding wave and spectral characteristics of binding wave of two layer woven fabrics at stitching area

6.4.2 FS approximation of whole binding wave of two layer stitched woven fabric in cross-section

It is not possible to use the approximation performed on separate parts of binding wave for the evaluation of properties of whole binding wave because we need the information about the whole interlacing, so we are approximating the whole binding wave as well. The linear description by means of straight lines for two layer stitched woven fabric has been shown in Figure 21 in the fabric geometry. The FS approximation of two layer stitched woven fabrics has been performed using equation (24). The linear description of the binding wave in longitudinal cross-sections for fabric sample (B4) is shown in Figure 60.

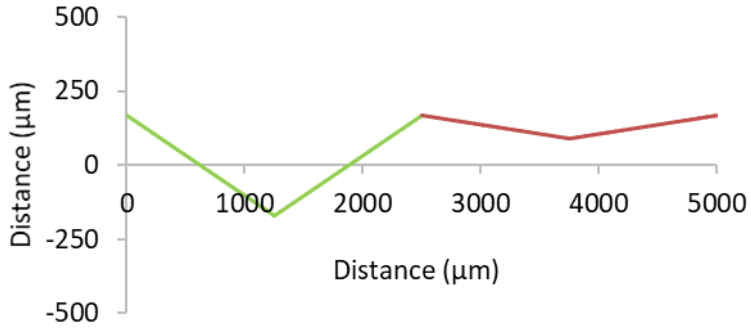

Figure 60. Graphical illustration of linear description of central line of thread in cross-section of two layers stitched woven fabric for sample (B4) in longitudinal cross-section

The real cross-section, experimental binding waves for the sample (B4), its approximation and spectral characteristics can be observed in Figure 61. It can be observed that the approximation done by Fourier series fits well to the experimental binding wave after certain number of components and our theoretical model for two layer stitched woven fabric samples holds good with the experimental binding wave. The spectral characteristics obtained by theoretically and experimentally approximated binding wave has been calculated using equation (32) for two layer stitched woven fabric (B4). It can be observed in Figure 61 that there is not big difference in the spectral characteristics obtained by theoretical and experimental data. It can also be observed the that the amplitude of first harmonic component *(A1)* is different from the one obtained by FS analysis of stitched portion, as shown in Figure 59, as these values are for both stitched and non-stitched sections. The amplitude of second harmonic component *(A2)* is quite high as the difference between first and second binding wave is high, while the amplitude of remaining components is not so high This explains that

a better approximation and fitting by Fourier model can be obtained by using just few number harmonic components and in this case, it is $F_3(x)$.

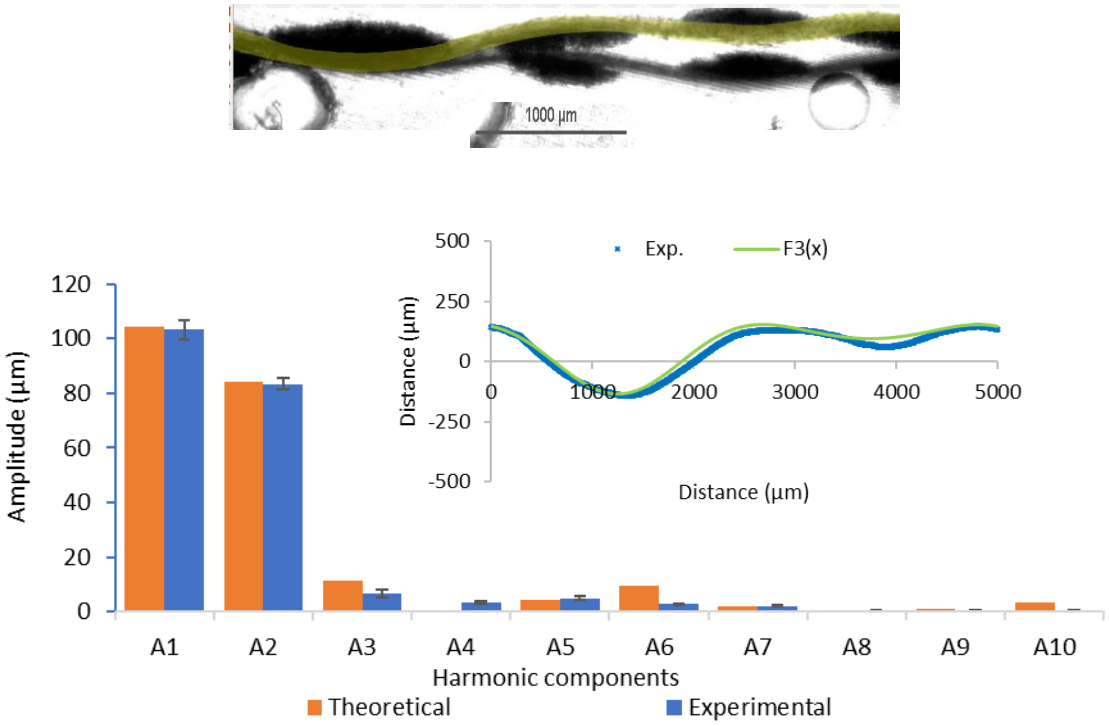

Figure 61. Cross-section of real binging wave of woven fabric, Fourier approximation and spectral characteristics of binding wave (B4) in longitudinal cross-section

6.5 Influence of plain weave repeat in non-stitched part of binding wave of two-layer stitched woven fabric in cross-section using Fourier series

In this chapter we want to present influence of number of repeats of plain weave in binding wave on the spectral characterization of Fourier spectrum. For modelling of geometry of cross-section of woven fabric, the Fourier series is still used with straight lines description of central line of the binding wave. For experimental part of work the fabric design of two layer woven fabrics (B4-B7) with varying stitching distance (period) and repeat size are shown in Figure 62. In the sample (B4) the repeat size is smallest which is one-time, while in (B5) to (B7) it is three, five and seven-times respectively. So, we have a possibility to use this plain weave by ‘n’ times and we can assume that which shape and spectral characteristics we will obtain. The non-stitching section which is just next to the stitching section, can be continuous depending upon the distance between two stitch points or repeat size. There will be higher elongation in fabric when the stitch points per meter are high and this can be used as reinforcement in composites where we need higher deformation instead of rigidity. So, it is

necessary to understand the effect of stitch distance or repeat size by FS approximation and spectrum analysis.

The linear description for two layer fabrics has already been describes in Figure 21 in the fabric geometry. This description allows us to evaluate the warp and weft threads in the interlacing at stitching and non-stitching sections for a complete binding repeat. For the approximation of a two layer woven fabric (B4-B7) by FS, the period of the periodic function has been taken *as P = T = 4A, 8A, 12A, 16A* respectively.

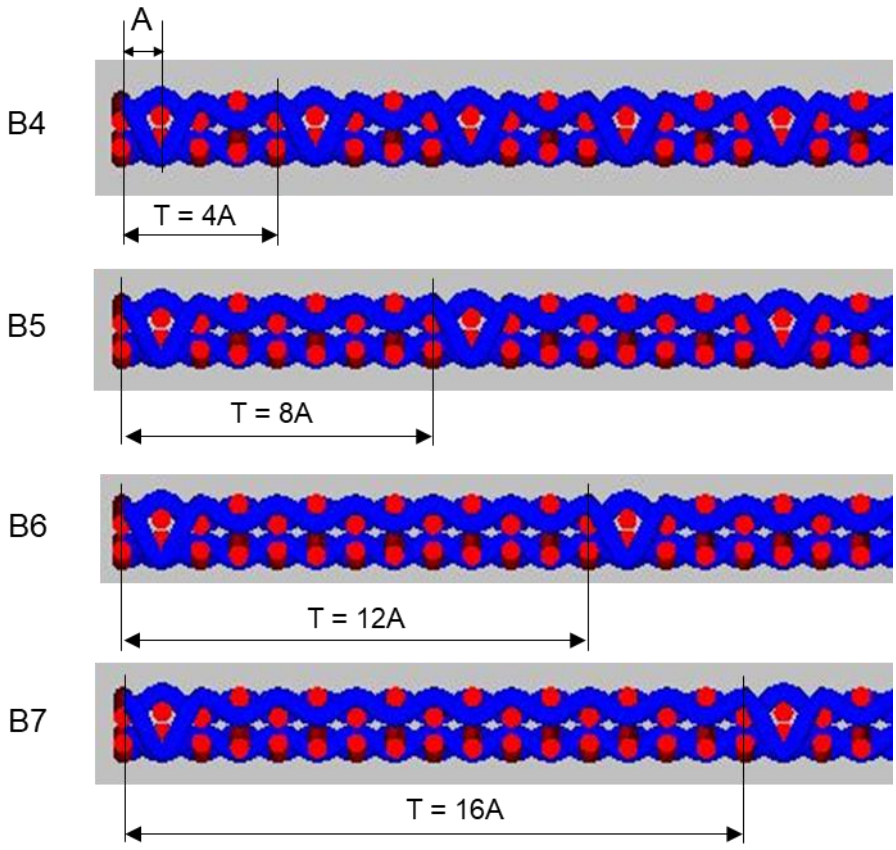

Figure 62. Geometry of two layer woven fabric samples (B4-B7) with varying repeat size

The FS approximation of two layer stitched woven fabrics has been performed using equation (24). The approximation of the complete repeat of all woven fabric samples (B4-B7) and their spectral characteristics can be observed in the Figure 63 to Figure 70. It can be observed that the approximation done by Fourier series is in accordance with the shape of the binding wave in fabric sample after certain number of components and our theoretical model for two layer stitched woven fabric samples holds good for different repeat sizes as well. It is continuous and can be applied to bigger repeat sizes. The woven fabric (B4) has the smallest

repeat size as it contains only one-time plain woven fabric in non-stitching section, while the sample (B5) contains three-times, sample (B6) five-times and sample (B7) holds seven-times plain woven fabric in non-stitching section. Fourier series is an expansion of a periodic function *F(x)* in terms of an infinite sum of sines and cosines. In the Figure 63 $F_3(x)$ is the sum of five terms of Fourier series to get better approximation. It can be observed in Figure 63 to Figure 70 that when the repeat size is increasing from (B4) to (B7), the number of binding waves required to get a better approximation as per woven structure are also increasing, so the repeat size has direct relation with the number of binding or crimp waves.

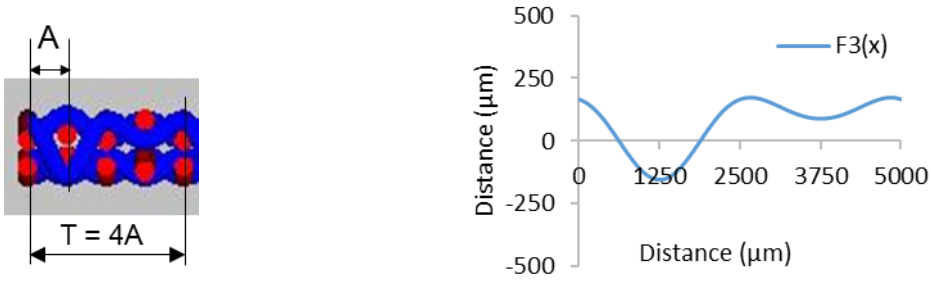

Figure 63. Graphical illustration of geometry of cross-section for one-time repeat of plain woven fabric in non-stitching section and Fourier approximation of complete repeat of binding wave (B4) in longitudinal cross-section

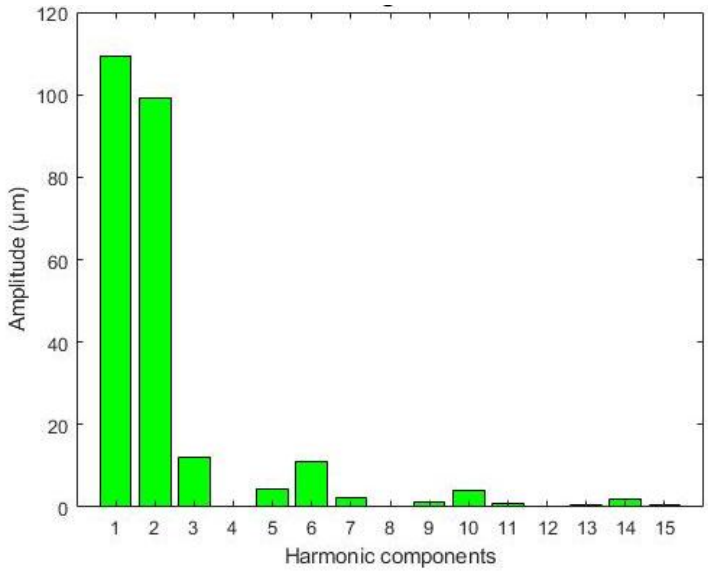

Figure 64. Spectral characteristics of the binding wave in two layer stitched woven fabric (B4) with repeat of one time of plain woven fabric in non-stitched part

Moreover, it can be analyzed accurately by the harmonic analysis. Each of the binding waves obtained by Fourier series (where $\alpha = 1,2,3,..$) has its own spectral characteristic which evaluates the course of the binding wave. The spectral characteristics of all the two layer fabric sample (B4-B7) in longitudinal cross-section has been calculated using equation (32). The first harmonic component *(A1)* represents the amplitude of the first binding wave, while second harmonic component *(A2)* is the difference between first and second binding wave. In the similar way, the difference between the other binding waves has been calculated and represented in figures for fifteen harmonic components. Moreover, it has also been observed that just by adding few number of sines and cosines series we can get a better approximation of binding wave.

It can be observed in Figure 64, Figure 66, Figure 68 and Figure 70 in the harmonic analysis that the amplitude of second component *(A2)* is quite high for woven sample (B4), fourth component *(A4)* for woven sample (B5), sixth component *(A6)* for woven sample (B6) and eighth component *(A7)* for woven sample (B7). After this highest amplitude the approximated crimp wave holds good with the sample crimp wave. We are getting this highest amplitude component after the exact number of plain weave units for each woven fabric sample. So, it can be concluded that when the repeat size is increasing from (B4) to (B7), the number of binding waves required to get a better approximation as per woven structure are also increasing, hence the repeat size is directly proportional to the number of harmonic components.

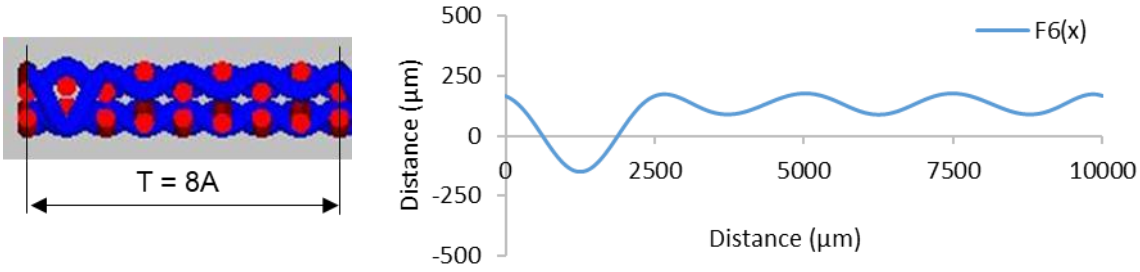

Figure 65. Graphical illustration of geometry of cross-section for three-times repeat of plain woven fabric in non-stitching section and Fourier approximation of binding wave (B5) in longitudinal cross-section

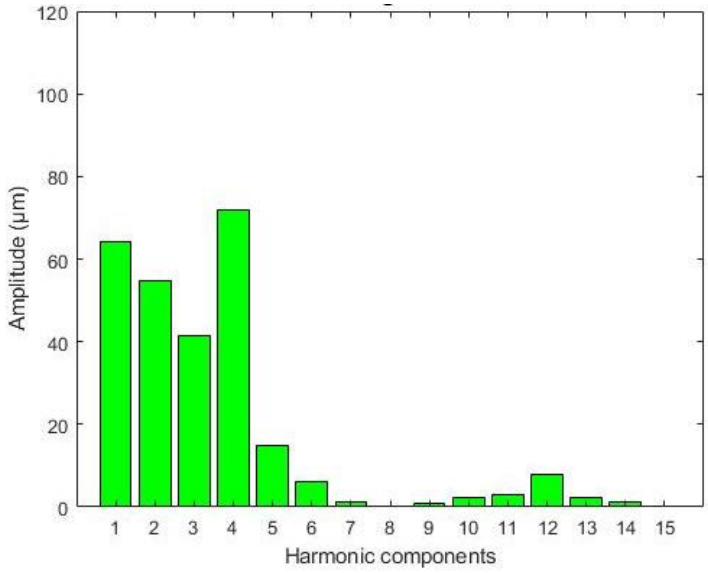

Figure 66. Spectral characteristics of the binding wave in two layer stitched woven fabric (B5) with repeat of three-time of plain woven fabric in non-stitched part

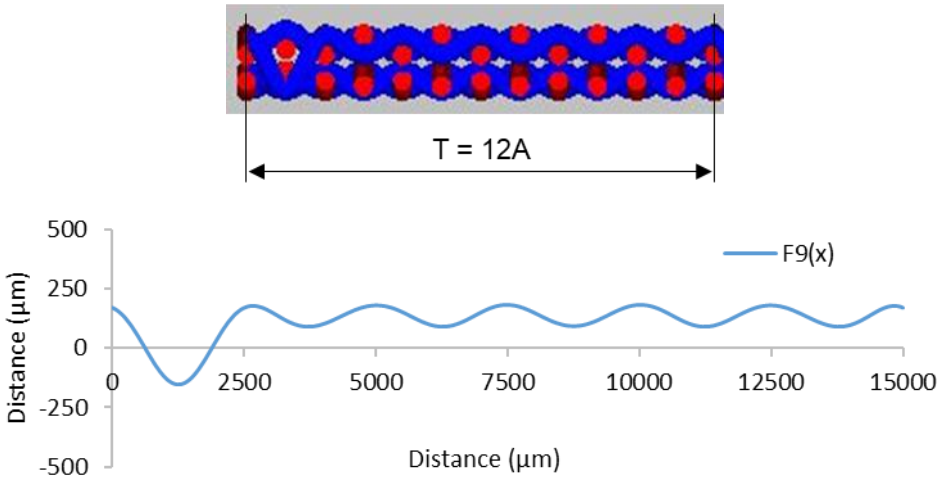

Figure 67. Graphical illustration of geometry of cross-section for five-times repeat of plain woven fabric in non-stitching section and Fourier approximation of binding wave (B6) in longitudinal cross-section

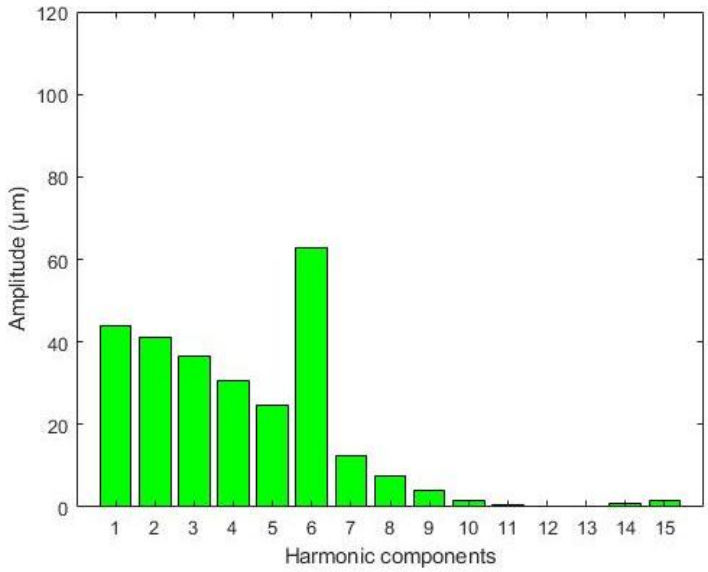

Figure 68. Spectral characteristics of the binding wave in two layer stitched woven fabric (B6) with repeat of five-times of plain woven fabric in non-stitched part

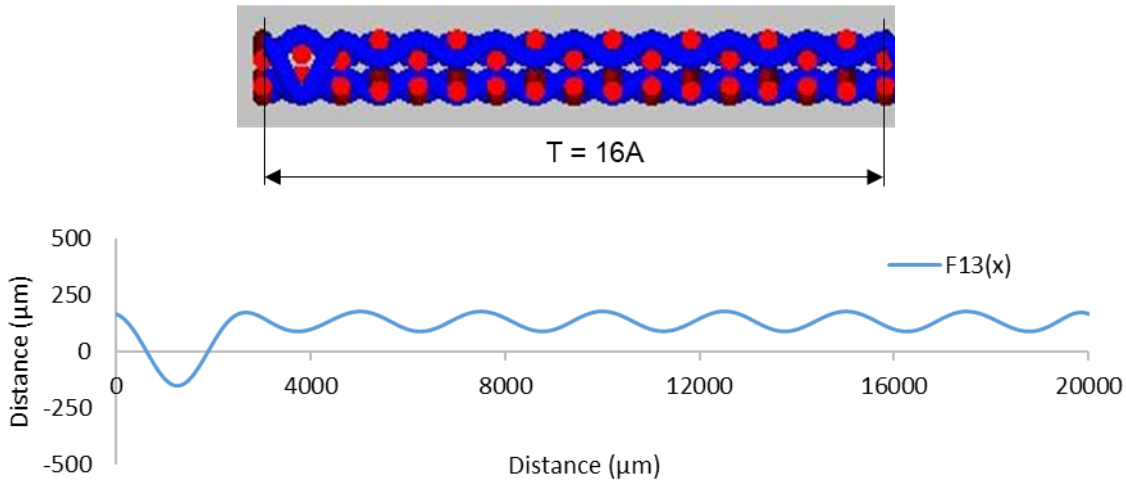

Figure 69. Graphical illustration of geometry of cross-section for seven-times repeat of plain woven fabric in non-stitching section and Fourier approximation of binding wave (B7) in longitudinal cross-section

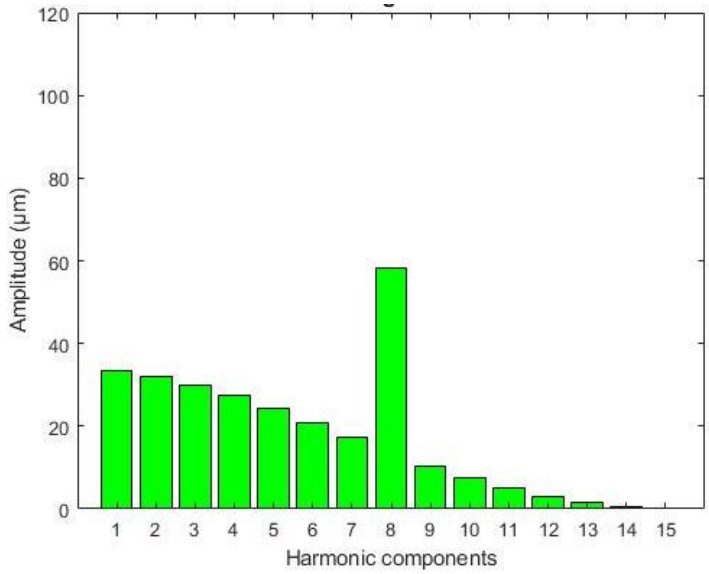

Figure 70. Spectral characteristics of the binding wave in two layer stitched woven fabric (B7) with repeat of seven-times of plain woven fabric in non-stitched part

7. CONCLUSIONS AND FUTURE WORK

The following conclusions can be drawn from this study.

- The work is focused on mathematical expression and description of geometry of binding wave of single as well as two-layer stitched woven fabric using Fourier series. For mathematical definition of binding wave as an input function f(x) in Fourier series, the linear description of the central line of the binding wave was used. Based on verification of model with real binding wave, the validity of the model is confirmed and verified.

- Fourier series analysis describe the whole binding wave repeat contrary to present models which describes only one interlacing point. Using Fourier series modelling, we can obtain not only the description of geometry of binding wave (length of binding wave or crimp of threads) but also spectral characterization for analyzing the individual components, which can react on deformation of the shape of binding wave.

- The final shape of binding wave of two layer stitched woven fabric is given by the definition of number of repeats of plain weave in interlacing in cross-section. The influence of repeats of plain weave in binding wave on the spectral characterization of Fourier spectrum was evaluated.

- FS approximation can be used for analysis of cross-section as well as the deformation of shape of binding wave in the single layer plain woven fabric (which is possible to use as reinforcement structure) and also for two layer plain woven structures where we have connections of the individual layers by the varying stitching points. The model has been validated with the experimental analyses of binding wave in cross-section of single layer and two layer stitched woven fabric.

- The effect of stitch distance (repeat size) in two layer woven structure has been analyzed in stitching section. The amplitude of harmonic component is increasing from (B4) to (B7). The fabric with more number of stitching points (B4) retains more deformation.

- Experimental analysis shows that the approximation done by the proposed theoretical model (idea) for description of geometry of cross-section of woven multifilament fabric structures (single and two layer stitched woven fabrics with plain weave) is in accordance

with experimental spectrum. Theoretical model for description of mutual interlacing of threads in two layer stitched woven structure, it is possible to use it as analytical prediction of geometry of woven structure, and shape of the binding wave.

- By predicting the geometry of the binding wave in two layers stitched woven fabric, it is possible to use it for the calculation of basic properties of woven fabric (length of threads in binding wave, crimp of threads, thickness of woven fabric, etc.).

- The model for description of geometry of binding wave in cross-section can be extended for the other weaves such as twill or satin weaves with longer floats, bigger repeat size and more number of layers. The spectrum will be different in that case.

- The deformation of the shapes of binding waves of the individual layers of the multilayer woven fabrics can be compared with the deformation of the binding waves in the individual layers in composites.

8. REFERENCES

[1] S. L. Edwards and J. A. Werkmeister, “Mechanical evaluation and cell response of woven polyetheretherketone scaffolds,” *J. Biomed. Mater. Res. Part A*, vol. 100A, no. May, pp. 3326–3331, 2012.

[2] P. Boisse, N. Hamila, E. Vidal-sallé, and F. Dumont, “Simulation of wrinkling during textile composite reinforcement forming. Influence of tensile in-plane shear and bending stiffnesses,” *Compos. Sci. Technol.*, vol. 71, no. 5, pp. 683–692, 2011.

[3] O. Erol, B. M. Powers, and M. Keefe, “A macroscopic material model for woven fabrics based on mesoscopic sawtooth unit cell,” *Compos. Struct.*, vol. 180, pp. 531–541, 2017.

[4] P. H. Dastoor, T. K. Ghosh, S. K. Batra, and S. P. Hersh, “Computer-assisted structural design of industrial woven fabrics Part III: Modelling of fabric uniaxial/biaxial load-deformation,” *J. Text. Inst.*, vol. 85, no. 2, pp. 135–157, 1994.

[5] T. M. McBride and J. Chen, “Unit-cell geometry in plain-weave fabrics during shear deformations,” *Compos. Sci. Technol.*, vol. 57, no. 3, pp. 345–351, 1997.

[6] F. T. Peirce, “5-The geometry of cloth structure,” *J. Text. Inst. Trans.*, vol. 28, no. 3, pp. T45–T96, 1937.

[7] A. Kemp, “An Extension of Peirce’s Cloth Geometry to the Treatment of Non-circular Threads,” *J. Text. Inst. Trans.*, vol. 49, no. 1, pp. T44–T48, 1958.

[8] B. Olofsson, “49-A general model of a fabric as a geometric-mechanical structure,” *J. Text. Inst. Trans.*, vol. 55, no. 11, pp. T541–T557, 1964.

[9] J. W. S. Hearle and W. J. Shanahan, “11—An Energy Method for Calculations in Fabric Mechanics Part I: Principles of the Method,” *J. Text. Inst.*, vol. 69, no. 4, pp. 81–91, 1978.

[10] W. J. Shanahan and J. W. S. Hearle, “12—an Energy Method for Calculations in Fabric Mechanics Part II: Examples of Application of the Method To Woven Fabrics,” *J. Text. Inst.*, vol. 69, no. 4, pp. 92–100, 1978.

[11] J. B. Hamilton, “7—a General System of Woven-Fabric Geometry,” *J. Text. Inst.*

Trans., vol. 55, no. 1, pp. T66–T82, 1964.

[12] R. B. Turan, "Three-dimensional computer simulation of 2/2 twill woven fabric by using B-splines," *October*, vol. 101, no. 10, pp. 870–881, 2010.

[13] M. K. Dolatabadi and R. Kovař, "Geometry of plain weave fabric under shear deformation. Part II: 3D model of plain weave fabric before deformation," *J. Text. Inst.*, vol. 100, no. 5, pp. 381–386, 2009.

[14] S. V. Lomov *et al.*, "Textile composites: modelling strategies," *Compos. Part A Appl. Sci. Manuf.*, vol. 32, no. 10, pp. 1379–1394, Oct. 2001.

[15] Y. Nawab, *Fabric Manufacturing Calculations Process and Product*. Islamabad, Pakistan: Higher Education Commission, 2017.

[16] C. G. Provatidis and S. G. Vassiliadis, "On the performance of the geometrical models of fabrics for use in computational mechanical analysis," *Int. J. Cloth. Sci. Technol.*, vol. 16, no. 5, pp. 434–444, 2004.

[17] J. Drasrova, "Analysis of fabric cross-section." PhD Thesis (in Czech), Technical University of Liberec, Czech, 2004.

[18] J. Escofet, M. S. Millán, and M. Ralló, "Modeling of woven fabric structures based on fourier image analysis," *Appl. Opt.*, vol. 40, no. 34, pp. 6170–6176, 2001.

[19] B. Košková and S. Vopička, "Determination of yarn waviness parameters for C/C woven composites," in *Proceedings of International Conference CARBON*, 2001, pp. 1–6.

[20] B. K. Sirková, "Study of approximations of individual models by a partial sum of Fourier Series.pdf," *Vlakna a Text.*, vol. 7, no. 4, pp. 189–194, 2000.

[21] S. Kawabata, M. Niwa, and H. Kawai, "The finite-deformation theory of plain-weave fabrics Part I: the biaxial-deformation theory.," *J Text Inst*, vol. 64, no. 1, pp. 21–46, 1973.

[22] A. Miravete, *3-D textile reinforcements in composite materials*. Cambridge CB1 6AH, England: Woodhead Publishing Limited, 1999.

[23] J. L. Hu and J. G. Teng, “Computational fabric mechanics: Present status and future trends,” *Finite Elem. Anal. Des.*, vol. 21, no. 4, pp. 225–237, 1996.

[24] Jinlian HU, “Structural properties of fabric,” in *Structure and mechanics of woven fabrics*, Cambridge CB1 6AH, England: Woodhead Publishing Limited, 2004, pp. 61–69.

[25] A. P. Mouritz, M. K. Bannister, P. J. Falzon, and K. H. Leong, “Review of applications for advanced three-dimensional fibre textile composites,” *Compos. Part A Appl. Sci. Manuf.*, vol. 30, no. 12, pp. 1445–1461, 1999.

[26] P. Amuthakkannan, V. Manikandan, and M. Uthayakumar, “Mechanical properties of basalt and glass fiber reinforced polymer hybrid composites,” *J. Adv. Microsc. Res.*, vol. 9, no. 1, pp. 44–49, 2014.

[27] E. M. Parsons, T. Weerasooriya, S. Sarva, and S. Socrate, “Impact of woven fabric: Experiments and mesostructure-based continuum-level simulations,” *J. Mech. Phys. Solids*, vol. 58, no. 11, pp. 1995–2021, 2010.

[28] S. Adanur, *Hand Book of Weaving*. Lancaster. Basel: Technomic Publishing Co., INC., 2001.

[29] Y. Nawab, *Textile Engineering - An introduction*. Germany: De Gruyter Oldenbourg, 2016.

[30] B. N. Cox and G. Flanagan, *Handbook of analytical methods for textile composites*, no. 4750. NASA, 1997.

[31] D. P. Adams, E. R. Schwarz, and S. Backer, “The relationship between the structural geometry of a textile fabric and its physical properties,” *Text. Res. J.*, vol. 16, no. 9, pp. 653–665, 1956.

[32] B. K. Sirková and I. Mertová, “Woven fabric structural pore models analysis,” in *21st Internation Confrence on Structure and Structural Mechanics of Textiles*, 2016, no. December, pp. 33–43.

[33] B. K. Sirková, “The structure and final properties of the woven fabrics,” in *2nd International textile, clothing & design conference*, 2004, pp. 6–9.

[34] Y. Nawab, S. T. A. Hamdani, and K. Shaker, *Structural Textile Design*. Boca Raton: CRC Press, Taylor & Francis Group, 2017.

[35] N. Gokarneshan, *Fabricc structure and design*. New Delhi: New Age International (P) Ltd., 2004.

[36] A. Majumdar, *Soft computing in textile engineering*. Cornwall, UK: Woodhead Publishing Limited, 2011.

[37] M. Azeem, Z. Ahmad, and A. Fraz, "Influence of Weave Design and Yarn Types on Mechanical and Surface Properties of Woven Fabric," vol. 1, no. 127, pp. 42–45, 2018.

[38] E. B. Berry, *Textile designing pure and applied*, 2nd ed. N.C.State, USA: North Carolina State College, 1964.

[39] A. C. Long, *Design and manufacture of textile composites*. Cambridge CB1 6AH, England: Woodhead Publishing Limited, 2005.

[40] B. K. Behera and P. K. Hari, *Woven Textile Structure-Theory and Applications*. Cambridge CB1 6AH, England: Woodhead Publishing Limited, 2010.

[41] P. S. Tung and S. Jayaraman, "Three-dimensional multilayer woven preforms for composites," USA: ACS Publications, 1989, pp. 53–80.

[42] M. Mcclain, R. Senior, T. E. Organic, and M. Composites, "Overview of Recent Developments in 3D Structures," *Albany Eng. Compos.*, pp. 1–12, 2012.

[43] N. Khokar, "3D-Weaving: Theory and Practice," *J. Text. Inst.*, vol. 92, no. 2, pp. 193–207, 2001.

[44] F. Stig, "An introduction to the mechanics of 3D-woven fibre reinforced composites," KTH School of Engineering Sciences, Stockholm, Sweden, 2009.

[45] S. Chou and H.-E. Chen, "The weaving methods of three-dimensional fabrics of advanced composite materials," *Compos. Struct.*, vol. 33, no. 3, pp. 159–172, Jan. 1995.

[46] B. K. Behera and R. Mishra, "3-Dimensional weaving," *Indian J. Fibre Text. Res.*, vol.

33, pp. 274–287, 2008.

[47] B. K. Behera, J. Militky, R. Mishra, and D. Kremenakova, “Modeling of Woven Fabrics Geometry and Properties,” in *Woven Fabrics*, Rijeka, Croatia: InTech, 2012, p. 296.

[48] R. Kovar, “Length of the yarn in plain-weave crimp wave,” *Journal of the Textile Institute*, vol. 102, no. 7. pp. 582–597, 2011.

[49] S. Vassiliadis, *Advanes in modern woven fabric technology*. Rijeka, Croatia: InTech, 2011.

[50] P. H. Dastoor, S. P. Hersh, S. K. Batra, and W. J. Rasdorf, “Computer-assisted structural design of industrial woven fabrics part I: Need, scope, background, and system architecture,” *J. Text. Inst.*, vol. 85, no. 2, pp. 89–109, 1994.

[51] S. Sockalingam, J. W. Gillespie, and M. Keefe, “On the transverse compression response of Kevlar KM2 using fiber-level finite element model,” *Int. J. Solids Struct.*, vol. 51, no. 13, pp. 2504–2517, 2014.

[52] Y. Wang, Y. Miao, D. Swenson, B. A. Cheeseman, C. Yen, and B. Lamattina, “Digital element approach for simulating impact and penetration of textiles,” *Int. J. Impact Eng.*, vol. 37, no. 5, pp. 552–560, 2010.

[53] G. Nilakantan, “Filament-level modeling of Kevlar KM2 yarns for ballistic impact studies,” *Compos. Struct.*, vol. 104, pp. 1–13, 2013.

[54] M. Grujicic, R. Yavari, J. S. Snipes, S. Ramaswami, and B. A. Cheeseman, “The effect of plain-weaving on the mechanical properties of warp and weft p -phenylene terephthalamide (PPTA) fibers / yarns,” *J. Mater. Sci.*, vol. 49, pp. 8272–8293, 2014.

[55] R. Samadi, “Particle-based modeling of the compaction of fiber yarns and woven textiles,” *Text. Res. J.*, vol. 84, no. 11, pp. 1159–1173, 2014.

[56] J. Zeman and M. Sejnoha, “Homogenization of balanced plain weave composites with imperfect microstructure : Part I — Theoretical formulation,” *Int. J. Solids Struct.*, vol. 41, pp. 6549–6571, 2004.

[57] N. Takano, Y. Uetsuji, Y. Kashiwagi, and M. Zako, "Hierarchical modelling of textile composite materials and structures by the homogenization method," *Model. Simul. Mater. Sci. Eng.*, vol. 7, no. 2, p. 207, 1999.

[58] A. E. Bogdanovich, *Multi-scale modeling, stress and failure analyses of 3-D woven composites*, vol. 41, no. 20. 2006.

[59] J. W. S. Hearle, "An energy method for calculations in fabric mechanics Part 2: Examples of application of the method to woven fabrics," *J. Text. Inst.*, vol. 69, p. 92, 1978.

[60] B. Ozgen and H. Gong, "Yarn geometry in woven fabrics," *Text. Res. J.*, vol. 81, no. 7, pp. 738–745, 2010.

[61] R. H. Gong, B. Ozgen, and M. Soleimani, "Modeling of Yarn Cross-Section in Plain Woven Fabric," *Text. Res. J.*, vol. 79, no. 11, pp. 1014–1020, 2009.

[62] "http://rsbweb.nih.gov/ij/, accessed on April 2018." .

[63] B. K. Sirková, "Mathematical model for description of thread's interlacing in fabric using Fourier series," Thesis, Technical University of Liberec, 2002.

[64] Y. Xiaobo, X. Binjie, G. Baciu, and H. Jinlian, "Fourier-Analysis Based Satin Fabric Density and Weaving Pattern Extraction," *Res. J. Text. Appar.*, vol. 11, no. 1, pp. 71–80, 2007.

[65] R. Pan, J. Zhang, Z. Li, W. Gao, and B. Xu, "Applying image analysis for automatic density measurement of high-tightness woven fabrics," *Fibres Text. East. Eur.*, vol. 2, no. 116, pp. 66–72, 2016.

[66] B. Xu and H. Ecology, "Identifying Fabric Structures with Fast Fourier Transform Techniques," *Text. Res. J.*, vol. 66, no. 8, pp. 496–506, 1996.

[67] P. Volf, "Automatic Assessing and Monitoring of Weaving Density 1," *Fibers Polym.*, vol. 10, no. 6, pp. 830–836, 2009.

[68] P. Potiyaraj, C. Subhakalin, B. Sawangharsub, and W. Udomkichdecha, "Recognition and re-visualization of woven fabric structures," *Int. J. Cloth. Sci. Technol.*, vol. 22,

no. 2/3, pp. 79–87, 2010.

[69] A. Moussa, D. Dupont, D. Steen, and X. Zeng, “Structure analysis and surface simulation of woven fabrics using fast Fourier transform techniques,” *J. Text. Inst.*, vol. 101, no. 6, pp. 556–570, 2010.

[70] A. Lachkar *et al.*, “Textile woven fabric recognition using Fourier image analysis techniques : Part II – texture analysis for crossed-states detection,” *J. Text. Inst.*, vol. 96, no. 3, pp. 179–183, 2016.

[71] G. Hu, Q. Wang, and G. Zhang, “Unsupervised defect detection in textiles based on Fourier analysis and wavelet shrinkage,” *Appl. Opt.*, vol. 54, no. 10, pp. 2963–2980, 2015.

[72] B. Xu, “Identifying Fabric Structures with Fast Fourier Transform Techniques,” *Text. Res. J.*, vol. 66, no. 8, pp. 496–506, 1996.

[73] C. Chan, S. Member, and G. K. H. Pang, “Fabric defect detection by fourier analysis - Industry Applications,” *IEEE Trans. Ind. Appl.*, vol. 36, no. 5, pp. 1267–1276, 2000.

[74] J. Zhang, R. Pan, W. Gao, and J. Xiang, “Weave pattern recognition by measuring fiber orientation with Fourier transform,” *J. Text. Inst.*, vol. 108, no. 4, pp. 622–630, 2017.

[75] S. Nosek, “The structure and geometry of the woven fabrics,” 1996.

[76] B. P. Dash, B. K. Behera, R. Mishra, and J. Militky, “Modeling of internal geometry of 3D woven fabrics by computation method,” *J. Text. Inst.*, vol. 104, no. 3, pp. 312–321, Mar. 2013.

[77] B. K. Sirková and M. Vyšanská, “Methodology for evaluation of fabric geometry on the basis of the fabric cross-section,” *Fibres Text. East. Eur.*, vol. 94, no. 5, pp. 41–47, 2012.

[78] A. Seyam and A. El-shiekh, “Mechanics of woven fabrics: Part II: Experimental study of weavability limit of yams with thickness variation,” *Text. Res. J.*, vol. 60, no. 8, pp. 457–463, 1990.

[79] N. Khokar, "3D Fabric-forming Processes: Distinguishing Between 2D-weaving, 3D-weaving and an Unspecified Non-interlacing Process," *J. Text. Inst.*, vol. 87, no. 1, pp. 97–106, 1996.

[80] N. Khokar, "3D-Weaving: Theory and Practice," *J. Text. Inst.*, vol. 92, no. 2, pp. 193–207, 2001.

[81] X. Chen, L. W. Taylor, and L. J. Tsai, "Three-dimensional Fabric Structures. Part 1 - An Overview on Fabrication of Three-Dimensional Woven Textile Preforms for Composites," *Handb. Tech. Text. Second Ed.*, vol. 1, pp. 285–304, 2015.

[82] H. Jeon, *Woven fabrics*. Rijeka, Croatia: InTech, 2012.

[83] K. Bilisik, "Multiaxis Three Dimensional (3D) Woven Fabric," *Adv. Mod. Woven Fabr. Technol.*, no. 1989, pp. 79–106, 2011.

[84] J. . Soden and B. . Hill, "Conventional weaving of shaped preforms for engineering composites," *Compos. Part A Appl. Sci. Manuf.*, vol. 29, no. 7, pp. 757–762, Jul. 1998.

[85] N. G. Novikov, "Structure and design of fabric."

[86] B. K. Sirková, "Spectral identification of the weaves in the woven fabrics."

[87] B. K. Sirkova, "Description of binding waves using the Fourier Series," in *Vlakna a Textil*, 2013, vol. 20, no. 2, pp. 32–40.

[88] Z. Ahmad and B. K. Sirková, "Tensile behavior of Basalt/Glass single and multilayer-woven fabrics," *J. Text. Inst.*, vol. 109, no. 5, pp. 686–694, 2017.

[89] "ISO 1973:1995,Textile fibres -- Determination of linear density -- Gravimetric method and vibroscope method," 1995.

[90] ASTM, "Standard Test Methods for Tire Cords , Tire Cord Fabrics , and Industrial Filament Yarns Made from Manufactured Organic-Base Fibers 1," *Astm*, no. June, pp. 1–39, 2015.

[91] ISO 2061:1995, "Textiles — Determination of twist in single spun yarns — Untwist / retwist method."

[92] ISO 1144:2016, “Textiles -- Universal system for designating linear density (Tex System),” 2016.

[93] B. Neckář, “Yarn diameter and hairiness,” Internal Standards No. 22-102-01/01, 2004.

[94] B. Neckář, “Yarns. Forming, structure, properties. SNTL.” Czech, Praha, 1990.

[95] D. Kremenakova, “Recommended procedure for preparation of samples. Soft and hard sections (slices),” Internal Standard No. 46-108-01/01, 2002.

[96] S. D. Kretzschmar and R. Furter, “The measurement of yarn diameter, density and shape of yarns,” 2009.

[97] Z. Ahmad, S. Iqbal, M. Eldeeb, and A. A. Mazari, “Effect of yarn structure on cover factor in woven fabrics,” *Ind. Textila*, vol. 69, no. 3, pp. 197–201, 2018.

[98] Z. Ahmad, B. K. Sirková, and M. Eldeeb, “Yarn cross-sectional deformation in woven fabric,” *Vlakna a Text.*, vol. 23, no. 4, pp. 36–41, 2016.

[99] F. T. Peirce, “Geometrical principles applicable to the design of functional fabrics,” *Text. Res. J.*, vol. 17, no. 3, pp. 123–147, 1947.

[100] Z. Ahmad, B. K. Sirkova, and A. R. R. Aboalasaad, “Yarn deformation in multifilament single layer woven structures using Fourier series,” in *18th AUTEX World Textile Conference*, 2018, no. ID no. 3180.

APPENDIX A

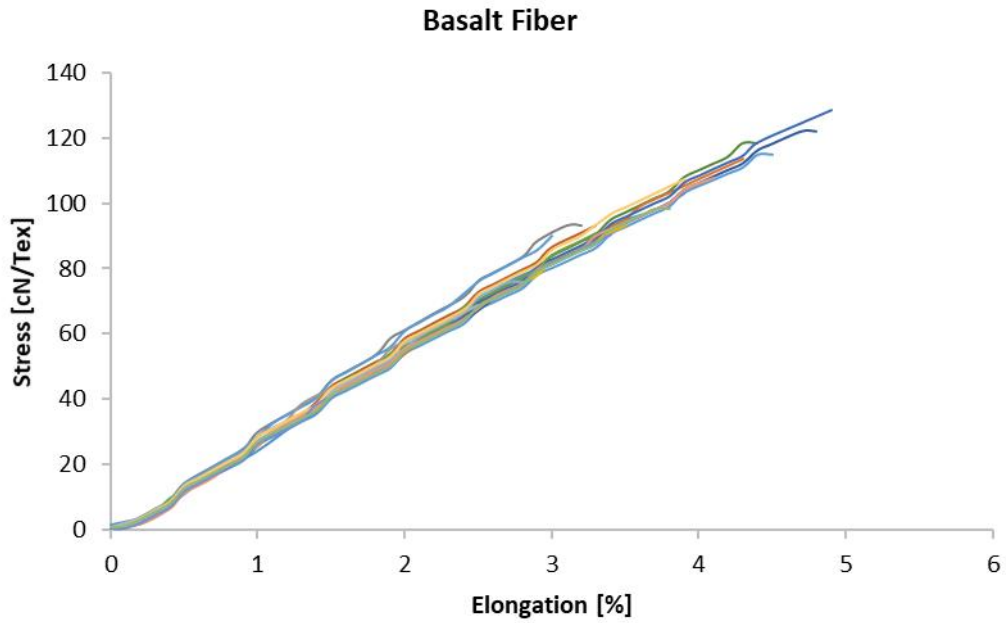

Figure 71. Stress-strain curves for Basalt fiber

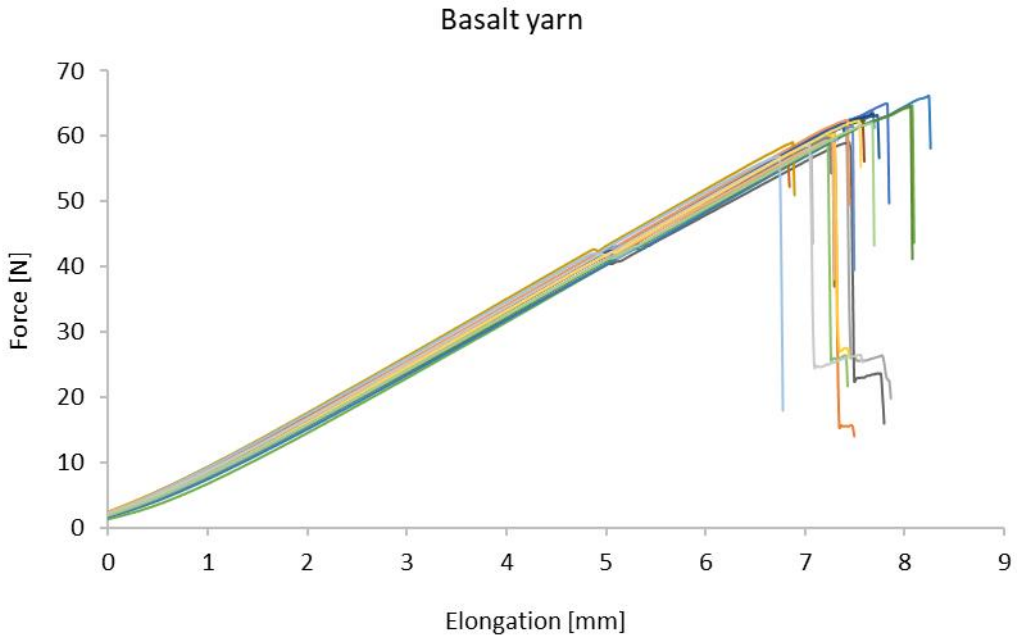

Figure 72. Force-elongation curves for Basalt yarn

APPENDIX B

Approximation for single layer Glass woven fabrics by Fourier series

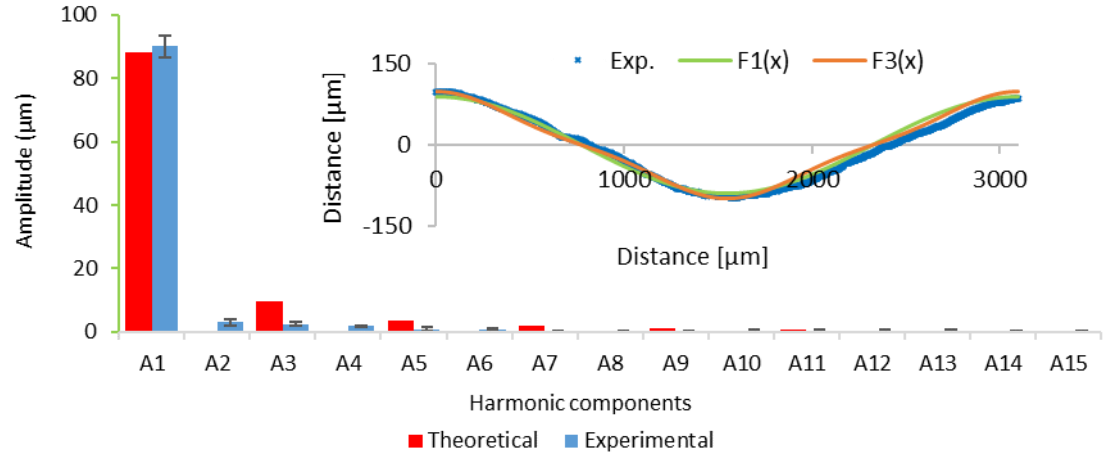

Figure 73. Fourier approximation and spectral characteristics of binding wave in longitudinal cross-section for fabric sample (G1)

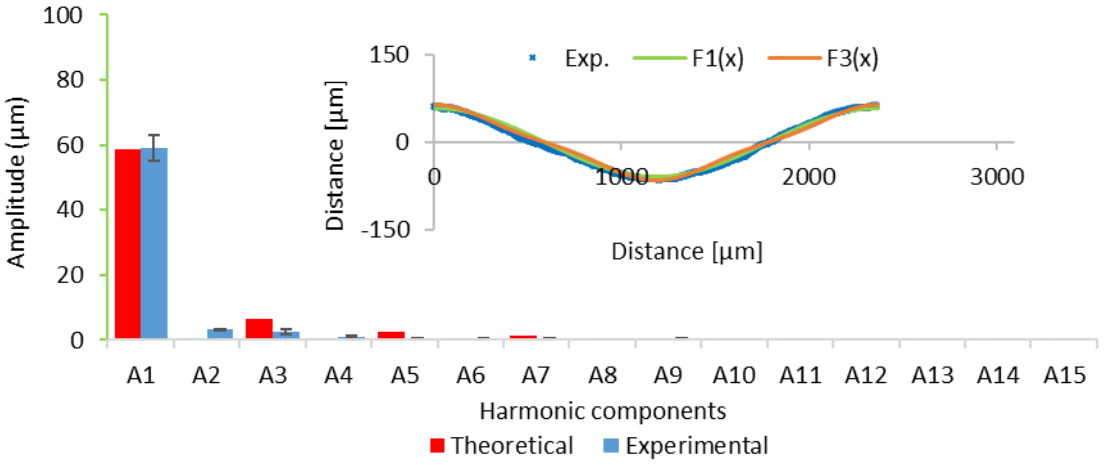

Figure 74. Fourier approximation and spectral characteristics of binding wave in longitudinal cross-section for fabric sample (G2)

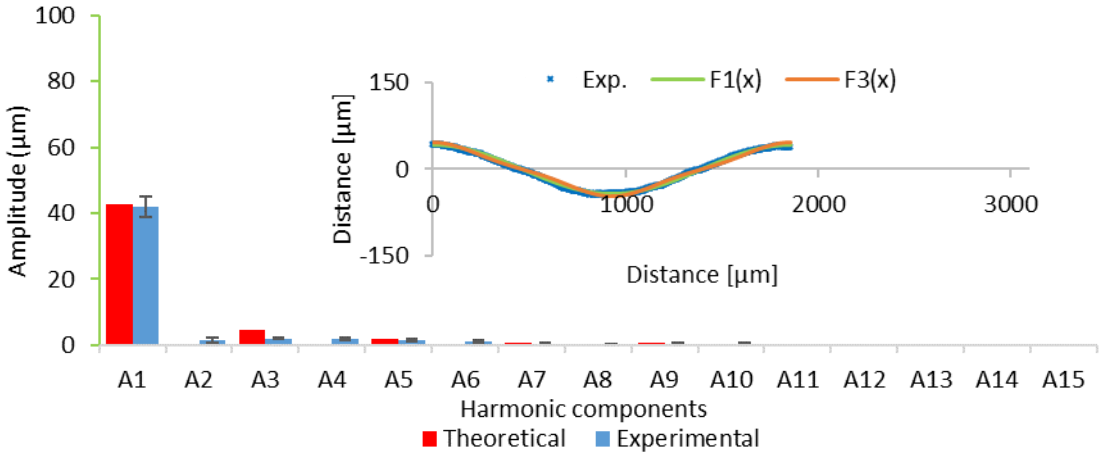

Figure 75. Fourier approximation and spectral characteristics of binding wave in longitudinal cross-section for fabric sample (G3)

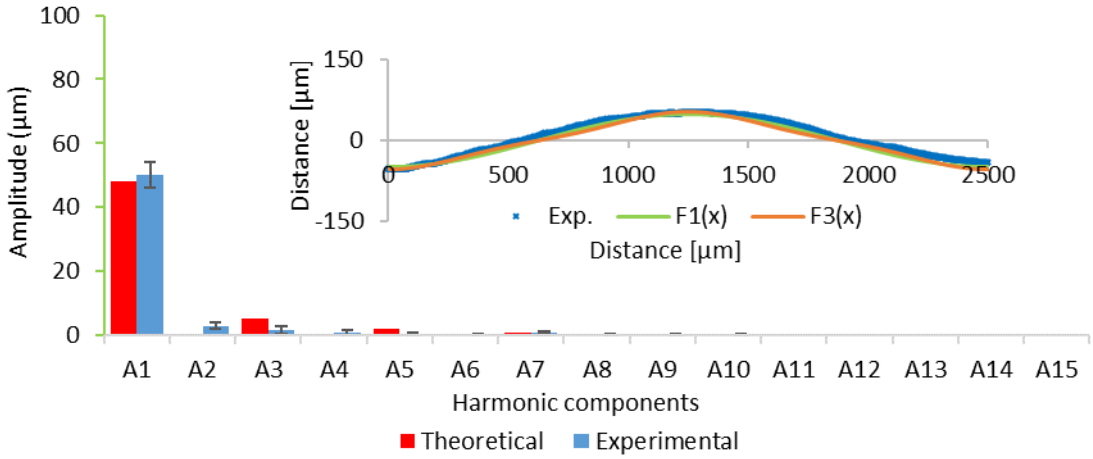

Figure 76. Fourier approximation and spectral characteristics of binding wave in transverse cross-section for fabric sample (G1)

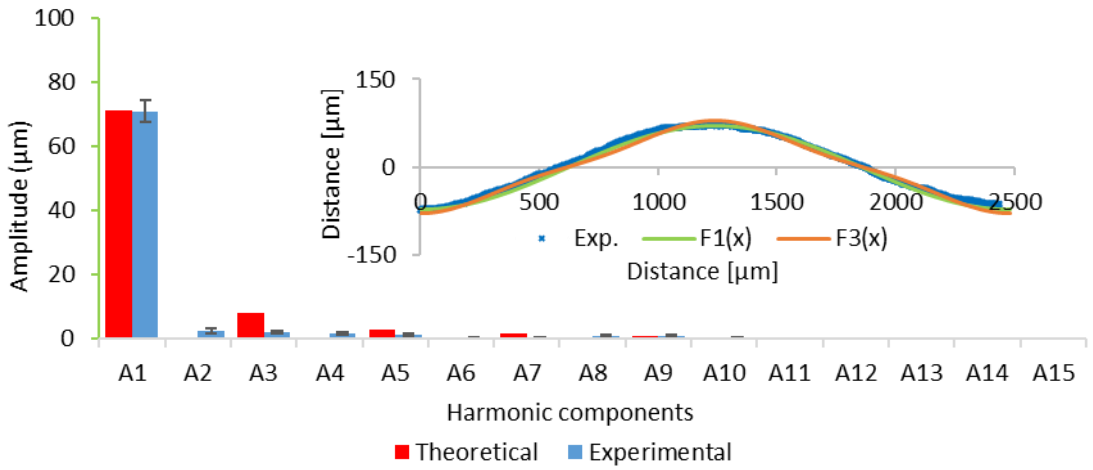

Figure 77. Fourier approximation and spectral characteristics of binding wave in transverse cross-section for fabric sample (G2)

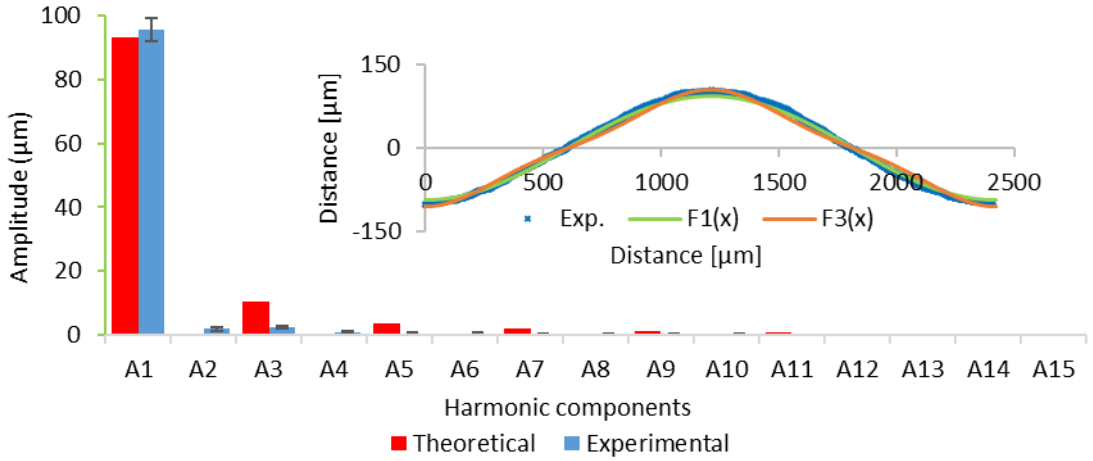

Figure 78. Fourier approximation and spectral characteristics of binding wave in transverse cross-section for fabric sample (G3)

RESEARCH ARTICLES

Publications in journals

1. **Ahmad Z**., Sirková B., Ahmad S., Naeem M.S., Hassan S.Z., "Effect of material and stitching on tensile properties of woven fabrics", IOP Conference Series: Materials Science and Engineering, 2018, 414(1): 012049, ISSN 1757-8981.
2. **Ahmad Z.**, Eldeeb M., Iqbal S., and Mazari, A., "Effect of yarn structure on cover factor in woven fabrics", Industria Textila, 2018, 69(3), p. 197-201, ISSN:1222-5347 [Thompson ISI/Scopus].
3. Azeem M., **Ahmad Z.**, Wiener J., Fraz A., Siddique H.F., and Havalka A., "Influence of weave design and yarn types on mechanical and surface properties of woven fabric", Fibres & Textiles in Eastern Europe, 2018, 26, 1(127), p. 42-45, ISSN:1230-3666, [Thompson ISI/Scopus].
4. **Ahmad Z.**, and Sirková B., "Tensile behavior of Basalt and Glass single layer and multilayer woven fabrics", Journal of Textile Institute, 2017, 109(5), p. 686-694, ISSN: 0040-5000 [Scopus Database].
5. Iqbal S., Eldeeb M., **Ahmad Z.**, and Mazari A., "Comparative study on yarn and knitted fabric made from Open end and Rieter airjet spun system", Journal of Textile & Apparel/Tekstil ve Konfeksiyon, 2017, 27(3), p. 234-240, ISSN: 1300-3356 [Thompson ISI/Scopus].
6. Mangat, A.E., Hes, L. Bajzik, V., and **Ahmad, Z.**, "Influence of air flow direction on thermal resistance and water vapor permeability of Rib knit fabrics", Journal of Textile & Apparel/Tekstil ve Konfeksiyon, 2017, 27(1), p. 32-37, ISSN: 1300-3356 [Thompson ISI/Scopus].
7. **Ahmad Z.**, Sirková B., and Eldeeb M., "Yarn cross-sectional deformation in woven fabric", Vlakna a Textil, 2016, 23(4), p. 36-41, ISSN: 1335-0617 [Scopus Database].

Articles under review

1. **Ahmad Z.**, and Sirková B., "Modelling of multifilament woven fabric structure using Fourier series", Journal of Textile Institute, ISSN: 0040-5000 (under review).
2. **Ahmad Z.**, and Sirková B., "Analysis of mutual interlacing of threads in multifilament single layer and two layer woven fabric structure using Fourier series", Journal of Textile Institute, ISSN: 0040-5000 (under review).

3. **Ahmad Z.**, and Sirková B., "Modelling of reinforcement two layer stitched woven fabric structure intended for composites", Composites Part B: Engineering, ISSN: 1359-8368 (under review).
4. Aboalasaad A.R.R., Sirková B., and **Ahmad Z**., "Influence of tensile stress on woven compression bandage structure and porosity", Autex Research Journal, ISSN: 1470-9589 (under review).

Publications in International Conferences

1. **Ahmad Z**., Sirková B., and Aboalasaad A.R.R., "Yarn deformation in multifilament single layer woven structures using Fourier series", AUTEX, Istanbul, Turkey 2018, ISBN 978-961-6900-17-1.
2. Zubair M., **Ahmad Z**., Javaid M.U., Drean J.Y., and Mathieu D., "Influence of fabric architecture and material on physical properties of 3D multilayer woven fabrics", In: 9th Central European Conference (proceedings). Liberec: Technical University in Liberec, 2017. ISBN 978-80-7494-355-3.
3. Naeem M.S., **Ahmad Z.**, Javed Z., Rasheed A., Ramzan B. and Abid H.A., "Removal of Acid Red from Aquous Media using Activated Carbon from Acrylic waste", Emerging Trends in Knitting, Venue: National Textile University, Faisalabad, Pakistan, 2018, ISBN 978-969-7549-03-0.
4. Naeem S., Javed S., Baheti V., Militky J., **Ahmad Z.**, and Behera P., "Effect of temperature, heating rate and holding time on the properties of Carbon web made from acrylic waste" In: 21st conference STRUTEX (proceedings). Liberec: Technical University in Liberec, 2016. ISBN 978-80-7494-269-3.
5. **Ahmad Z.**, Sirková B. and Eldeeb M., "Influence of weft setting on shape of yarn cross section in woven." In: Světlanka Workshop (Proceedings), Rokytnice nad Jizerou: Světlanka, 2015-08-14. ISBN 978-80-7494-229-7.
6. **Ahmad Z.**, Nazir I., Ibrahim S., Iqbal S., and Naeem M.S., "Effect of weave design on comfort properties of fabric made of Bamboo yarn" In: 20th conference STRUTEX (proceedings). Liberec: Technical University in Liberec, 2014. ISBN 978-80-7494-139-9.
7. Javaid M.U., **Ahmad Z.**, Iqbal S., Naeem M.S., "Viscose Fiber Strength and Degree of Polymerization", In: First International Young Engineers Confrence, At University of Engineering and Technology, Lahore, April 2014

RESEARCH PROJETCS

1. Member of the student grant completion (SGS) project 2017 (project no.21198), titled, “Preparation of modified carbon sorbents”, Faculty of Textile Engineering, Technical University of Liberec, Czech Republic.
2. Leader of the student grant completion (SGS) project 2016 (project no.21153), titled, “3D construction and structure of woven fabric”, Faculty of Textile Engineering, Technical University of Liberec, Czech Republic.
3. Member of the student grant completion (SGS) project 2015 (project no.21086), titled, “Effect of plying process on air jet yarn properties”, Faculty of Textile Engineering, Technical University of Liberec, Czech Republic.